

# **THESIA** 3

## This is to certify that the dissertation entitled

# SURVIVAL AND EXPERIMENTAL EVOLUTION OF ESCHERICHIA COLI UNDER FREEZE-THAW STRESS

presented by

#### **SEAN CHRISTIAN SLEIGHT**

has been accepted towards fulfillment of the requirements for the

Ph.D. degree in Microbiology and Molecular Genetics

Richard E. Lucki

Major Professor's Signature

May 9, 2007

Date

MSU is an affirmative-action, equal-opportunity employer

### LIBRARY Michigan State University

PLACE IN RETURN BOX to remove this checkout from your record.

TO AVOID FINES return on or before date due.

MAY BE RECALLED with earlier due date if requested.

DATE DUE	DATE DUE	DATE DUE

6/07 p:/CIRC/DateDue.indd-p.1

# SURVIVAL AND EXPERIMENTAL EVOLUTION OF ESCHERICHIA COLI UNDER FREEZE-THAW STRESS

Ву

Sean Christian Sleight

#### A DISSERTATION

Submitted to
Michigan State University
in partial fulfillment of the requirements
for the degree of

DOCTOR OF PHILOSOPHY

Department of Microbiology and Molecular Genetics

2007

#### ABSTRACT

#### SURVIVAL AND EXPERIMENTAL EVOLUTION OF ESCHERICHIA COLI UNDER FREEZE-THAW STRESS

Ву

#### Sean Christian Sleight

This dissertation presents experiments on survival and evolution of *Escherichia coli* under freeze-thaw (FT) stress. The initial chapter describes the survival experiments necessary to identify conditions and suitable progenitors for the freeze-thaw-growth (FTG) evolution experiment. The following chapters illustrate this FTG evolution experiment as well as the phenotypic and genetic differences of the FTG-evolved lines relative to their progenitors. The FTG-evolved lines consisted of two groups. One group is derived from a single clone from each of the 12 populations of the long-term evolution experiment (Lenski et al. 1991) at the 20,000 generation timepoint. The other group is derived from three replicates of the ancestor from this long-term evolution experiment.

Chapter 1 illustrates that the 12 long-term lines are more susceptible to repeated FT cycles relative to the ancestor, but have no significant changes to prolonged freezing. There is significant variation among the long-term lines in FT survival and this variation corresponds with differences in fitness. It was hypothesized that these 12 long-term lines would have a greater potential for evolutionary adaptation to the FT component of the FTG cycle and thus were chosen as progenitors for the FTG evolution experiment along with three replicates of the ancestor.

Chapter 2 describes the FTG evolution experiment and various phenotypic measurements of the FTG-evolved lines relative to their progenitors.

Competition experiments demonstrated evolutionary adaptation to FTG conditions that can be attributed to both improved FT survival and a shorter transition to growth after the FT cycle. Growth curve experiments measure the lag phase and growth rate after a FT cycle and stationary phase.

Chapter 3 describes the candidate gene sequencing and insertion sequence (IS) fingerprinting analysis performed to identify genetic changes in FTG-evolved lines. Multiple FTG-evolved lines acquired mutations in the *cls* gene and *uspA/B* intergenic region. In selected evolved lines, these mutations are beneficial in FTG conditions under the genomic context that they arose in. Mutations in the *cls* gene contribute to maintaining membrane fluidity after a FT cycle. The IS150 insertion in the intergenic region of *uspA/B* disrupts *uspB* transcription in FTG conditions, but the exact physiological benefit is unknown.

This dissertation is illness.	s dedicated to the	e recovery of Dr.	Thomas Whittam	ı from his

#### **ACKNOWLEDGEMENTS**

I would like to thank my advisor Dr. Richard Lenski for his tremendous support and advisement, allowing me to join his lab, and for obtaining funding for my research. He gave me the independence necessary to develop my critical thinking skills that are essential for performing scientific research, yet provided guidance whenever I needed it that no doubt steered my research in the right direction and improved its quality. Dr. Lenski is a top-notch scientist as evidenced by his elegant long-term evolution experiment, critical analysis skills, and brilliant writing. As a mentor, I could not ask for better and will always be grateful for this opportunity.

I'd also like to thank Dr. Dominique Schneider, who took the time to advise me via e-mail the best way to perform the insertion sequence analysis and how to make isogenic constructs. These experiments were key to discovering the genetic adaptations of my evolved lines and their significance. Dr. Schneider is essentially an unofficial committee member and made wonderful suggestions that helped guide my research.

I want to also thank all my committee members, Drs. Thomas Whittam,
Mike Thomashow, Thomas Schmidt, and John Breznak. Their insightful
questions, comments, and suggestions at committee meetings tremendously
helped shape and advance the bulk of my research, not to mention the time and
effort needed to read my dissertation proposal and this dissertation.

There are many past and present members of the Lenski lab that I want to thank for their help in the lab, helpful discussions, friendship, and suggestions at

lab meeting presentations: Neerja Hajela, Christian Orlic, Nicholas Wigginton, Gabe Yedid, Zachary Blount, Mike Wiser, Drs. Bob Woods, Kristina Hillesland, Chris Borland, Christopher Marx, Susi Renold, Tim Cooper, Dusan Misevic. Elizabeth Ostrowski, Jeff Barrick, and all of Neerja's lab assistants over the years. I especially want to thank Neerja Hajela for all her help in the lab and making lab supplies needed for my research, Christian and Nick for helping me with experiments vital to my research, Bob Woods for advising me on techniques for making isogenic constructs and helpful discussions, Kristina Hillesland and Chris Borland for reading and critiquing my dissertation proposal, and Zachary Blount for reading a postdoctoral fellowship proposal draft and helpful discussions. I also need to thank Jeff Landgraf at RTSF for his help with my RT-PCR experiments and analysis, Jorge Rodrigues for his help with fluorescence microscopy (live-dead count) experiments, the Department of Microbiology and Molecular Genetics, and the NASA Astrobiology Institute for funding my research.

I want to thank my entire family for their continued support and fun conversations about my research and science in general. Last, but certainly not least, I'd like to thank my amazing girlfriend Malia Moren. Not only has she continued to support my graduate studies endeavor, but is always there for me through the rough patches. And I almost forgot to thank my cat Sy for keeping my lap warm while I finish writing this dissertation.

#### **TABLE OF CONTENTS**

LIST OF TABLES	VIII
LIST OF FIGURES	ix
CHAPTER 1: CHANGES IN FREEZE-THAW SURVIVAL FOLLOWING EVOLUTION IN A BENIGN ENVIRONMENT.  Abstract.  Background.  Materials and Methods.  Results and Discussion.  Conclusions.  Figures.  Tables.	1 1 2 5 9 13 16 21
CHAPTER 2: ADAPTATION TO CYCLES OF FREEZING, THAWING, AND GROWTH: PHENOTYPIC EVOLUTION.  Abstract.  Background.  Materials and Methods.  Results.  Discussion.  Figures.	22 22 23 29 36 46 52
CHAPTER 3: ADAPTATION TO CYCLES OF FREEZING, THAWING, AND GROWTH: GENETIC EVOLUTION	64 64 65 69 81 97 108
REFERENCES	128
APPENDIX 1: Supplementary figures and tables for Chapter 2	143
APPENDIX 2: Supplementary figures and tables for Chapter 3	158

#### LIST OF TABLES

in mortality rates under the repeated freeze-thaw regime	21
Table 2. ANOVA testing for heterogeneity among the evolved lines in mortality rates under the prolonged freezing regime	21
Table 3. IS changes in FTG-evolved lines relative to progenitors	125
Table 4. Mutations in <i>cls</i> and <i>uspA/B</i> genes	125
Table 5. <i>cls</i> mutations in FTG-evolved lines through time	126
Table 6. <i>uspA/B</i> mutations in FTG-evolved lines through time	126
Table 7. 2-way ANOVA testing for differences in the <i>cls</i> allele, progenitor or evolved background, and interaction effects in laurdan anisotropy after freeze-thaw treatment	127
Table 8. 2-way ANOVA testing for differences in the <i>cls</i> allele, progenitor or evolved background, and interaction effects in laurdan anisotropy after stationary phase	127
Table A1.1. Phenotypic measurements between individual FTG-evolved lines relative to their progenitors	156
Table A1.2. Statistical tests for FTG-evolved groups and their progenitors	157
Table A2.1. Primer pairs used to PCR amplify candidate genes	165
Table A2.2. Primer pairs used to PCR amplify IS element probes for RFLP analysis	166
Table A2.3. Primer pairs used to PCR amplify sequences adjacent to IS elements	167
Table A2.4. IS band differences between individual FTG-evolved lines relative to their progenitors	168
Table A2.5. Laurdan anistropy differences between individual FTG-evolved clones, their progenitors, and isogenic strains	169

#### LIST OF FIGURES

Figure 1. Survival of ancestral <i>E. coli</i> strain under the freeze-only (prolonged freezing) and repeated freeze-thaw cycle regimes	16
Figure 2. Comparison of mortality rates between the evolved <i>E. coli</i> and their ancestor under the repeated freeze-thaw regime	17
Figure 3. Comparison of mortality rates between the evolved <i>E. coli</i> and their ancestor under the prolonged freeze-only regime	18
Figure 4. Heterogeneity of mortality rates among the 12 evolved lines under the repeated freeze-thaw regime	19
Figure 5. Correlation between freeze-thaw mortality and fitness in the benign environment	20
Figure 6. Evolutionary histories of freeze-thaw-growth (FTG) populations	52
Figure 7. Schematic illustration showing how the apparent duration of lag phase is corrected for FT survival to calculate the actual duration of the physiological lag prior to growth	53
Figure 8. Relative fitness of FTG evolved groups A and B and their progenitors over the two-day FTG cycle	54
Figure 9. Relative fitness of the 15 FTG evolved lines and their progenitors	55
Figure 10. Decomposition of overall fitness gains under the FTG regime into changes in (A) FT survival and (B) growth performance	56
Figure 11. Growth dynamics of the FTG-evolved lines and their progenitors following (A) FT treatment and (B) stationary phase at 37°C.	58
Figure 12. Lag phases following the FT treatment for two FTG-evolved lines and their progenitors	60
Figure 13. Lag phases following stationary phase at 37°C for two FTG-evolved lines and their progenitors	62
Figure 14. Evolutionary histories of individual freeze-thaw-growth (FTG) populations	108

Figure 15. Southern hybridization of <i>Hin</i> cII-digested genomic DNA with the IS <i>150</i> probe	109
Figure 16. Schematic representation of mutations in <i>cls</i>	110
Figure 17. Schematic representation of IS150 insertions in <i>uspA/B</i> intergenic region	111
Figure 18. Relative fitness components of the following clones:  A-2 cls <sup>-</sup> construct, A-2 cls <sup>+</sup> progenitor, A-2/FTG cls <sup>+</sup> construct, and  A-2/FTG cls <sup>-</sup> evolved clone	112
Figure 19. Growth dynamics following (A) FT treatment and (B) stationary phase at 37°C	115
Figure 20. Laurdan anisotropy differences following (A) FT treatment and (B) stationary phase	117
Figure 21. Relative fitness components of the following clones: ancestor ( <i>uspA/B</i> -IS150), evolved clone AncB/FTG <i>uspA/B</i> +IS150, and the constructed clone AncB/FTG <i>uspA/B</i> -IS150	119
Figure 22. Growth dynamics following (A) FT treatment and (B) stationary phase at 37°C	122
Figure 23. Relative <i>uspB</i> transcription differences using Real-Time PCR	124
Figure A1.1. Relative freeze-thaw survival of the 15 FTG-evolved lines and their progenitors	144
Figure A1.2. Comparison of mortality rates between individual FTG-evolved lines and their progenitors under the repeated freeze-thaw regime	145
Figure A1.3. Comparison of mortality rates between the FTG-evolved groups and their progenitors under the repeated freeze-thaw regime	146
Figure A1.4. Relative growth fitness after freezing and thawing of the 15 FTG-evolved lines and their progenitors	147
Figure A1.5. FTG timecourse for two FTG-evolved lines and their progenitors	148
Figure A1.6. Growth timecourse after stationary phase for two FTG-evolved lines and their progenitors	150

Figure A1.7. Fluorescence microscopy of the Evolved Group A (AncB/FTG) clone and the ancestor at different timepoints in the FTG cycle	152
Figure A1.8. Fluorescence microscopy of the Evolved Group B (A+1/FTG) clone and its progenitor (A+1) at different timepoints in the FTG cycle	154
Figure A2.1. cls and uspA/B isogenic constructs and reconstructs	159
Figure A2.2. Southern hybridization of <i>Eco</i> RV-digested genomic DNA to the IS1 probe	160
Figure A2.3. Southern hybridization of <i>Eco</i> RV -digested genomic DNA to the IS3 probe	161
Figure A2.4. Southern hybridization of <i>Eco</i> RV-digested genomic DNA to the IS <i>186</i> probe	162
Figure A2.5. Southern hybridization of <i>Eco</i> RV-digested genomic DNA to the IS <i>186</i> probe (second blot)	163
Figure A2.6. Relative <i>uspA</i> transcription differences using Real-Time PCR	164

#### CHAPTER 1

### CHANGES IN FREEZE-THAW SURVIVAL FOLLOWING EVOLUTION IN A BENIGN ENVIRONMENT

BMC Evolutionary Biology 2006, 6:104

#### **ABSTRACT**

In order to study the dynamics of evolutionary change, 12 populations of E. coli B were serially propagated for 20,000 generations in minimal glucose medium at constant 37°C. Correlated changes in various other traits have been previously associated with the improvement in competitive fitness in the selective environment. This study examines whether these evolved lines changed in their ability to tolerate the stresses of prolonged freezing and repeated freeze-thaw cycles during adaptation to a benign environment. All 12 lines that evolved in the benian environment for 20,000 generations are more sensitive to freeze-thaw cycles than their ancestor. The evolved lines have an average mortality rate of 54% per daily cycle, compared to the ancestral rate of 34%. By contrast, there was no significant difference between the evolved lines and their ancestor in mortality during prolonged freezing. There was also some variability among the evolved lines in susceptibility to repeated freeze-thaw cycles. Those lines that had evolved higher competitive fitness in the minimal glucose medium at 37°C also had higher mortality during freeze-thaw cycles. This variability was not associated, however, with differences among lines in DNA repair functionality and mutability. The consistency of the evolutionary declines in freeze-thaw tole rance, the correlation between fitness in glucose medium at 37°C and

mortality during freeze-thaw cycles, and the absence of greater declines in freeze-thaw survival among the hypermutable lines all indicate a trade-off between performance in minimal glucose medium at 37°C and the capacity to tolerate this stress. Analyses of the mutations that enhance fitness at 37°C may shed light on the physiological basis of this trade-off.

#### **BACKGROUND**

Most research in evolution pursues the comparative method, in which the present-day patterns of organismal diversity are examined in order to infer historical processes of change (Harvey and Pagel 1991). Research in paleontology allows a more direct examination of the past (Gould 1989), but fossil data are limited in certain respects, including the inability to measure the performance abilities of organisms. A third approach for studying evolution is to perform long-term studies, either observational (Grant 1999) or experimental (Bell 1997), that allow one to observe evolution in action across many generations. In recent years, bacteria and viruses have become especially popular for experimental evolution, owing to their rapid generations that allow studies to run for hundreds or even thousands of generations (Lenski et al. 1991; Bennett and Lenski 1993; Burch and Chao 2000; Elena and Lenski 2003; MacLean et al. 2004; Wichman et al. 2005).

In a long-term experiment, Lenski and colleagues have propagated 12 populations of *E. coli* for more than 20,000 generations at 37°C in a minimal-salts medium supplemented with glucose (Lenski et al. 1991; Lenski and Travisano 1994; Lenski 2004). The dynamics of both phenotypic (Sniegowski et al. 1997;

Lenski et al. 1998; Cooper and Lenski 2000; Rosen and Lenski 2000; Cooper et al. 2001a; de Visser and Lenski 2002; Novak et al. 2006) and genomic (Cooper et al. 2001b; Cooper et al. 2003; Lenski et al. 2003; Crozat et al. 2005; Rosen et al. 2005; Woods et al. 2006; Pelosi et al. 2006) evolution have been characterized in a variety of ways. During the 20,000 generations, the bacteria have genetically adapted to their selective environment, such that their mean fitness relative to the ancestor increased by about 70%, based on direct competitions (Cooper and Lenski 2000). Interestingly, four of the 12 populations evolved defects in their DNA repair mechanisms, which caused them to become hypermutable (Sniegowski et al. 1997; Cooper and Lenski 2000). The evolving bacteria also increasingly became ecological specialists, in the sense that their performance in some, but not all, other test environments tended to decline (Lenski et al. 1998; Cooper and Lenski 2000; Cooper et al. 2001a; Pelosi et al. 2006). The parallel trajectories between increasing fitness in the selective environment and declining performance in other environments suggest that most of the decline in other environments is the result of pleiotropic side-effects of the same mutations that produce adaptation in the selective environment (Cooper and Lenski 2000). The fact that the four populations that became mutators do not show much more specialization is also consistent with this interpretation (Cooper and Lenski 2000).

Stressful environments, such as prolonged freezing or repeated freezethaw cycles, may reveal other performance tradeoffs in the evolved lines. In fact, freezing and thawing impose several interconnected stresses including

dehydration, hyperosmotic stress, ice formation, oxidative stress, and low temperature (Cox and Heckly 1973; Calcott 1985; Gao and Critser 2000). The acute responses of bacterial cells to freezing and thawing, including the effects of prior exposure to cold and other stresses on survival (Thammavongs et al. 1996; Jeffreys et al. 1998; Panoff et al. 1998; Wouters et al. 1999a; Wouters et al. 1999b; Drouin et al. 2000; Leebanon and Drake 2001), are reasonably well understood. Many other variables also contribute to whether bacteria survive freezing and thawing, including their nutritional status and growth phase as well as the cooling rate employed (Calcott 1985; Gao and Critser 2000; Packer et al. 1965). Freezing and thawing E. coli cells without an exogenously supplied cryoprotective agent, such as glycerol, severely decreases their viability (Calcott and MacLeod 1975; Calcott and Gargett 1981). Loss of viability is proportional to the number of freeze-thaw cycles that cells experience (Packer et al. 1965; Ingraham 1987; Calcott et al. 1983). Therefore, the elapsed time that cells are frozen generally influences viability less than the processes of freezing and thawing.

By contrast, much less is known about how and why different bacterial strains and species vary in their capacity to survive these stresses (Calcott 1985; Drouin et al. 2000; Young et al. 1964; Scher et al. 1964). In this study, we examine how evolutionary adaptation by populations of *E. coli* to serial propagation on a minimal glucose medium at a constant temperature of 37°C affected survival during prolonged freezing and repeated freeze-thaw cycles in the absence of cryoprotectant. In particular, we test whether there was an

evolutionary trade-off such that adaptation to this benign environment led to correlated losses in survival capacity under these stresses. We also evaluate whether replicate lines that evolved under the same regime show heterogeneous changes in their stress responses. One of our motivating interests in this research is to identify strains and conditions suitable for a future experiment that will investigate evolutionary adaptation to repeated freeze-thaw-growth cycles. We want to identify conditions in which some survival is possible, but where there is sufficient mortality to impose strong selection. Also, evidence for heritable variation among lines in survival under these extreme conditions would indicate the potential, at least, for evolutionary adaptation in that future experiment.

#### **MATERIALS AND METHODS**

#### Long-term evolution experiment and bacterial strains

The long-term evolution experiment is described in detail elsewhere (Lenski et al. 1991; Lenski 2004). In brief, 12 populations were founded using an *E. coli* B ancestor and then propagated at 37°C for 20,000 generations (3,000 days) in Davis minimal medium supplemented with glucose at 25 mg/L (DM25). The populations were diluted 100-fold daily into fresh medium, and their regrowth allowed about 6.6 (= log<sub>2</sub> 100) generations per day. The source strain, REL606, cannot grow on arabinose (Ara<sup>-</sup>), and it was used to start six populations; the other six were started with a spontaneous Ara<sup>+</sup> mutant, REL607, of the source strain. The Ara marker is selectively neutral in the experimental environment (Lenski et al. 1991). The 12 evolved lines used in this study were

isolated as single clones at generation 20,000, after which they have been stored in glycerol at -80°C.

Methods for measuring survival under freeze-only and freeze-thaw regimes

Culture media and experimental pre-conditioning

Bacteria used for testing were removed from storage in the freezer, inoculated into LB (Luria-Bertani) medium, and incubated for 24 h at 37°C. A culture was then diluted 1:10,000 into DM25 and incubated for 24 h at 37°C. A final 1:100 dilution was made into fresh DM25 and incubated for 24 h at 37°C, at which time cells were well into stationary phase, having exhausted the glucose in the first 8 h or so. Hence, all cells in the experiments were physiologically acclimated to the same environmental conditions before their survival was measured during repeated freeze-thaw cycles or during prolonged freezing.

#### Measuring cell density

Colony forming units (CFU) were used to estimate viable cell densities. A pilot study was performed to find a range of serial dilutions that would allow accurate cell counts as populations declined during repeated freeze-thaw cycles. For the evolved lines that were most sensitive, no dilution was made on the final day of the freeze-thaw experiment, so that no line fell below the detection limit of ~10 cells/mL. Diluted or undiluted cell cultures were plated on tetrazolium-arabinose (TA) indicator agar (Lenski et al. 1991) and incubated at 37°C for 24 h before counting.

#### Freeze-thaw regime

After pre-conditioning, 1 mL of a stationary-phase culture was transferred into each of three replicate vials, which were then immediately placed in a –80°C freezer. Each day the tubes were kept frozen for 22.5 h and allowed to thaw at room temperature (about 22°C) for 1.5 h. Viable cell density was measured after the desired number of freeze-thaw cycles. For example, in order to measure survival after 1 day, the vials were frozen for 22.5 h and thawed for 1.5 h before measuring cell density. To measure survival after 7 days, the vials were subjected to seven freeze-thaw cycles and the cell density was measured after the last thaw.

#### Freeze-only regime

After pre-conditioning, 1 mL of a stationary-phase culture was transferred into each of three replicate vials and placed in a –80°C freezer. After the desired duration, a vial was thawed for 1.5 h and viable cell density measured. For example, to measure the freeze-only survival after 1 day, vials were frozen for 22.5 h and thawed for 1.5 h before measuring cell density. To measure the freeze-only survival after 7 days, vials were frozen for 166.5 h (= 7 days minus 1.5 h) and thawed for 1.5 h. Thus, the elapsed time at –80°C is varied experimentally, and only a single thaw occurs regardless of duration under this regime.

#### Calculations and statistical methods

The first experiment was performed to measure and compare the survival of the ancestral strain under two different 28-day regimes, one with daily freeze-thaw cycles and the other representing the freeze-only regime. In each case,

linear regression was performed on the log<sub>10</sub>-transformed viable cell densities to estimate the daily mortality rate and determine whether it differed significantly from zero. Data from all 28 days, including day 0, were used to calculate the mortality rate under the freeze-thaw regime, whereas that initial value was excluded when calculating the mortality rate during the freeze-only regime in order to adjust for effect of the single episode of thawing that was experienced in all subsequent days.

The second experiment compared the survival of the ancestral and evolved lines under the freeze-only and freeze-thaw regimes. It also allowed us to test for heterogeneity in survival rates among the 12 independently evolved lines. This experiment lasted 10 days; given the temporal constancy of the mortality rates observed in the first experiment, we estimated viable cell densities on days 0 and 10 only. For each assay, we calculated the percentage survival as  $s = n_{10} / n_0$ , where  $n_0$  and  $n_{10}$  denote initial and final densities, respectively. For the freeze-thaw regime, we then computed the mortality rate per day as  $m_{FT} = 1 - s^{1/10}$ . For the freeze-only regime, we took into account that there were nine days of sustained freezing and one freeze-thaw cycle. Therefore, the freeze-only mortality rate was calculated as  $m_{FO} = 1 - (s/(1 - m_{FT}))^{1/9}$ . For example, if the mortality rate per freeze-thaw cycle were 30%, then one would expect s = 0.7 under the freeze-only regime even with perfect survival during the other nine days. If there were also 2% daily mortality during the constant freezing, then one would expect overall survival under the freeze-only regime to be  $s = 0.7 \times (0.98)^9 \approx 0.58$ . Also, to preserve the statistical independence of the

replicate  $m_{FO}$  estimates, each one was calculated using a unique paired estimate of  $m_{FT}$ .

For each mortality rate parameter,  $m_{FT}$  or  $m_{FO}$ , we compared the evolved lines with the ancestral strain as follows. We first computed the mean of the three replicate assays for each evolved line, and then we computed the grand mean and standard deviation from the individual means of the 12 independently evolved lines. For the ancestor, we computed the mean and standard deviation over the six assays (three each for the two marker states). We performed a two-tailed t-test with unequal variances, which allows for the fact that the evolved lines may have diverged from one another as well from their common ancestor. For the freeze-thaw and prolonged freezing mortality rates, we also tested for heterogeneity among the evolved lines by performing a one-way analysis of variance (ANOVA), with the three replicate assays per line providing statistical replication.

#### **RESULTS AND DISCUSSION**

#### Effects of freeze-only and freeze-thaw regimes on survival of the ancestor

Figure 1 shows the survival trajectories for the *E. coli* B ancestral strain under the  $-80^{\circ}$ C freeze-only and freeze-thaw regimes over the course of 28 days. With daily freeze-thaw cycles, the density of viable cells declined by about five orders of magnitude. As evidenced by the log-linear trajectory ( $r^2 = 0.97$ , p < 0.0001), the bacteria experienced a nearly constant mortality rate of 34.4% killed per freeze-thaw cycle.

It is quite clear that most of this mortality was caused by the repeated bouts of freezing and thawing, as opposed to the time that cells spent frozen, because the cumulative mortality under the freeze-only regime was far less. In fact, over the entire 28 days at –80°C, with one thaw, the viable population size declined by only 35.2%. This decline almost exactly matches the cell death observed after one day in the freeze-thaw regime (Fig. 1), implying that no further death occurred during the other 27 days at constant –80°C. In fact, the slope of the cell-survival trajectory from day 1 to day 28 under the freeze-only regime was not significantly different from zero (p = 0.3483). Thus, there was little or no mortality, even over several weeks, beyond that caused by the single freeze-thaw cycle that was a necessary part of the survival assay procedures for all samples, regardless of how long they had spent at –80°C.

Therefore, the ancestral strain used for the long-term evolution experiment at 37°C is quite hardy with respect to prolonged freezing at –80°C. However, it is much more sensitive to repeated cycles of freezing and thawing. In the next section, we examine whether the lines that previously evolved for 20,000 generations in a benign environment became less tolerant of either prolonged freezing or repeated freeze-thaw cycles.

# Effects of freeze-only and freeze-thaw regimes on survival of the evolved lines in comparison with the ancestor

We performed 10-day experiments under both freeze-only and freeze-thaw regimes using the 12 lines that evolved by serial propagation on a minimal glucose medium at constant 37°C for 20,000 generations and their ancestor.

Each evolved line had three replicates, while the ancestor was replicated six-fold (three each for the Ara<sup>-</sup> and Ara<sup>+</sup> marker variants). Figure 2 compares the average mortality rates of the evolved lines and their ancestor under the freeze-thaw regime. The ancestor experienced a mortality rate of 34.0% per day under the freeze-thaw regime, a value almost identical to our first experiment. By contrast, all 12 evolved lines experienced greater mortality, with an average rate of 53.7% per day. The difference in freeze-thaw mortality rates between ancestral and evolved rates is highly significant (two-tailed t-test with unequal variances, p < 0.0001).

However, we observed no significant difference between the evolved lines and their ancestor in mortality rates during prolonged freezing at –80°C (Fig. 3; two-tailed t-test with unequal variances, p = 0.7689). Mortality rates under this regime were calculated, as described in the Materials and Methods, such that they correct for the effect of one cycle of freezing and thawing. The average mortality rates estimated for the ancestor and evolved lines under the freeze-only regime were 5.8% and 6.6% per day, respectively. The ancestral value is somewhat higher than estimated in the first experiment, but it is still much lower than the mortality rates measured during repeated freeze-thaw cycles in either experiment.

Thus, the 37°C-evolved lines as a group remained about as robust as their ancestor to the effects of prolonged freezing at –80°C. However, the evolved lines are much more sensitive than their ancestor to the effects of repeated freeze-thaw cycles, with the average mortality rate increasing from 34.0% to

53.6% per daily cycle. In the section that follows, we examine variation among the evolved lines in their freeze-thaw sensitivity.

# Heterogeneity among the evolved lines in freeze-thaw and prolonged freezing survival

Figure 4 shows the mortality rate per daily freeze-thaw cycle for each of the 12 lines that independently evolved at 37°C. The 95% confidence intervals were calculated by using the three replicate assays performed for each line. Estimated mortality rates vary from 40.2% to 78.0% per day. An analysis of variance confirms that variation among the evolved lines is highly significant (Table 1, p < 0.0001). Moreover, Figure 5 shows there is a significant correlation between competitive fitness measured in the benign selective environment (Cooper and Lenski 2000) and mortality rates measured in the freeze-thaw regime (r = 0.5882, n = 12, two-tailed p = 0.0442). This correlation provides further support for the trade-off between fitness in the benign environment of serial propagation on glucose minimal medium at constant 37°C and survival during repeated freeze-thaw cycles. In the prolonged freezing regime, an ANOVA shows there is also significant variation in the ability to survive prolonged freezing among the long-term lines (Table 2, p < 0.0001). Thus, while there is heterogeneity among these lines in both repeated freeze-thaw and prolonged freezing survival, there is no directional trend across these lines as a group.

The four lines that evolved defects in DNA repair, and which have much higher mutation rates (A-2, A-4, A+3, and A+6; Sniegowski et al. 1997; Cooper and Lenski 2000), do not have consistently higher freeze-thaw mortality rates, as

a group, than do the other evolved lines. Also, there is no significant correlation between competitive fitness in the benign environment and survival under the freeze-only treatment (r = 0.0756, n = 12, two-tailed p = 0.8154), consistent with the absence of any significant difference between the ancestor and evolved lines as a group in this stress-related capacity.

The variation among lines that evolved in the benign selective environment indicate that they acquired different sets of mutations that differentially affect their sensitivity to freeze-thaw cycles. The differences between lines are not associated with variation in DNA repair function and mutability, which implies that pleiotropic effects of the mutations that were selected for their beneficial effects during the evolution experiment in minimal glucose medium at 37°C are responsible for the increased susceptibility to freezing and thawing. If, alternatively, mutations that harmed freeze-thaw survival had accumulated by neutral drift, then we would expect significantly higher susceptibility among the four lines with defective DNA repair functions (Lenski and Cooper 2000; Funchain et al. 2000).

#### CONCLUSIONS

E. coli B cells experience little mortality during prolonged freezing at -80°C, even in the absence of added cryoprotectant. However, they are much more susceptible to repeated freezing and thawing, consistent with earlier studies (Packer et al. 1965; Ingraham 1987; Calcott et al. 1983). Twelve lines that previously evolved for 20,000 generations in a benign environment, consisting of serial transfer in a minimal glucose medium at constant 37°C, all

became more susceptible to freeze-thaw mortality than was their ancestor. Moreover, those evolved lines with higher fitness gains in the benign selective environment also tended to have greater susceptibility to freeze-thaw cycles, further supporting the trade-off in performance between these environments. However, the variation among the evolved lines was not associated with differences in DNA repair function and mutability that arose during the evolution experiment (Sniegowski et al. 1997; Cooper and Lenski 2000). Therefore, increased susceptibility to freeze-thaw cycles in the evolved lines probably reflects pleiotropic effects of mutations that were beneficial to the bacteria during evolution in the benign environment with minimal glucose medium and constant 37°C. In any case, significant variation among the lines in their freeze-thaw survival implies that there is genetic variation for this trait, such that it can be selected, which will be a focus of our future research.

Future research directions include evolving *E. coli* populations under freeze-thaw-growth cycles. The growth phase will allow populations to recover from mortality caused by freezing and thawing; selection should favour a reduction in freeze-thaw mortality, a faster transition to growth after thawing, or both. Another future direction includes identifying individual mutations responsible for increased susceptibility to freezing and thawing in the lines evolved in the benign environment of constant 37°C, or increased resistance in lines evolved under the freeze-thaw-growth regime. Finally, phenotypic and genetic analyses of freeze-thaw resistance could be extended to natural isolates of *E. coli*. Comparisons between food-borne pathogens and commensals would

be of particular interest because the ability to survive and recover from freezing and thawing might be an important adaptation of some food-borne pathogens.

#### **FIGURES**

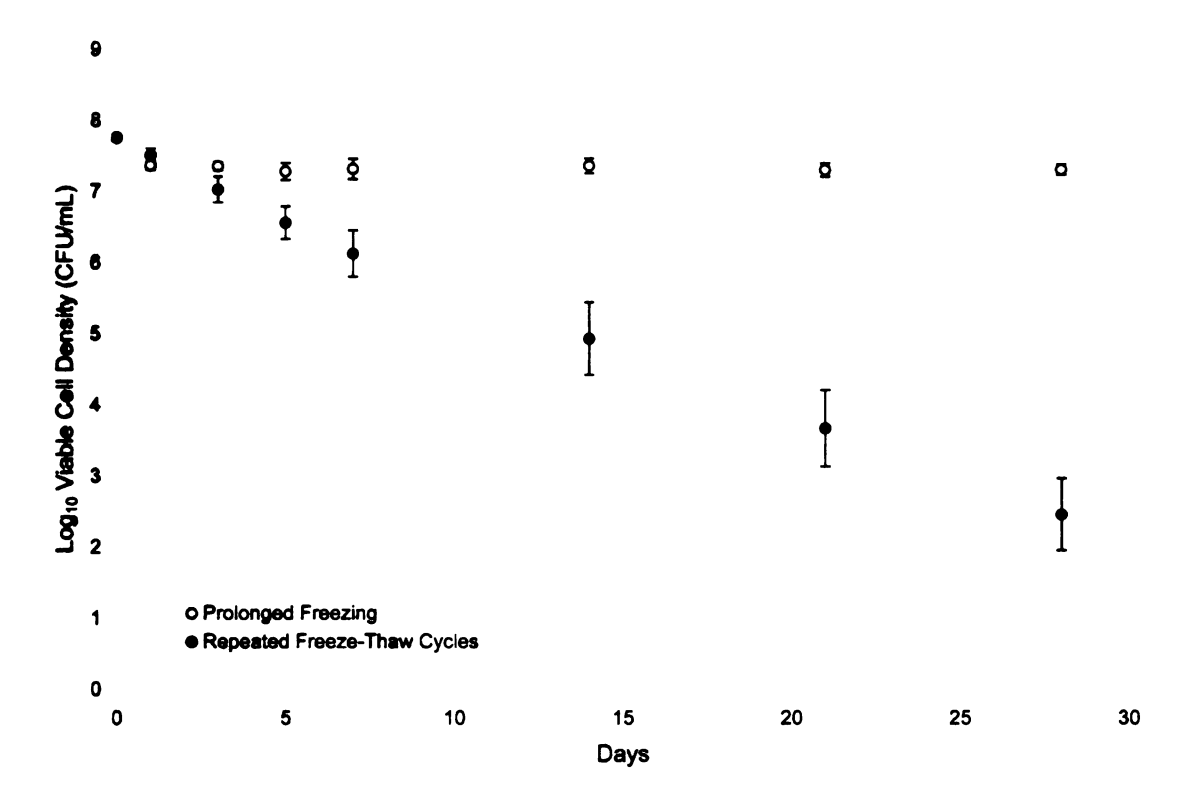


**Figure 1. Survival of ancestral** *E. coli* **strain under the freeze-only (prolonged freezing) and repeated freeze-thaw cycle regimes.** Each point is the log<sub>10</sub>-transformed viable cell density (CFU/mL) averaged over six replicates. Closed circles show the repeated freeze-thaw regime, and open circles show the prolonged freeze-only regime. Error bars are 95% confidence intervals and, when not visible, are smaller than the corresponding symbol.

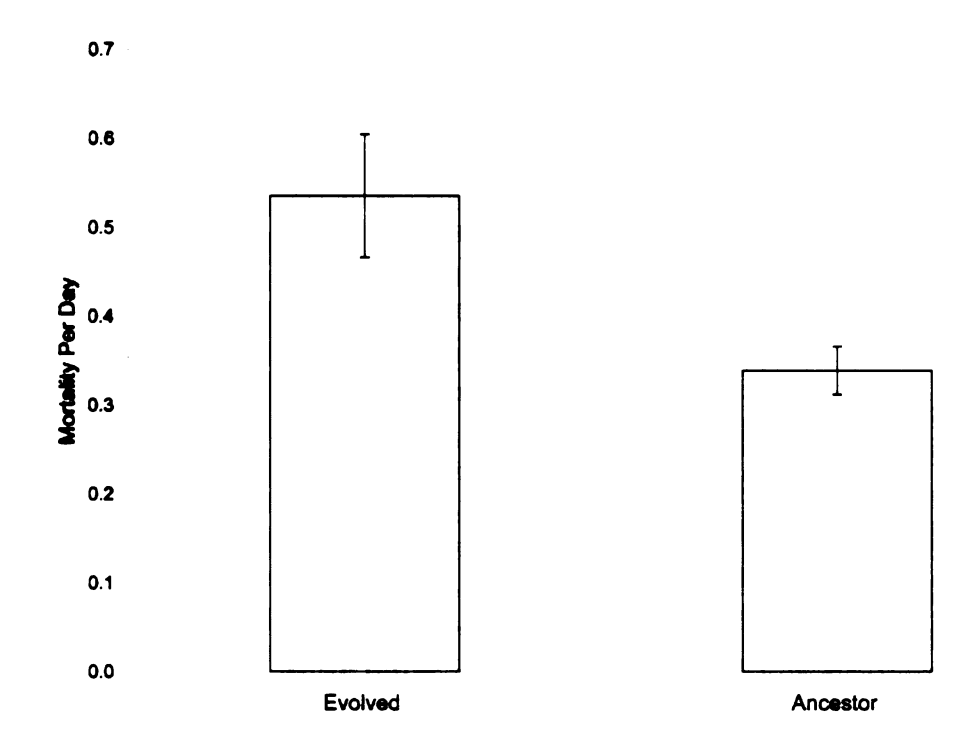
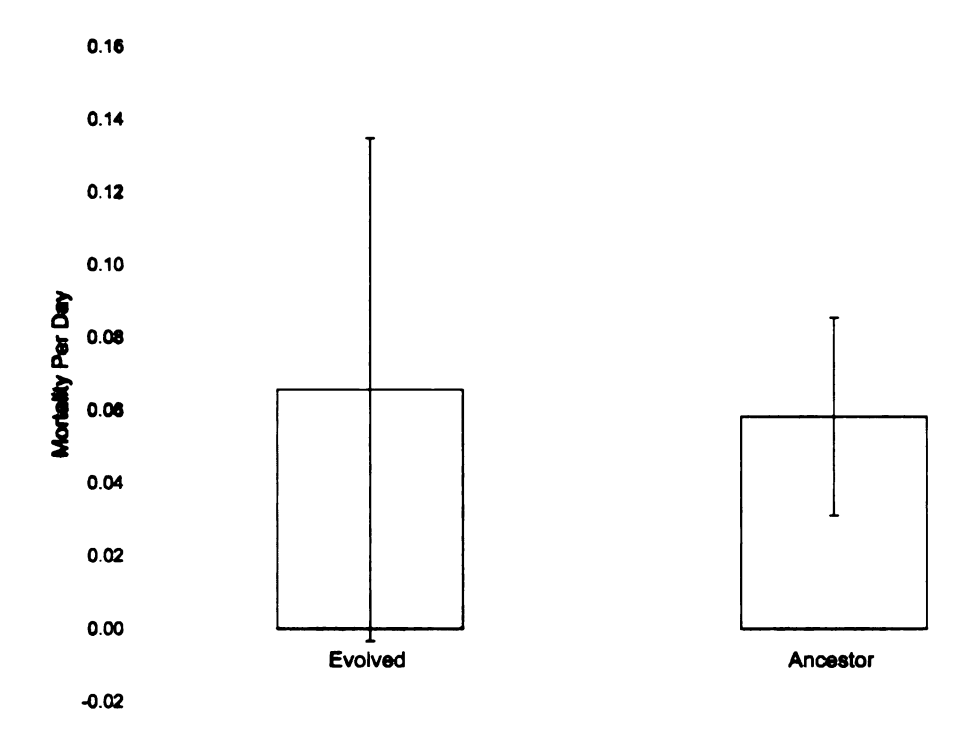


Figure 2. Comparison of mortality rates between the evolved *E. coli* and their ancestor under the repeated freeze-thaw regime. The height of each bar shows the mean mortality rate per day for the evolved lines or their ancestor, measured over ten daily freeze-thaw cycles. For the evolved bacteria, the mean is calculated over all 12 lines, with three assays for each line. For the ancestor, the mean is calculated over two marked variants (Ara<sup>+</sup> and Ara<sup>-</sup>), again with three assays for each one. See the Materials and Methods section for the mortality rate calculation. Error bars are 95% confidence intervals based on the number of lines (evolved) or total assays (ancestor).



**Figure 3.** Comparison of mortality rates between the evolved *E. coli* and their ancestor under the prolonged freeze-only regime. The height of each bar shows the mean mortality rate per day for the evolved lines or their ancestor, measured over ten days at -80°C. For the evolved bacteria, the mean is calculated over all 12 lines, with three assays for each line. For the ancestor, the mean is calculated over two marked variants (Ara<sup>+</sup> and Ara<sup>-</sup>), with three assays for each one. See the Materials and Methods section for the mortality rate calculation, which includes an adjustment for the mortality caused by thawing in the final day. Error bars are 95% confidence intervals based on the number of lines (evolved) or total assays (ancestor).

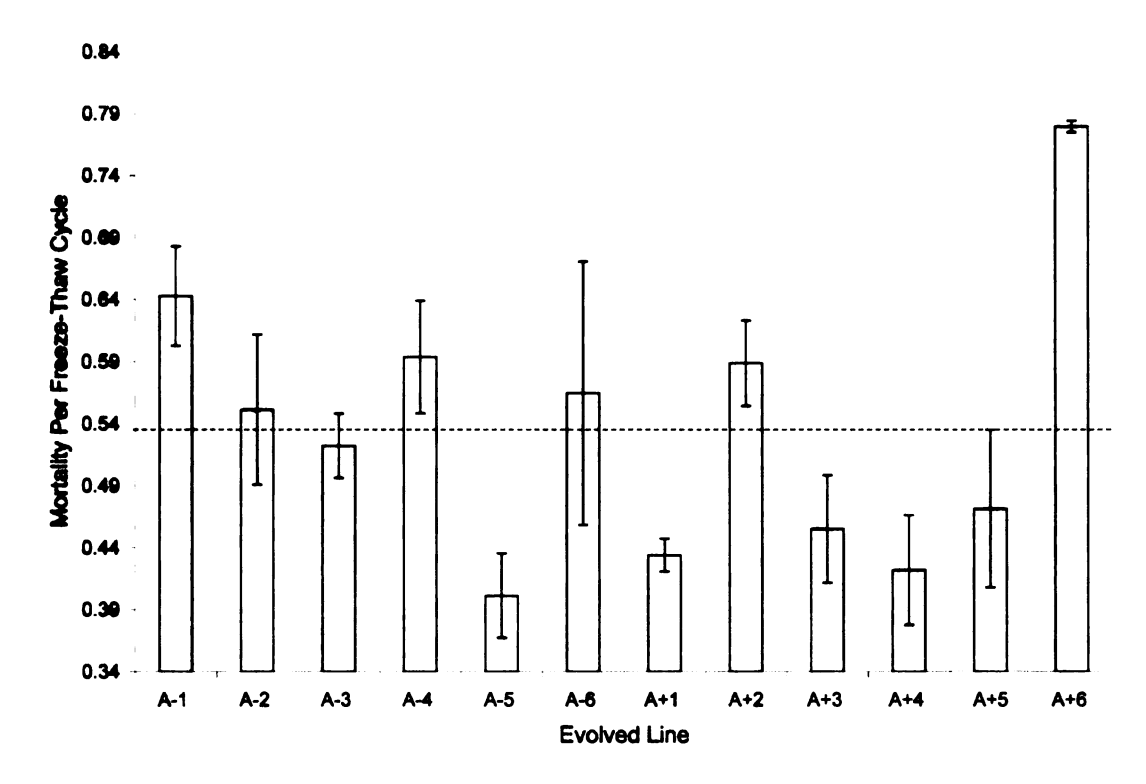
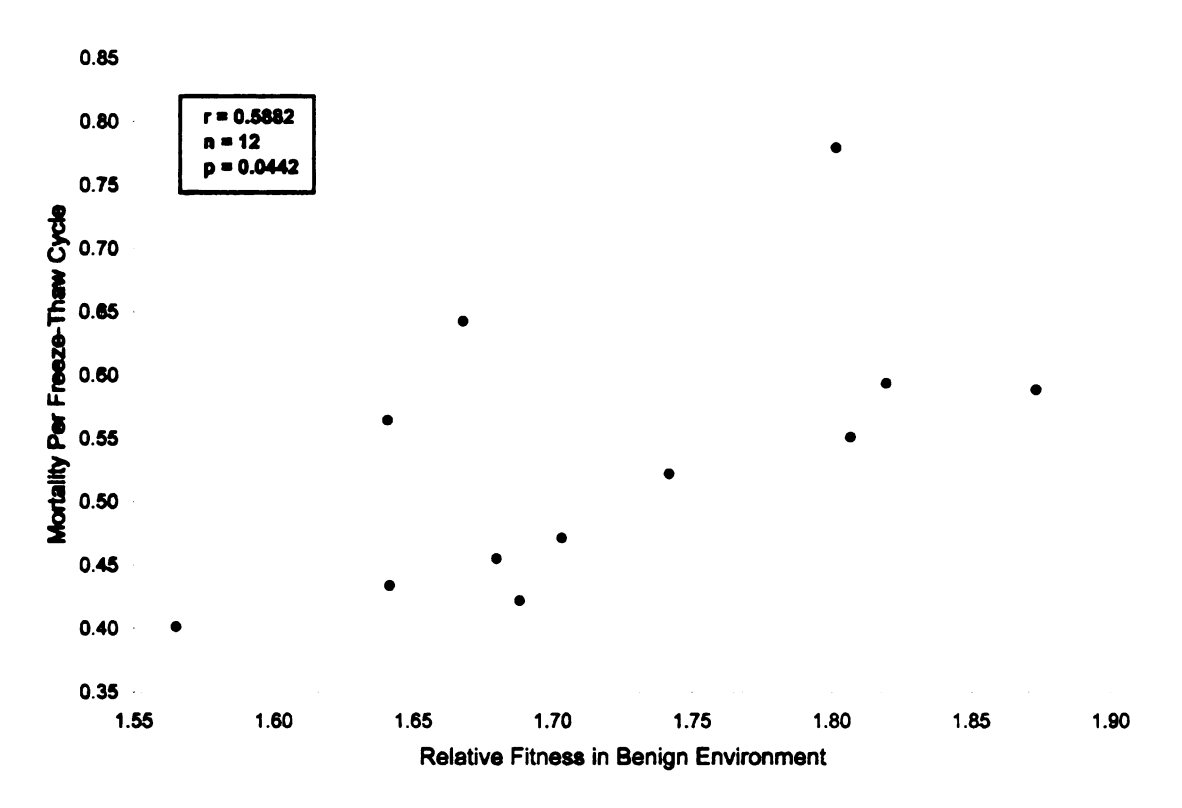


Figure 4. Heterogeneity of mortality rates among the 12 evolved lines under the repeated freeze-thaw regime. The height of each bar shows the mean mortality rate per day for one of the evolved lines, measured over ten daily freeze-thaw cycles, calculated from three assays for each line. The x-axis value (34%) is the estimated mortality rate of the ancestor; the dashed line shows the average mortality rate for the 12 evolved lines. Error bars are 95% confidence intervals calculated using the replicate assays for each line. See Table 1 for the statistical analysis testing for variation among the evolved lines.



**Figure 5. Correlation between freeze-thaw mortality and fitness in the benign environment.** Each point shows the mortality rate per freeze-thaw cycle measured in this study, and the relative fitness measured previously (Cooper and Lenski 2000) in the benign environment, for one of the 12 evolved lines.

#### **TABLES**

Source	df	SS	MS	F	р
Line	11	0.3906	0.03551	88.67	< 0.0001
Error	24	0.0096	0.00040		

Table 1. ANOVA testing for heterogeneity among the evolved lines in mortality rates under the repeated freeze-thaw regime. Mortality rates were estimated with three-fold replication for each of the 12 evolved lines. The very low p-value indicates significant heritable variation among these lines in their survival capacity under the freeze-thaw regime.

Source	df	SS	MS	F	р
Line	11	0.1912	0.01738	22.06	< 0.0001
Error	24	0.0189	0.00079		

Table 2. ANOVA testing for heterogeneity among the evolved lines in mortality rates under the prolonged freezing regime. Mortality rates were estimated with three-fold replication for each of the 12 evolved lines. The very low p-value indicates significant heritable variation among these lines in their survival capacity under the prolonged freezing regime.

#### CHAPTER 2

## ADAPTATION TO CYCLES OF FREEZING, THAWING, AND GROWTH: PHENOTYPIC EVOLUTION

Physiological and Biochemical Zoology 2007, in press.

#### **ABSTRACT**

Fifteen populations of Escherichia coli were propagated for 150 freezethaw-growth (FTG) cycles in order to study the phenotypic and genetic changes that evolve under these stressful conditions. Here, we present the phenotypic differences between the evolved lines and their progenitors as measured by competition experiments as well as growth curves. Three FTG lines evolved from an ancestral strain that was previously used to start a long-term evolution experiment, while the other twelve FTG lines are derived from clones that had previously evolved for 20,000 generations at constant 37°C. Competition experiments indicate that the former FTG group improved their mean fitness under the FTG regime by about 90% relative to their progenitor, while the latter FTG group gained on average about 60% relative to their own progenitors. These increases in fitness result from both improved survival during freezing and thawing and more rapid recovery to initiate exponential growth after thawing. This shorter lag phase is specific to recovery after freezing and thawing. Future work will seek to identify the mutations responsible for evolutionary adaptation to the FTG environment, and use them to explore the physiological mechanisms that allow increased survival and more rapid recovery.

#### **BACKGROUND**

Most physiological and genetic studies of adaptation to stressful environments focus on the proximate mechanisms that promote survival and growth. By contrast, research on the evolutionary adaptation of organisms to stressful environments examines how new stress responses evolve, or existing stress responses are reshaped, by selection. One immediate question is whether a population can survive the stress and persist on an evolutionary timescale, or whether it will go extinct, and many factors influence this outcome: the frequency of stress conditions, the conditions for growth between bouts of stress, and so on. Assuming that a population survives, then there exists the potential for evolutionary changes that improve survival and recovery under the same or similar stresses in the future.

The direct study of evolutionary changes can be accomplished by observing populations of bacteria or other organisms with suitably short generations while they are propagated in controlled and reproducible laboratory environments (Rose 1984; Lenski et al. 1991; Bennett et al. 1992; Bennett and Lenski 1999; Wichman et al. 1999, 2000; Elena and Lenski 2003; Lenski 2004; Riehle et al. 2005; Chippindale 2006; Herring et al. 2006; Leu and Murray 2006; Schoustra et al. 2006; Zeyl 2006). Advantages of using bacteria in experimental evolution include their rapid generations and large populations, as well the capabilities of establishing replicate populations from the same ancestral clone and reviving ancestral and derived cells stored at different times in an experiment. Also, bacteria reproduce asexually, and thus stable genetic markers

can be used to distinguish ancestral from derived genotypes during competition experiments to measure their relative fitness. Moreover, a wealth of genetic, biochemical, and physiological information exists for model species, including *Escherichia coli*, that can enrich and inform analyses built around evolution experiments.

In a long-term evolution experiment, Lenski and colleagues have studied the dynamics of phenotypic and genomic evolution in twelve initially identical populations of E. coli while they were propagated on a glucose-supplemented minimal medium at 37°C for more than 20,000 generations (Lenski et al. 1991; Lenski and Travisano 1994; Cooper and Lenski 2000; Rozen and Lenski 2000; Schneider et al. 2000; Cooper et al. 2003; Lenski et al. 2003; Pelosi et al. 2006; Woods et al. 2006). Bennett and colleagues performed related experiments in which bacteria derived from this long-term study were used to found several sets of new populations that continued to evolve in the same medium but under different thermal regimes, including constant lower and higher temperatures as well as in temporally fluctuating environments (Bennett et al. 1992; Lenski and Bennett 1993; Leroi et al. 1994; Travisano et al. 1995; Mongold et al. 1996, 1999; Bennett and Lenski 1999; Cullum et al. 2001; Riehle et al. 2001, 2003, 2005). The latter studies have shown adaptation that is often temperature specific, with frequent but not universal tradeoffs in performance at other temperatures. There is evidence from these studies, as well as others, to suggest that rates of evolutionary adaptation to stressful environments may often exceed corresponding rates in non-stressful environments (Parsons 1987; Hoffman and

Parsons 1993; Lenski and Bennett 1993; Bennett and Lenski 1997; Rutherford and Lindquist 1998; Queitsch et al. 2002).

In this study, we examine the evolutionary adaptation of *E. coli* populations to a regime of alternating days of freezing without added cryoprotectant at -80°C and thawing at room temperature, followed by growth at the benign temperature of 37°C. In preliminary work we found that repeated freeze-thaw (FT) cycles cause mortality such that, without intervening opportunities for growth, populations go extinct. Therefore, the opportunity for growth every other day allows populations to recover and multiply, including the generation of new mutations that might allow improved survival during or faster recovery following FT cycles. Our aims here are to report the basic experimental design, provide evidence for adaptation to this regime, and determine whether adaptation occurs by improved survival, faster recovery, or both. Also, our study shows how evolutionary history can influence evolutionary changes because the populations were founded by strains that had different histories prior to this experiment. We will conclude by outlining our future plans to identify the genetic and physiological bases of the adaptations reported here.

Before turning to this evolution experiment, we now provide a brief overview of bacteria in nature that experience freezing and thawing conditions, their physiological responses to freezing and thawing, and a preliminary experiment that we performed to identify the conditions for our evolution experiment. Many different bacterial species live in environments subject to freezing and thawing, including Siberian permafrost (Rivkina et al. 2000), Arctic

tundra (Eriksson et al. 2001), and Antarctic ponds (Mountfort et al. 2003). Some of these bacteria live as parts of mat communities that include diatoms and green algae as well as cyanobacteria. Metabolic activity and growth have been reported for some permafrost bacteria at temperatures as low as -10°C (Bakermans et al. 2003). Comparative evidence suggests that evolutionary adaptation to these freeze-thaw environments has involved changes in coldshock or cold-active proteins (Cloutier et al. 1992; Hebraud and Potier 1999; Siddiqui and Cavicchioli 2006), membrane fluidity (Russell 1990; Hebraud and Potier 1999, Ponder et al. 2005), and enzymes that inhibit or promote ice nucleation (Muryoi et al. 2004; Walker et al. 2006). In general, however, little is known about the time scale over which such changes have occurred, the number of mutations needed to allow survival starting from a freeze-thaw sensitive progenitor, whether survival during freezing or recovery upon thawing is the more important target of selection, and other such issues that can be explored by experimental evolution.

Freezing and thawing are multi-faceted stresses that involve not only low temperature but also potentially lethal intracellular ice formation and dehydration resulting from hyperosmotic shock (Mazur 1984; Gao and Crister 2000). Also, freezing and thawing cause oxidative damage (Cox and Heckly 1973) and can thus be mutagenic (Grecz et al. 1980; Calcott and Gargett 1981). In the face of all these potentially damaging effects, many bacteria nonetheless can protect themselves or otherwise recover under the right circumstances (Calcott 1985). Several variables have been shown to affect whether bacteria can survive

freezing and thawing, including nutritional status, growth phase, and cooling rate (Calcott 1985; Gao and Crister 2000). For example, bacteria harvested in stationary phase survive freezing and thawing much better than those harvested during exponential growth (Souzu 1989). Furthermore, pre-exposure to cold, osmotic, and other stresses can increase subsequent FT survival, presumably owing to changes in levels of particular proteins or other cell components that provide cross-tolerance (Drouin et al. 2000; Thammavongs et al. 1996; Panoff et al. 2000).

Various approaches could be pursued to investigate the molecular genetic basis of FT tolerance. The traditional genetic approach screens sets of insertion mutants to identify those that are deficient in FT survival, but not in their ability to grow under permissive conditions, presumably owing to knock-outs of genes whose products are specifically required for FT survival or recovery. Analyses of changes in mRNA and protein levels might allow the identification of other genes whose expression levels are altered during freezing, thawing, or subsequent recovery. An evolutionary approach, such as the one we have pursued, differs because it allows the study of improvements in the stress response, and not just the basis of the tolerance as it presently exists in a particular strain or species. Indeed, there may be many different types of evolutionary adaptations that could improve FT survival and recovery, some of which might involve genes other than those already known to be important for this stress response. By studying the evolution of multiple experimental lines, including ones started with different ancestral strains, one can observe the uniformity or diversity of responses to any

given stress. Also, the use of a mesophilic organism such as *E. coli*, instead of a psychrophilic species that is already cold-adapted, may increase the opportunity to see new evolutionary adaptations to FT conditions on an experimental timescale. In a previous study by another group, *Lactobacillus delbrueckii* were found to evolve greater FT tolerance after serial propagation in milk with intermittent freezing and thawing (Monnet et al. 2003).

We performed a pilot experiment to isolate cryotolerant mutants of E. coli that could better survive repeated freezing and thawing. The ancestor of the long-term experimental populations was subjected to daily FT cycles without added nutrients, but no viable cells remained after 40 days. Therefore, for this study we introduced a growth phase after the FT cycle to allow populations to recover and, potentially, to evolve. Elsewhere, we have also reported that 12 populations of E. coli that evolved in a minimal salts medium with glucose at 37°C for 20,000 generations all became more sensitive to repeated FT cycles than their ancestor, although the extent of this change varied among the derived lines (Sleight et al. 2006). These findings demonstrate genetic variation in FT tolerance, and they also indicate that some of the mutations responsible for improved fitness in that warm environment are detrimental under FT conditions. Also, because these lineages are pre-adapted to the growth conditions at 37°C, they are interesting progenitors to start an evolution experiment under the FTG regime. We can compare the adaptation to the FTG regime of the 37°C-evolved lines and their progenitors, with our a priori expectations that the 37°C-evolved

lines have more scope for improvement with respect to FT cycles but less opportunity to improve further during the growth phase.

#### MATERIALS AND METHODS

## Culture media and experimental pre-conditioning

The bacterial clones used in our experiments, including those evolved in our experiment as well as their progenitors, are kept in long-term storage at -80°C with glycerol added as a cryoprotectant. However, in the FTG evolution experiment and in our assays of FT survival and relative fitness under the FTG regime, we used medium without added glycerol in order to investigate the evolution of changes in survival and recovery. To ensure that cells were in comparable physiological states at the start of assays of FT survival and competitive fitness, cells were removed from the freezer; inoculated into LB (Luria-Bertani) medium independently for each replicate assay and incubated at 37°C for 24 h; then diluted 10,000-fold into Davis minimal medium supplemented with glucose at 25 mg/L (DM25) and incubated at 37°C again for 24 h, at which point these cells were used to start all assays.

### Long-term evolution experiment and bacterial strains

The long-term evolution experiment at constant 37°C is described in detail elsewhere (Lenski et al. 1991; Lenski 2004). In brief, 12 replicate populations evolved for 20,000 generations (3,000 days) starting from two variants of the same ancestral strain of *E. coli* B. One variant (REL606) cannot grow on arabinose, while the other (REL607) is a spontaneous Ara<sup>+</sup> mutant; six

populations were founded from each type. The Ara marker is neutral in the long-term experimental environment (Lenski et al. 1991), which consists of daily 1:100 transfers into flasks that contain DM25 and incubation with shaking at 37°C. The dilution and subsequent re-growth allow about 6.6 (= log<sub>2</sub> 100) generations per day.

## Freeze-thaw-growth evolution experiment

Figure 6 gives an overview of our freeze-thaw-growth (FTG) evolution experiment. The 15 FTG populations include three replicates, designated group A, founded by the Ara<sup>+</sup> variant of the original ancestor, and twelve populations founded by clones sampled from each of the long-term populations at generation 20,000, designated group B. These 15 populations evolved for 150 two-day FTG cycles, which equals some 1,000 generations based on the 100-fold dilution and re-growth in alternating days; in fact, somewhat more generations occurred because additional cell growth also offset death during the freeze-thaw cycle in alternating days. To start the evolution experiment, 1 mL of stationary-phase DM25 culture was transferred into a freezer tube and put in a -80°C freezer for 22.5 h. The tubes were then thawed at room temperature (~22°C) for 1.5 h, after which time the contents were diluted 1:100 into fresh DM25 and incubated at 37°C without shaking for 24 h. The use of unshaken tubes, rather than shaken flasks, during the growth phase represents a small departure from the methods used in the long-term evolution experiment. This change allowed us to handle more cultures simultaneously. Any effect on oxygen levels is small, owing to the low sugar concentration used in our experiments and the resulting low population density (about  $3-5 \times 10^7$  cells per mL in stationary phase, roughly two orders of magnitude below the density in most research with *E. coli*). In a previous study, there was no discernible difference in relative fitness between shaken flasks and unshaken tubes under conditions similar to those used in our study (Travisano 1997).

Thus, the populations in our evolution experiment experienced cycles of a day of freezing and thawing that alternated with a day in which they grew in the same medium and at the same temperature as in the long-term evolution experiment. Populations and clones were sampled and stored every 100 generations (30 days) in freezer vials with glycerol for future study. During the long-term evolution experiment at 37°C, unique mutations were substituted at certain loci in each population (Woods et al. 2006); we have confirmed by sequencing the presence of at least one such mutation in each group B line, which demonstrates they were all derived from their intended progenitors (S. C. Sleight and R. E. Lenski, unpublished data).

# FTG competition experiments

We performed competitions to measure the extent of evolutionary adaptation of the FTG-evolved lines relative to their progenitors. Competitions were performed in the exact same environment as used in the FTG evolution experiment. For group A, the FTG-evolved lines competed directly against the ancestor with the opposite Ara-marker state. For group B, the FTG-evolved lines and their 37°C-evolved progenitors each competed separately against the original ancestor bearing the opposite marker state.

The densities of two competitors were estimated by serially diluting cultures on tetrazolium-arabinose (TA) indicator plates, except for one FTG evolved line and its progenitor that form poor colonies on TA medium and whose densities were estimated from minimal glucose plates. Plates were incubated for 24 h at 37°C, and the resulting number of colony forming units was used to estimate the corresponding density. Ara<sup>+</sup> and Ara<sup>-</sup> cells form white and red colonies, respectively, when grown on TA plates. As a control for any effect of the Ara marker, the Ara<sup>+</sup> and Ara<sup>-</sup> ancestral variants also competed in each batch of competition experiments; the Ara marker is neutral in the FTG regime, as was previously shown under the growth conditions of the long-term experiment.

Prior to starting a competition, each competitor was separately conditioned as described previously. Equal volumes of each competitor were then mixed, and 1 mL was transferred into a tube and placed in a –80°C freezer. After 22.5 h, the tube was thawed at room temperature for 1.5 h. Then 0.1 mL was diluted into 9.9 mL of DM25 and incubated at 37°C for 24 h. Measurements of the densities of the competitors were taken at the start (before freezing), after thawing, and again after the growth phase that completes the full FTG cycle. From these data, we estimated the relative fitness of the two competitors over the course of the complete FTG cycle by using the initial and final samples, as described below. In addition, we partitioned the overall FTG fitness into two components that reflect FT survival and subsequent growth by using the middle sample, also as described below.

the single ancestor of group A where the mean was based on the replicate assays. Details of the statistical analyses are given below.

#### **Growth curves**

We obtained separate growth curves, based on optical density (OD), for the evolved clones and their progenitors in order to estimate the durations of their lag phase prior to commencing growth as well as their doubling times during the growth phase. These growth parameters were first calculated for each line by averaging nine replicate growth trajectories for that line. Group means were then calculated by averaging the estimates for each line in the group, except for the single ancestor of group A whose parameters were estimated directly from the nine replicates. OD measurements were made at the 420-nm wavelength on 0.2 mL cultures in 96-well microtiter plates incubated at 37°C. The data were collected following either a FT cycle or stationary phase at 37°C, with a comparison between the two curves permitting an estimate of the effect of the FT cycle on the time required to achieve exponential growth following dilution into fresh DM25 medium, as described below.

# Calculations of lag phase duration and doubling time

Calculations of the duration of lag phase used the general method given by Lenski et al. (1994) with modifications as described here. OD values from growth curve experiments were standardized by dividing by the initial OD (measured immediately after the FT cycle before dilution, and divided by 100 to take the dilution factor into account) and log<sub>2</sub>-transformed in order to express changes as doublings. The transformed data were then plotted and inspected to

identify the window of exponential growth, and linear regression was performed on those exponential-phase data. The doubling time was calculated as the inverse of the slope of the regression. The "apparent" lag phase was then estimated by extrapolating the exponential growth back in time until the regression intersected the initial OD measurement (Fig. 7). Note, however, that this apparent lag phase does not take into account any contribution of dead cells to OD, and so it over-estimates the actual duration of the lag phase. We corrected for this mortality by independently measuring the FT survival of the clone, then transforming the proportion surviving to a log<sub>2</sub> scale; that proportion is generally below one, and hence the value is negative on a log scale, with more negative values corresponding to higher mortality. As shown schematically in Figure 7, the log<sub>2</sub>-transformed survival value was plotted as a horizontal line on the graphs showing the exponential-phase growth data, where the intersection of this line with the extrapolated regression then provides an estimate of the actual duration of the physiological lag (i.e., the duration corrected for FT mortality).

## Statistical methods

We performed t-tests to compare performance measures between the FTG evolved lines and their progenitors. Paired tests were always used when comparing B group evolved lines with their progenitors, owing to their unique relationships. Paired tests were also used to compare the A group evolved lines with the common ancestor when the relevant assays for each evolved line were paired with particular assays for the ancestor. Otherwise, we used a t-test for comparing a single specimen, the ancestor, with a sample, the three evolved

identify the window of exponential growth, and linear regression was performed on those exponential-phase data. The doubling time was calculated as the inverse of the slope of the regression. The "apparent" lag phase was then estimated by extrapolating the exponential growth back in time until the regression intersected the initial OD measurement (Fig. 7). Note, however, that this apparent lag phase does not take into account any contribution of dead cells to OD, and so it over-estimates the actual duration of the lag phase. We corrected for this mortality by independently measuring the FT survival of the clone, then transforming the proportion surviving to a log<sub>2</sub> scale; that proportion is generally below one, and hence the value is negative on a log scale, with more negative values corresponding to higher mortality. As shown schematically in Figure 7, the log<sub>2</sub>-transformed survival value was plotted as a horizontal line on the graphs showing the exponential-phase growth data, where the intersection of this line with the extrapolated regression then provides an estimate of the actual duration of the physiological lag (i.e., the duration corrected for FT mortality).

#### Statistical methods

We performed t-tests to compare performance measures between the FTG evolved lines and their progenitors. Paired tests were always used when comparing B group evolved lines with their progenitors, owing to their unique relationships. Paired tests were also used to compare the A group evolved lines with the common ancestor when the relevant assays for each evolved line were paired with particular assays for the ancestor. Otherwise, we used a t-test for comparing a single specimen, the ancestor, with a sample, the three evolved

group A lines (Sokal and Rohlf 1981, pp. 229-231). This test assumes equal standard deviations for the distributions from which the single specimen and the sample are drawn; in fact, the ancestor, being a homogenous type, should have a lower standard deviation than the independently derived lines, which makes our inferences conservative. We used one-tailed tests for those hypotheses with clear a priori expectations about the direction of the outcome; otherwise, two-tailed tests were used conservatively, including those cases with potentially opposing effects. For example, we expect overall fitness and its components to increase for all FTG evolved lines when measured in the FTG environment. We also expect the lines in group B, which previously evolved in the same medium at 37°C and suffered correlated losses in FT survival, to show less improvement in growth rate, but greater gains in FT survival, than the lines in group A.

# Supporting data and supplementary analyses

Appendix 1, which can be found at the back of this dissertation, provides some supporting data and supplementary analyses relevant to this Chapter. All information pertaining to the Materials and Methods is included in the figure legend if not already described.

#### RESULTS

# **Evolutionary adaptation to the FTG regime**

Figure 8 shows that the lines evolved under the FTG regime improved in their overall fitness when measured under that same regime. The three lines in group A increased their fitness, on average, by 89% relative to the ancestral strain. The twelve lines in group B improved relative to their 37°C-evolved

progenitors by 60%, on average. Notice that the progenitors of group B were themselves much more fit than the common ancestor under the FTG regime; this result indicates that their improvements in growth during 20,000 generations at  $37^{\circ}$ C more than offset their losses in FT survival. The fitness gains in groups A and B relative to their own progenitors were both significant (one-tailed paired t-tests: group A, 2 df, p = 0.0034; group B, 11 df, p < 0.0001). Also, the proportional gains in group A, relative to their ancestor, were significantly greater than those observed in group B, relative to their progenitors, during the FTG evolution (two-tailed t-test with unequal variances, 13 df, p = 0.0417), although B had a final mean fitness that was significantly higher than A (two-tailed t-test with unequal variances, 13 df, p = 0.0003).

Figure 9 illustrates the extent of variation among the 15 evolved lines and their progenitors in overall fitness under the FTG regime. The three group A lines improved to a similar extent, and their fitness gains were all highly significant (p < 0.0001, based on one-tailed t-tests comparing six replicate assays for an evolved line and two assays for the ancestor that were paired with each evolved line). The group B lines showed much more variability, reflecting differences in their progenitors' fitness as well as their subsequent gains. Eleven of the B lines improved significantly (all p < 0.05, based on one-tailed t-tests comparing six replicate assays for each evolved line with six replicate assays for its own progenitor), while the gain in line A+5 was not significant. The A+5 progenitor had the highest FT survival of all group B progenitors; therefore, it had less scope to improve in this respect.

The fitness values for the B progenitors, which previously evolved at constant 37°C for 20,000 generations, vary by about two-fold under the FTG regime (Figure 9), whereas they vary much less, although significantly, in the benign environment where they evolved (Lenski et al. 1991; Lenski and Travisano 1994; Cooper and Lenski 2000). There is no significant correlation between the FTG fitness values measured here and the fitness values measured previously, on the same generational samples (Cooper and Lenski 2000), in that benign environment (r = -0.1673, 10 df, two-tailed p = 0.6033). Although the medium per se is the same, the ancestral and FTG environments are so dissimilar overall that performance in one does not predict performance in the other. However, we recently showed that, while all the B progenitors have greater sensitivity to FT mortality than the common ancestor, the extent of their increased sensitivity was significantly correlated with their fitness gains in the benign environment (Sleight et al. 2006). Thus, prior adaptation by the B progenitors reduced the scope for adaptation to the growth period of the FTG regime, while increasing potential adaptation to the FT treatment.

The overall adaptation to the FTG regime can be partitioned into improvements in FT survival and subsequent growth performance. Figure 10A shows the changes in FT survival (see also supplementary information in Appendix 1, Figure A1.1, for changes in FT survival between individual FTG evolved lines and their progenitors). Both group A and group B lines survived freezing and thawing better than their progenitors (one-tailed paired t-tests: group A, 2 df, p = 0.0014; group B, 11 df, p = 0.0023). The improvement in survival

was significantly greater in group B than in group A (one-tailed t-test with unequal variances, 13 df, p = 0.0432), as expected given the higher initial mortality in B progenitors. The resulting final survival values did not differ significantly between groups A and B (two-tailed t-test with unequal variances, 13 df, p = 0.3691).

As an aside, repeated FT survival to 10 FT cycles was also measured between all FTG evolved lines and their progenitors (see Appendix 1, Figure A1.2). Note that repeated FT survival is shown on a different scale as that in Figure 10A, which is only survival after one FT cycle measured in competition with the ancestor, to compare against previous repeated FT survival measurements (Figures 2 and 4). Figure A1.3 in Appendix 1 shows the mean repeated FT survival differences between the evolved groups and their progenitors. On average, Evolved Group A experienced 6% less mortality per FT cycle (one-tailed t-test p = 0.0652) and Evolved Group B improved by 14% in this respect (one-tailed t-test p > 0.0001). Repeated FT survival of the ancestor is about the same as Evolved Group B on average. Thus, the 12 long-term lines that evolved for 20,000 generations in a benign environment overcame their repeated FT sensitivity relative to the ancestor (Sleight et al. 2006) by evolution in a FTG regime.

Figure 10B shows the corresponding changes in growth performance after a FT cycle and dilution into fresh medium (see Appendix 1, Figure A1.4, for changes in growth after FT measurements between individual FTG evolved lines and their progenitors). Both groups underwent significant improvement (one-tailed paired t-tests: group A, 2 df, p = 0.0042; group B, 11 df, p < 0.0001). The

proportional gain in growth performance was greater for group A than for group B (one-tailed t-test with unequal variances, 13 df, p = 0.0056), as expected given the higher initial level for the group B progenitors. However, the final growth performance was still higher in B than in A (two-tailed t-test with unequal variances, 13 df, p = 0.0001).

The fact that group B lines showed such large improvements in their growth performance in the second day of the FTG cycle, despite their progenitors having evolved at 37°C for 20,000 generations, may be surprising at first glance. However, when we performed one-day competitions in the same medium, without a FT cycle, the evolved group B lines did not show any improvement in growth performance (S. C. Sleight and R. E. Lenski, unpublished data). As we will show in the next section, their improvement comes not from faster rates of exponential growth, but instead they evolved faster recovery of their growth capacity following the FT treatment.

# Changes in growth dynamics including the duration of lag phase

Figure 11 shows the growth dynamics, based on optical density, for both FTG-evolved groups and their progenitors under two slightly different conditions. In Figure 11A, the growth data correspond precisely to day 2 of the FTG regime, with cells having been frozen and thawed prior to their dilution into fresh medium at 37°C. In Figure 11B, the populations were started from stationary-phase cultures grown at 37°C without the intervening FT cycle.

Several interesting features are apparent from the growth dynamics following the FT cycle (Fig. 11A). First, notice that both evolved groups (grey

curves) increase much sooner than their respective progenitors (black curves). Second, the group B evolved lines (solid grey curve) perform better, on average, than the group A lines (dashed grey curve), although the difference is much less than between their progenitors (solid black and dashed black curves, respectively). Third, the improvement in group A (dashed grey curve) relative to its ancestor (dashed black curve) appears to involve both earlier and faster growth.

Now compare these dynamics with those observed without the intervening FT treatment (Fig. 11B). First, notice that all four growth trajectories now rise earlier than before. These differences imply that some portion of the lags after the FT treatment reflect demographic recovery, physiological recovery, or both from that stress. Second, the trajectories for the group B lines and their progenitors (solid grey and solid black curves, respectively) are almost perfectly superimposed. This similarity, in contrast to the difference seen after the FT treatment, implies that the group B lines have adapted by accelerating their recovery from the stress. Third, the trajectories for group A and the ancestor (dashed grey and dashed black curves, respectively) are much closer to than they were following the FT treatment. The remaining difference between them appears to reflect faster growth by the evolved A lines, rather than a shorter lag phase. After quantifying these differences, we will turn in the next section to more intensive experiments to disentangle the roles of demographic and physiological recovery from the FT treatment.

For each FTG-evolved line and its progenitor, we calculated its doubling time during exponential-phase growth and the "apparent" lag duration (without adjusting for FT mortality), as described in the Materials and Methods section. Considering first the growth trajectories after the FT treatment (Fig. 11A), group A lines evolved much faster exponential growth rates, with their mean doubling time almost 13 minutes shorter than the ancestor (one-tailed p = 0.0075 using a t-test for comparing a single specimen, the ancestor, with the three evolved group A lines). The group A lines also dramatically shortened the mean duration of the apparent lag phase by 153 minutes relative to their ancestor (one-tailed p = 0.0066, same test as above). By contrast, the group B lines, on average, did not evolve faster exponential growth than their progenitors, with the trend slightly in the opposite direction (p > 0.5). However, the B lines also evolved a much faster transition into exponential growth, with the average duration of the apparent lag phased reduced by about 105 minutes (one-tailed paired t-test, 11 df, p = 0.0001).

Without the preceding FT cycle (Fig. 11B), group A lines again showed faster exponential growth rates relative to their progenitors, with the average reduction in doubling time estimated to be about 9 minutes from these data (one-tailed p = 0.0058 using a t-test for comparing a single specimen with a group). However, the A lines did not evolve any shorter lag phase under this treatment, with the observed trend in the opposite direction (p > 0.5). Relative to their immediate progenitors, the group B lines did not improve, on average, in either their doubling time (one-tailed paired t-test, 11 df, p = 0.3007) or the duration of

the lag phase prior to growth, which trended very slightly in the opposing direction (p > 0.5).

# Demographic and physiological contributions to shorter lag phases

The data in the previous section clearly show that the FTG-evolved bacteria evolved much shorter apparent lag phases, and that these changes were specific to the FT treatment. However, these reductions in apparent lag phase do not distinguish between reduced cell death, such that population growth recommenced from a higher level after the FT treatment, and faster physiological recovery of surviving cells. To distinguish between these two effects, one must adjust the apparent lag phase by taking into account mortality during the FT treatment. Recall Figure 7, which shows schematically how the actual duration of the physiological lag phase is corrected for this FT mortality. Whereas the apparent lag is calculated by extrapolating exponential growth back to the initial optical density, which includes both living and dead cells, the actual lag is calculated by extrapolating back to the density of surviving cells only.

To address this issue, we performed more intensive experiments, including growth trajectories and FT survival assays, for single representatives of each evolved group and their progenitors. For group A, we used the middle of the three evolved lines and the common ancestor; for group B, we used the evolved line designated as A+1 and its progenitor (Fig. 9). Figure 12A shows the estimation of the duration of the physiological lag for that group A evolved line and its ancestor. The ancestor (black symbols) had an apparent lag of 324 minutes, while the apparent lag for the evolved line (grey symbols) was only 155

minutes, with the difference being 169 minutes. The physiological lags, adjusted for cell mortality, were 282 minutes for the ancestor and 135 minutes for the evolved line. Thus, the physiological lag was reduced by 147 minutes during the evolution of this FTG-adapted line. The other 22 minutes of the difference in the duration of the apparent lag reflects improved survival during the FT treatment.

Figure 12B shows the same analysis for the group B evolved line and its own immediate progenitor, which had evolved previously at 37°C for 20,000 generations. The apparent lag for this evolved line was 76 minutes, while that of its progenitor was 192 minutes, with the duration reduced during FTG-evolution by 116 minutes. After adjusting for mortality during freezing and thawing, the physiological lags estimated for the evolved line and its progenitor were 56 and 148 minutes, respectively, indicating that evolution had reduced the physiological lag by about 92 minutes in this group B line.

Figure 13 shows the calculation of lag durations for the same evolved lines and their progenitors, except in this case without a FT treatment prior to growth. There were no adjustments for death, which does not occur at any measurable rate under these conditions (Vasi et al. 1994). For both evolved lines and their progenitors, lag-phase durations were shorter than those seen after a FT treatment. Moreover, the differences between the FTG lines and their progenitors were much smaller and, in the group A case, the order was reversed. Without a FT treatment, the group A evolved line had a lag duration of 84 minutes, whereas that of the ancestor was only 52 minutes (Fig. 13A). Notice, too, that this group A line evolved faster exponential-phase growth, consistent

with the shorter doubling times reported earlier for its group. The group B line showed no improvement in exponential growth rate, as expected given its progenitor's prior evolution in the same medium and again consistent with earlier results (Fig. 13B). This group B progenitor experienced a lag of 34 minutes without a FT treatment, while its FTG-evolved derivative had a lag of 6 minutes. The resulting difference of 28 minutes is much less than the 92-minute difference in lag duration observed for the same B line and its progenitor after the FT treatment (Fig. 12B).

These experiments demonstrate that greater survival during the FT treatment and faster physiological recovery of growth capacity both contributed to the improved fitness of lines that evolved under the FTG regime. We obtained additional evidence for the evolution of faster physiological recovery in two subsidiary experiments. First, we obtained some population-growth trajectories by plating and counting cells, rather than by combining measurements of optical densities and cell survival (see Appendix 1, Figures A1.5-6). These experiments showed the faster recovery of growth in the same two evolved lines relative to their progenitors. Second, we performed fluorescence microscopy at multiple times after a FT cycle in order to visualize actively dividing cells (see Appendix 1, Figures A1.7-8). These observations revealed that cell division began much earlier in the FTG-evolved lines than in their progenitors, consistent with the evolution of faster physiological recovery of growth capacity following this stressful treatment.

#### DISCUSSION

We performed an experiment to investigate the evolutionary adaptation of 15 *E. coli* populations to 150 two-day cycles of freezing, thawing, and growth. No glycerol or other cryoprotective compound was added prior to freezing, unlike the standard method used to store bacteria. The entire experiment encompassed over 1,000 generations. Twelve of these freeze-thaw-growth (FTG) lines were founded by progenitors that had previously evolved for 20,000 generations in the same medium and at the same growth temperature of 37°C, except without the freeze-thaw (FT) treatment between reaching stationary phase and dilution in fresh medium (Fig. 6). The 37°C-evolved progenitors had higher growth rates than did the ancestor of the other three FTG lines, but these 37°C-evolved progenitors also suffered greater mortality during the FT treatment.

Almost all of the evolved lines showed large fitness gains in the FTG regime (Figs. 8 and 9). We identified three distinct fitness components that contributed to the improvement in overall performance. First, both groups of the evolved lines exhibited substantial improvement in FT survival, although the magnitude of improvement was greater for the group B lines, whose progenitors had evolved in the same medium at constant 37°C (Fig. 10A). During evolution in that benign environment, the progenitors became more sensitive to FT mortality (Sleight et al. 2006); hence, there was greater opportunity for better survival, which indeed occurred. However, these larger proportional gains in FT survival in Group B were not inevitable. The same mutations giving a fitness improvement in minimal glucose at 37°C could very well have not allowed for

compensatory mutations to increased FT survival. Second, the group A lines, whose progenitors had not experienced the same medium, evolved faster exponential-phase growth (Figs. 11-13). By contrast, the group B lines showed no measurable gains in their exponential growth (Figs. 11-13). Evidently, the B progenitors had largely exhausted the potential for faster exponential growth rate during their 20,000-generation history in the same culture medium.

Third, and perhaps most interesting, both groups showed striking improvement in the speed of their physiological recovery from FT stress. To demonstrate and quantify this third component of adaptation, we had to disentangle two confounding effects. One such factor is mortality during the FT cycle, which contributes to delayed recovery at the population level, but does not bear directly on the speed of recovery by surviving cells. We addressed this issue by independently measuring FT mortality, and using the data to calculate the physiological lag (Figs. 7, 12, and 13). The second complication arises because physiological lags occur following starvation, even without the FT treatment, upon dilution into fresh medium. Thus, one must distinguish between recovery from starvation and from freezing and thawing, which we did by measuring the duration of physiological lags following starvation with and without the intervening FT treatment (Figs. 11-13). Both groups of FTG-evolved lines showed much faster recovery of their surviving cells, with growth commencing an hour or more sooner than it did in their progenitors. This accelerated recovery provides a substantial head-start during the subsequent exponential growth. We also performed fluorescence microscopy on populations while they were

recovering from the FT treatment; these observations confirmed that many more viable cells were in the process of doubling for the FTG-evolved lines than for their progenitors during the early recovery period.

In addition to the differences in adaptation between the two groups of evolved lines, substantial variation also exists among lines in the same group, especially in the B group. The differences in adaptation between groups A and B reflect differences in their selective histories, but this explanation cannot explain the striking diversity among the B lines (Fig. 9), which shared the same original ancestor and the same two-stage history (Fig. 6). Evidently, the 12 lines in the B group have, by chance, accumulated different sets of mutations that cause the differences in their performance. At present, we do not know the identity of all those mutations. However, we can ask whether the variation among them reflects, at least in part, heterogeneity that was already present in their progenitors that diverged for 20,000 generations at constant 37°C. In fact, there is a significant positive correlation between the FTG fitness levels of the evolved B lines and their progenitors (r = 0.6769, 10 df, one-tailed p = 0.0079), indicating that some of the differential success among the diverse B lines reflects variation in the extent of pre-adaptation among their progenitors. However, it is also clear that most or all the B lines underwent substantial evolutionary adaptation during the FTG experiment (Figs. 8 and 9). With only one derived line from each progenitor, we cannot explicitly test whether the different B progenitors predisposed different final states (cf. Travisano et al. 1995). However, we might still examine this issue, in the future, by finding the mutations that contribute to

differences among the progenitors, finding other mutations responsible for adaptation during the FTG evolution experiment, and then systematically recombining these mutations from different lineages to ask whether the beneficial effects of the later mutations are conditional on or, alternatively, independent of the earlier mutations.

Many more experiments remain to be done, of course, and so we will close by discussing briefly our on-going research and future directions. In this study, we have demonstrated evolutionary adaptation to the FTG regime and we have partitioned the improvement into three distinct fitness components – survival, recovery, and growth – but we have not yet identified the physiological, biochemical, and genetic bases of the improvements in organismal performance. One can imagine approaching this general problem by beginning at a physiological scale and working down toward the genetic level, or vice versa. The approach that we are undertaking begins at the genetic level, which reflects our own expertise as well as the power of molecular genetic analyses in bacteria. Once we have found some of the mutations responsible for the improved performance of the FTG-evolved lines, we can then explore the resulting biochemical and physiological mechanisms. By having gene identities in hand, we can then target future studies to particular pathways based on the wealth of information that links the genetics, biochemistry and physiology of *E. coli* (Bock et al. 2006).

There are several different genetic approaches that one could pursue to find mutations substituted in experimental populations. These approaches

include DNA fingerprinting methods to find genes with new insertions or deletions (Papadopoulos et al. 1999; Schneider et al. 2000; Riehle et al. 2001); sequencing candidate genes based on specific phenotypic changes or other prior information (Notley-McRobb and Ferenci 2000; Cooper et al. 2001b; Crozat et al. 2005; Maharjan et al. 2006; Woods et al. 2006), analyzing changes in gene-expression profiles to suggest additional candidates (Cooper et al. 2003; Riehle et al. 2003; Pelosi et al. 2006); and even whole-genome sequencing (Shendure et al. 2005; Velicer et al. 2006; Herring et al. 2006).

Finding mutations, although certainly not trivial, is becoming much easier and less costly. But finding mutations is also only a first step in the genetic analysis. An extremely important subsequent step is to manipulate the affected gene, for example by constructing isogenic strains that differ by a single mutation (Cooper et al. 2001b, 2003; Crozat et al. 2005; Pelosi et al. 2006). Such work is possible using powerful molecular genetic approaches available in this system, but it is also painstaking and challenging work. Once such strains have been constructed, they can be competed to test whether a particular mutation did, in fact, contribute to the observed evolutionary adaptation or, alternatively, merely hitchhiked and was inconsequential to any gains in performance. Of course, the same strains can also be used to examine changes in biochemical and physiological traits, and the connections between genotype, phenotype, performance, and fitness can thus be elucidated.

There are many candidate biochemical and physiological pathways by which the FTG-evolved lines might have improved their FT survival as well as

their subsequent recovery and transition to growth. Some possibilities are as follows: altered induction of stress responses, including molecular chaperones; better repair of damage to DNA or other cell components; and regulatory or structural changes affecting membrane fluidity, osmosis, DNA supercoiling, and ribosomes or other components of the translational machinery. We are proceeding by a two-pronged approach. First, we have chosen a set of six candidate genes of interest given their known involvement in some of the relevant pathways, and these genes are being sequenced in the FTG-evolved lines and their progenitors. Second, we are performing a genomic-fingerprinting approach to look for insertions and deletions caused by the movement of IS insertion-sequence elements that are native to *E. coli* genomes (Papadopoulos et al. 1999; Schneider et al. 2000, 2002; Cooper et al. 2001b).

Without giving away the results of future papers, we have found two genes in which many FTG-evolved lines have substituted parallel mutations. Such parallelism is a hallmark of adaptive evolution (Wichman et al. 1999; Cooper et al. 2003; Woods et al. 2006). These genes and their products are in two different physiological pathways, one probably affecting membrane fluidity and the other encoding a stress response. We are presently attempting to construct isogenic strains that differ only by mutations in these genes. We will then use these strains to analyze the effects of the mutations on the relevant pathways, as well as on the demographic and physiological components of survival and recovery that produce the evolutionary adaptation to the FTG regime.

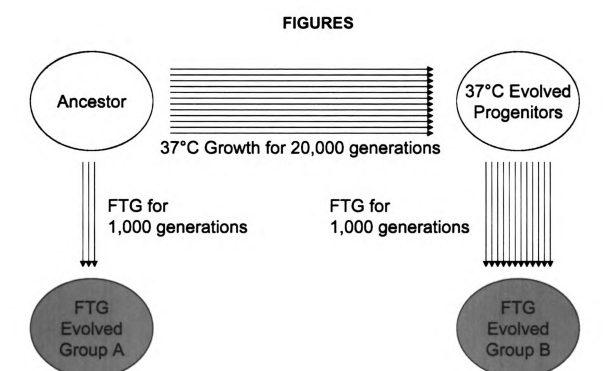


Figure 6. Evolutionary histories of freeze-thaw-growth (FTG) populations. Three lines in FTG-evolved group A were founded by the ancestor of another evolution experiment. Twelve lines in FTG-evolved group B were founded by clones sampled from populations that previously evolved for 20,000 generations at 37°C. All 15 of the FTG lines evolved for 1,000 generations under the FTG regime, with alternating days of a FT cycle and growth at 37°C. The culture medium used for growth days was the same one used during the evolution of the progenitors of FTG group B.

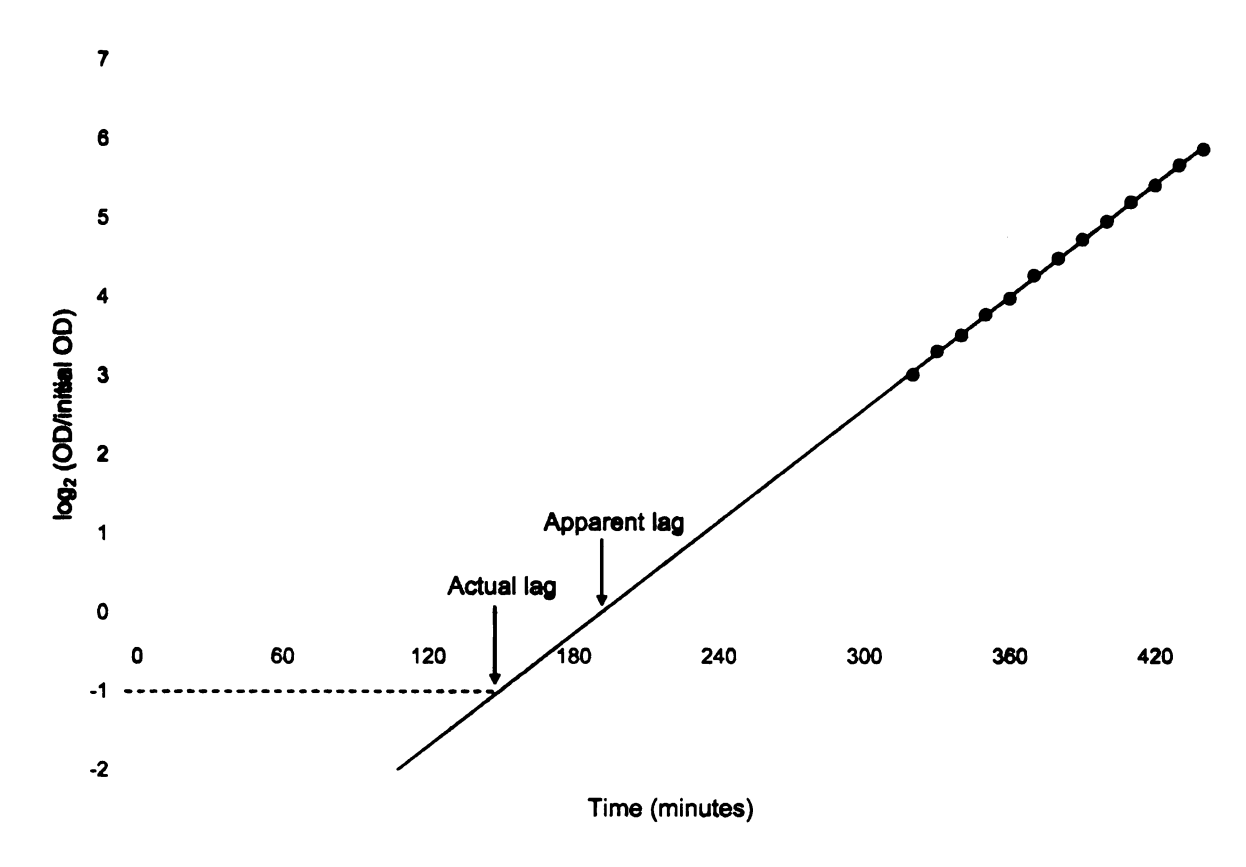


Figure 7. Schematic illustration showing how the apparent duration of lag phase is corrected for FT survival to calculate the actual duration of the physiological lag prior to growth. The apparent duration is calculated by extrapolating the regression line based on exponential growth back to the initial optical density. In this hypothetical example, 50% of the cells survived the FT treatment; therefore, the initial density of viable cells is half that implied by the initial optical density ( $\log_2 0.5 = -1$ ). The actual duration of the physiological lag is then obtained by extending the extrapolated growth trajectory until it intersects the initial density of viable cells.

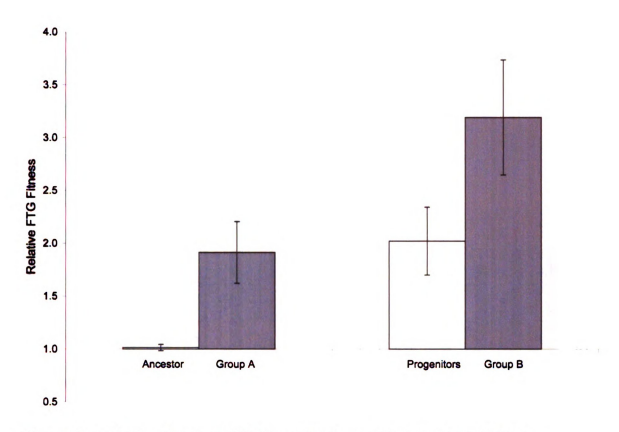


Figure 8. Relative fitness of FTG-evolved groups A and B and their progenitors over the two-day FTG cycle. For group A, each of the three evolved lines competed against the ancestor with the opposite Ara-marker state. For group B, each of the twelve evolved lines and their progenitors competed separately against the original ancestor with the opposite marker state. The mean value for each evolved group (grey) is adjacent to the corresponding mean for its progenitors (white). Means for each group were calculated from the average values for each member in the group, except for the single ancestor of group A where the mean is based on six independent measurements. Error bars are 95% confidence intervals based on the number of independently evolved lines, except for the ancestor, for which the interval is based on the six replicate assavs.

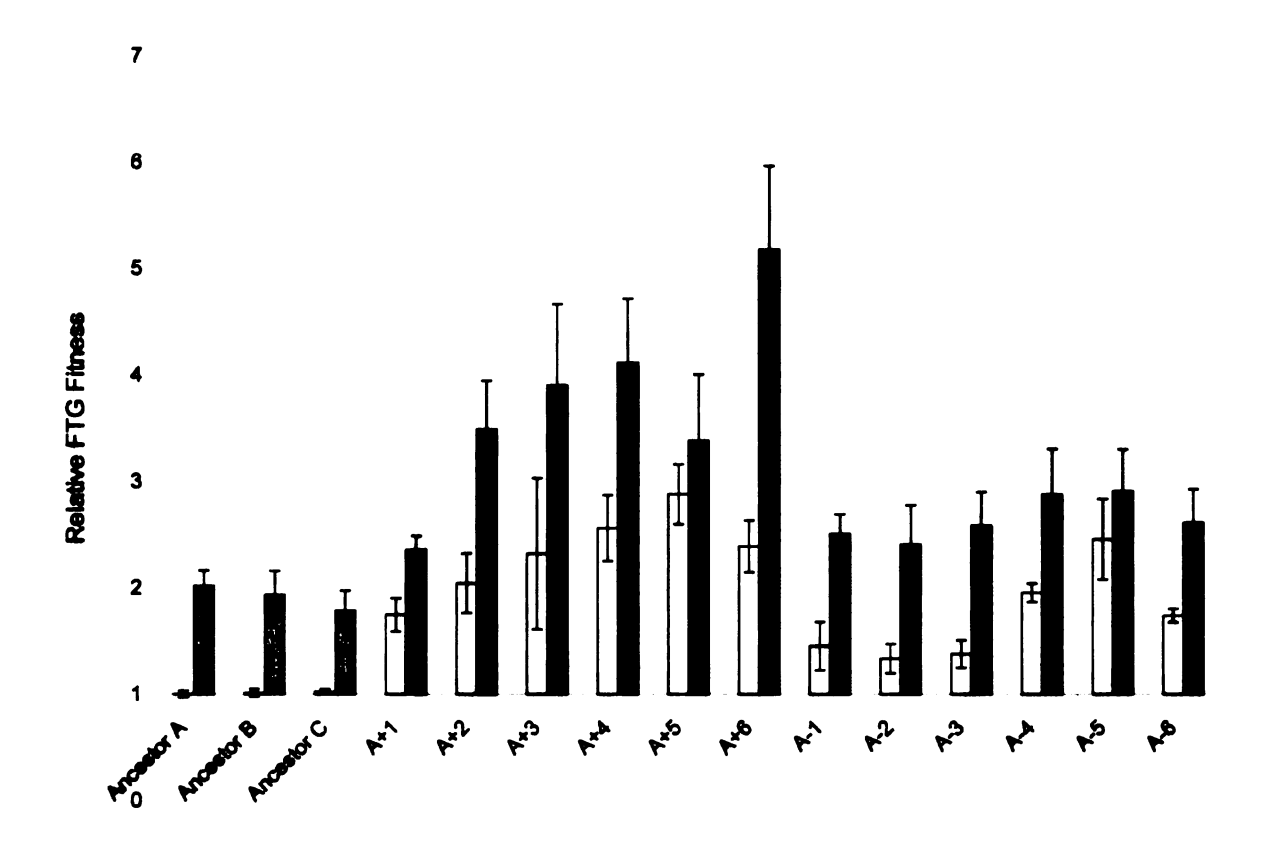


Figure 9. Relative fitness of the 15 FTG-evolved lines and their progenitors. Fitness values were measured in competition with the common ancestor over the two-day FTG cycle. Each evolved line (grey) is paired with its progenitor (white). The three group A lines are shown with different ancestral replicates (designated A, B, and C). The twelve group B lines were derived from long-term lines, designated A+1 to A-6, that previously evolved for 20,000 generations at 37°C. Error bars show 95% confidence intervals based on six replicate fitness assays for each line or progenitor, except for the group A ancestor, where two of the replicate assays were paired with each of the three evolved lines in that group.

Figure 10.

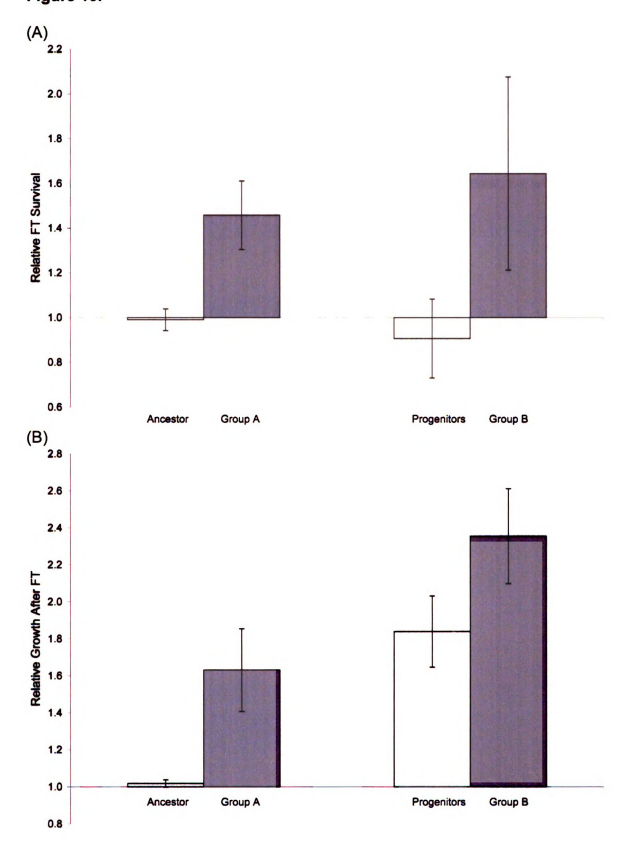
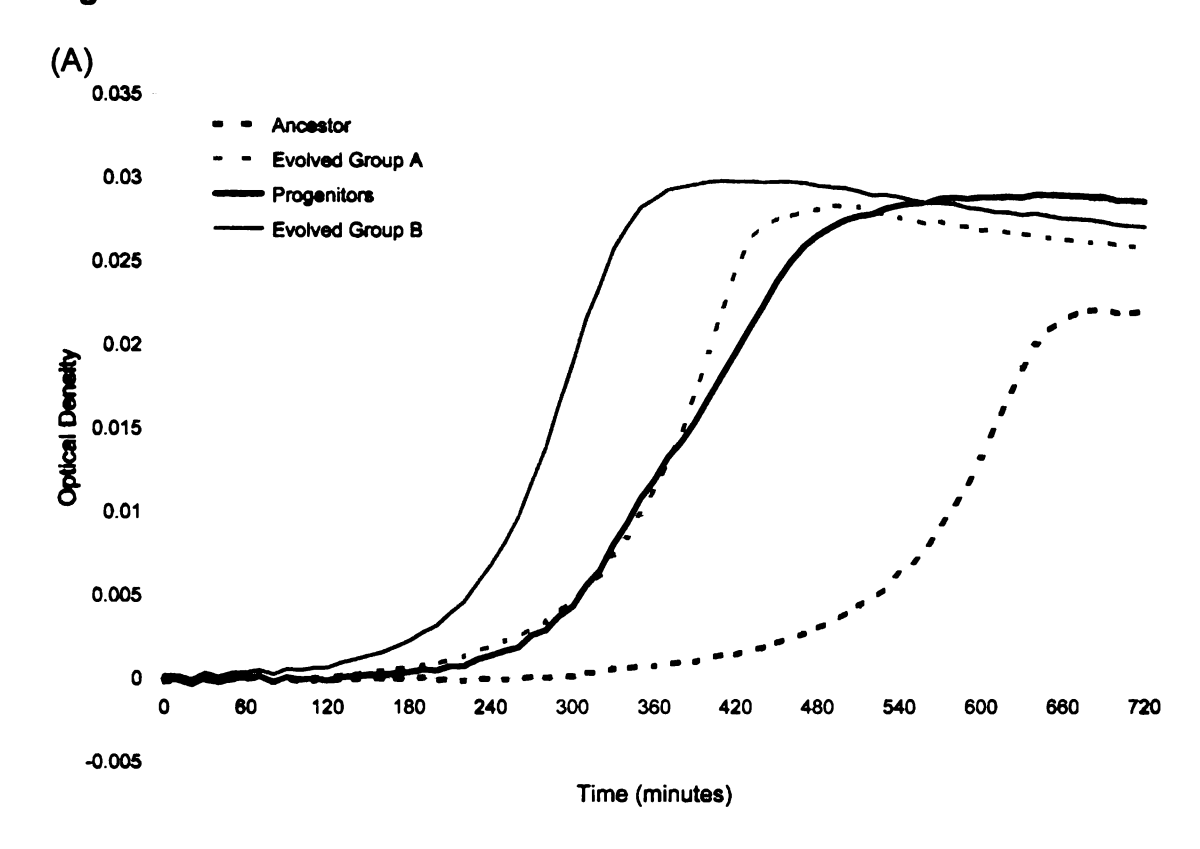


Figure 10. Decomposition of overall fitness gains under the FTG regime into changes in (A) FT survival and (B) growth performance. All values were measured with, and are shown relative to, a marked variant of the common ancestor. FT survival reflects changes in viable cell density during the first day of FTG competitions. Growth performance reflects the net rate of increase on the second day after dilution into fresh medium. The mean for each evolved group (grey) is adjacent to the corresponding mean for its progenitors (white). Means for each group were calculated from average values for each member in the group, except for the single ancestor of group A where the mean is based on six independent measurements. Error bars are 95% confidence intervals based on the number of independently evolved lines, except for the ancestor, for which the interval is based on the six replicate assays.

Figure 11.



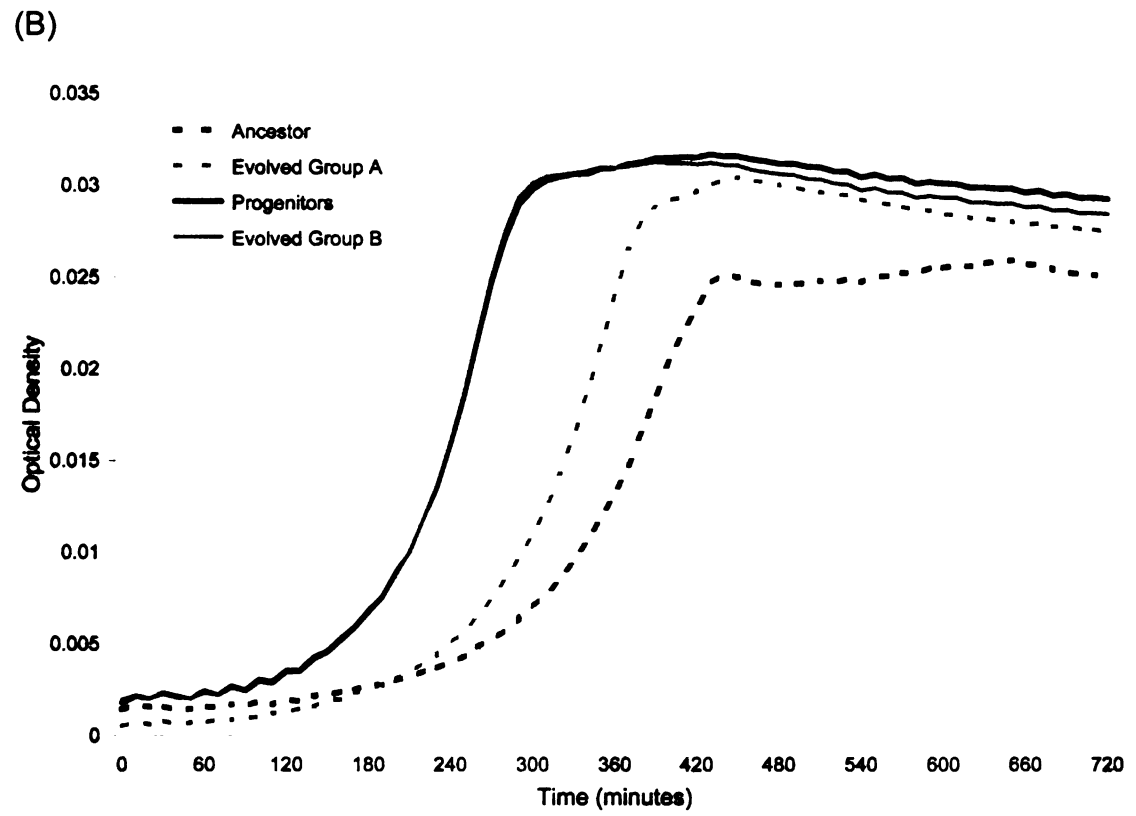
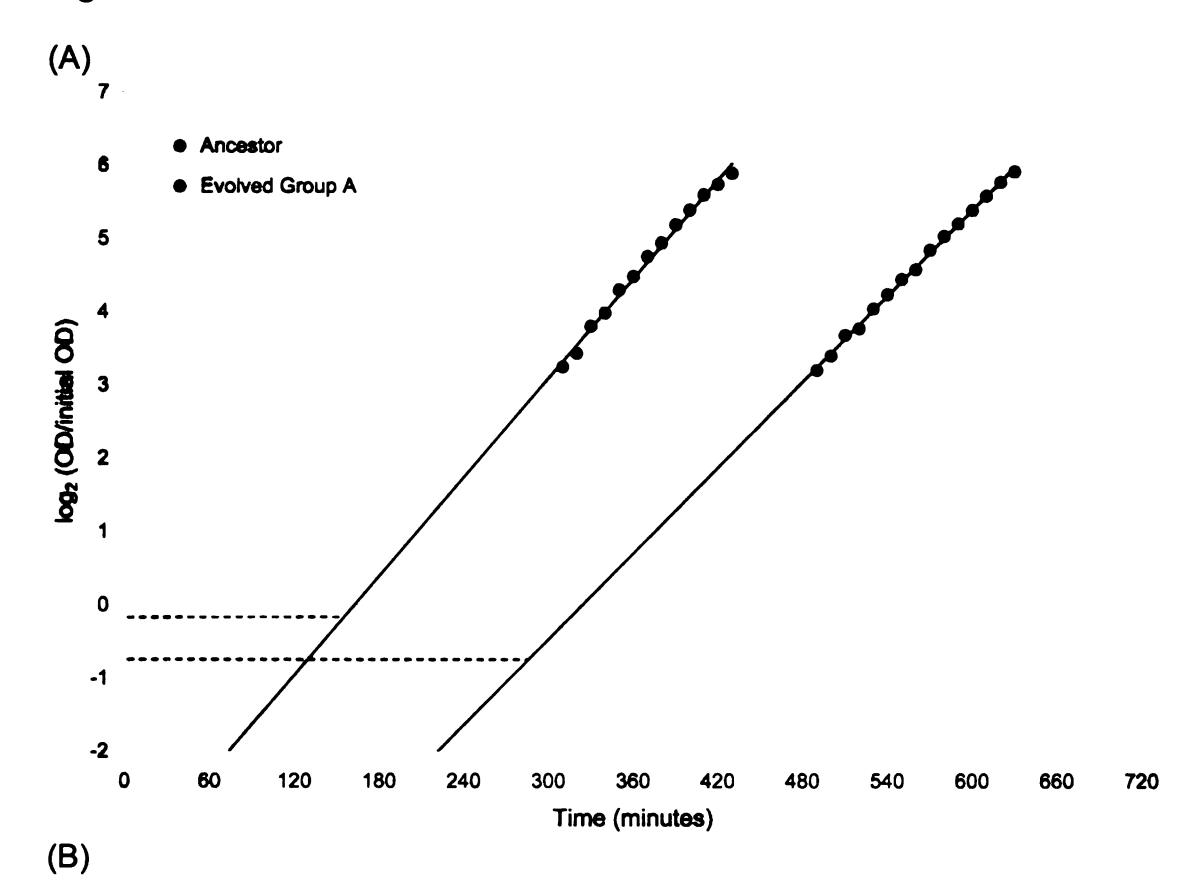


Figure 11. Growth dynamics of the FTG-evolved lines and their progenitors following (A) FT treatment and (B) stationary phase at 37°C. Evolved group A and the ancestor are shown by dashed-grey and dashed-black curves, respectively. Evolved group B and progenitors are shown as solid-grey and solid-black curves, respectively. Each trajectory shows the mean calculated over all of the evolved lines or progenitors in a group, except for the single group A ancestor. In each case, the underlying trajectories were replicated nine-fold for each evolved line or progenitor, including the group A ancestor.

Figure 12.



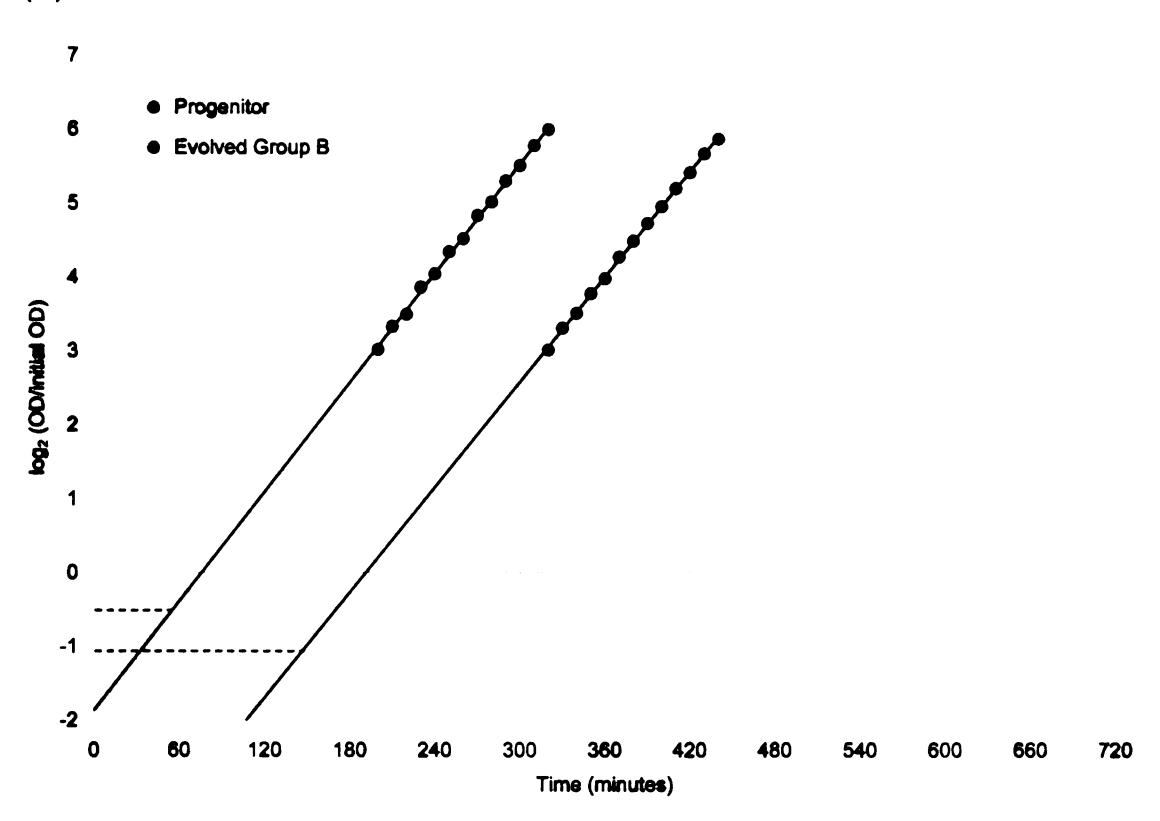
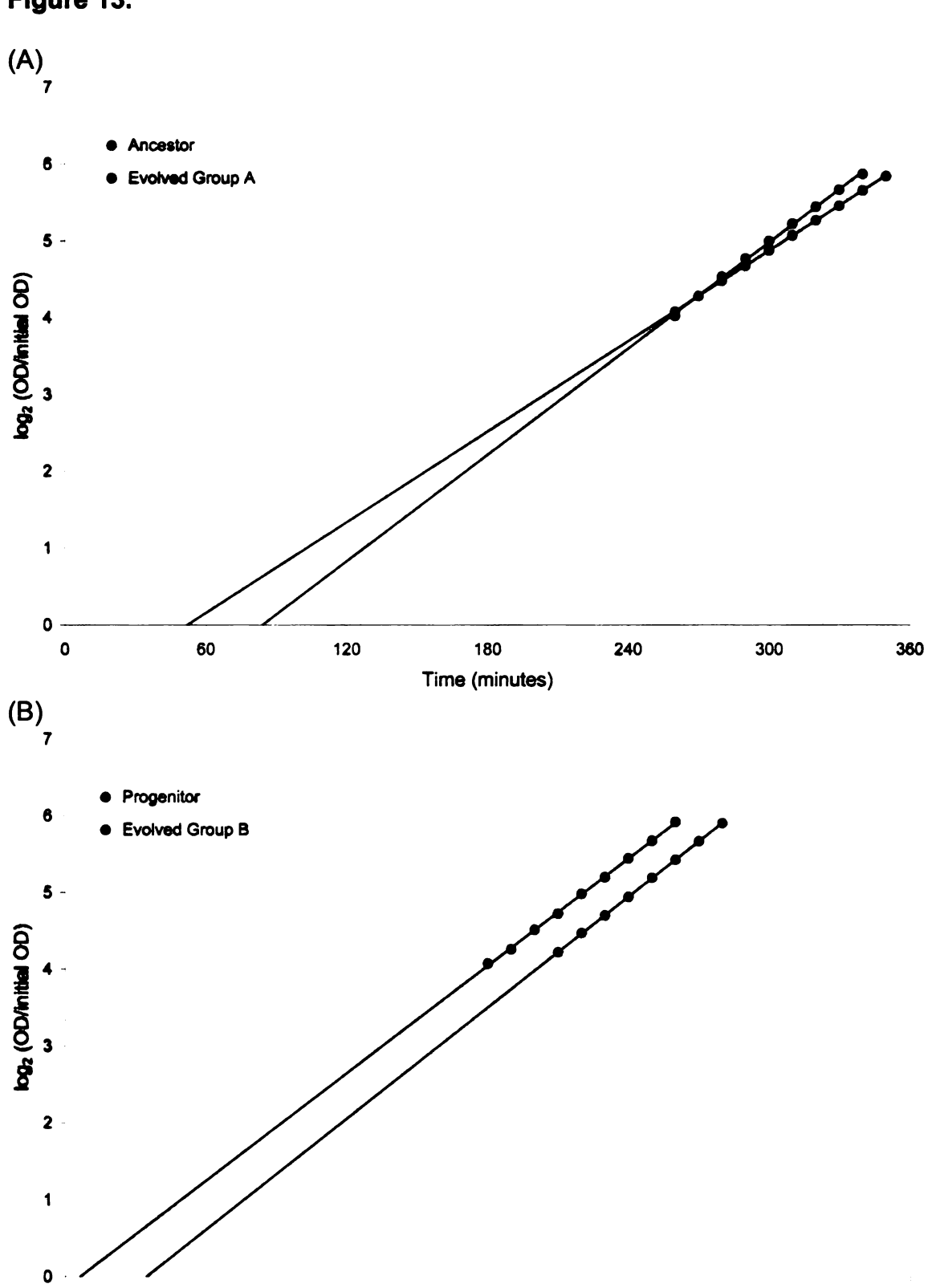


Figure 12. Lag phases following the FT treatment for two FTG-evolved lines and their progenitors. (A) Group A evolved line and the ancestor; (B) group B evolved line and its immediate progenitor. The evolved lines are shown as grey symbols, and their progenitors as black symbols. The apparent duration of the lag phase is where the log-linear regression crosses the initial optical density. The actual physiological duration occurs when the regression crosses the density adjusted for the proportion of surviving cells in the initial population, shown by the dashed horizontal lines. Growth trajectories and survival calculations are means of 27 replicate assays for each evolved line and progenitor.

Figure 13.



Time (minutes)

Figure 13. Lag phases following stationary phase at 37°C for two FTG-evolved lines and their progenitors. (A) Group A evolved line and the ancestor; (B) group B evolved line and its immediate progenitor. The evolved lines are shown as grey symbols, and their progenitors as black symbols. The duration of the lag phase extends to where the log-linear regression crosses the initial density; there is no appreciable mortality under this regime. Growth trajectories are means of 27 replicate assays for each evolved line and progenitor.

#### CHAPTER 3

# ADAPTATION TO CYCLES OF FREEZING, THAWING, AND GROWTH: GENETIC EVOLUTION

#### **ABSTRACT**

Microbial evolution experiments offer a powerful approach for coupling changes in complex phenotypes, including fitness and its components, with specific mutations. Here we investigate mutations substituted in 15 lines of E. coli that evolved for 1,000 generations under freeze-thaw-growth (FTG) conditions. To investigate the genetic basis of their improvements, we first sequenced six candidate genes in two lines, but found no changes. We then screened many of the lines for mutations involving insertion sequence (IS) elements, and identified two genes where multiple lines had similar mutations. Three lines had IS150 insertions in cls, which encodes cardiolipin synthase, and eight lines had IS150 insertions in the uspA-uspB intergenic region, encoding two universal stress proteins. Another line had an 11-bp deletion mutation in the cls gene. Strain reconstructions and competitions demonstrated that this deletion is beneficial under the FTG regime in its evolved genetic background. Further experiments showed that this cls mutation helps maintain membrane fluidity, and enhances survival, during freeze-thaw cycles. Reconstruction of isogenic strains also showed that the IS150 insertions in uspA/B are beneficial under the FTG regime. The evolved insertions reduce *uspB* transcription and enhance recovery of growth after thawing, although the physiological mechanism for faster recovery remains unknown.

#### BACKGROUND

Evolutionary biologists have long been interested in elucidating the genetic bases of adaptation to particular environments, including especially those environments that are novel or stressful to the organism. Evolution experiments using bacteria and other microorganisms (Elena and Lenski 2003; Poon and Chao 2005; Riehle et al. 2005; Herring et al. 2006; Schoustra et al. 2006, Velicer et al. 2006) offer a powerful context for studying the genetics of evolutionary adaptation, because one can couple changes in phenotypic traits, including fitness and its components, with specific mutations. Previous studies on evolutionary adaptation to stressful environments, for example, have examined how known stress-responsive genes evolve, and can also provide new insights into the physiology of organisms when there are unexpected changes in other genes (Riehle et al. 2001; de Visser et al. 2004). More generally, it is of considerable interest to know whether independent populations, when confronted with the same environmental challenges, will evolve along parallel or divergent paths. The convergence of multiple evolving lines on similar phenotypes, and even the same underlying genetic changes, provides a strong indication that the changes are adaptive as opposed to the product of random genetic drift (Bull et al. 1997; Ferea et al. 1999; Wichman et al. 1999; Cooper et al. 2001b, 2003; Colosimo et al. 2005; Wood et al. 2005; Woods et al. 2006; Pelosi et al. 2006).

Advantages to using bacteria for experimental evolution include the ability to establish and propagate replicate populations from a single clone, their rapid generations, and the ability to store and revive the ancestral clone and evolved

lines from different evolutionary time-points. Also, asexual reproduction allows the use of a stably inherited neutral genetic marker that can distinguish different competitors in assays designed to measure their relative fitness. This is particularly relevant for competition experiments between isogenic constructs that differ by a single mutation, to measure its fitness effect in either the exact same selection environment or another environment (Cooper et al. 2001, 2003; Crozat et al. 2005). This approach allows one to distinguish rigorously those mutations that cause fitness improvement from others that may have merely hitchhiked without producing any adaptation. The physiological effects of adaptive mutations can then be elucidated by appropriate phenotypic comparisons between the same isogenic constructs.

Here, we examine the genetic basis of evolutionary adaptation that occurred in 15 populations that evolved under stressful freeze-thaw-growth (FTG) conditions. This FTG regime consisted of a two-day cycle including 22.5 h spent frozen at -80°C and 1.5 h thawing at room temperature, followed by 1:100 dilution into fresh medium and incubation at 37°C for 24 h. During this last step, cells underwent a complete growth cycle including lag, growth, and stationary phases. The evolved lines achieved large increases in fitness relative to their progenitors when competed under the FTG regime, and these gains resulted from both improved survival after the freeze-thaw (FT) cycle and faster recovery to initiate exponential growth after thawing (Sleight and Lenski 2007). This shorter lag phase is specific to recovery after freezing and thawing, and not some more general improvement in recovery of growth following stationary phase per

se. Thus, it is of interest to identify and characterize some of the genetic changes responsible for these adaptations to the FTG regime.

Various approaches have been used to find beneficial mutations substituted in bacterial evolution experiments: sequencing candidate genes suggested by phenotypic changes (Treves et al. 1998; Cooper et al. 2001b) including global gene expression profiles (Cooper et al. 2003; Pelosi et al. 2006), genomic fingerprinting including the use of native insertion sequence (IS) elements as probes (Papadopoulos et al. 1999; Schneider et al. 2000; Zinser et al. 2003; Schneider and Lenski 2004), and most recently even whole-genome sequencing (Velicer et al. 2006; Herring et al. 2006). In this study, we have pursued a two-prong strategy. First, we sequenced six candidate genes whose diverse functions seemed particularly relevant to the stresses that cells would experience during freezing and thawing. When these candidate genes were sequenced in two FTG-evolved lines, however, we found no mutations in any of them relative to their progenitors. Second, we screened the entire genomes of many of the FTG-evolved lines and their progenitors by using a fingerprinting approach with IS elements as probes. This approach led us to the discovery of multiple IS-associated mutations at each of two loci, and these genes and mutations then became the focus of this study. In the paragraphs below, we describe some of the salient features of IS elements for our work.

IS elements are generally small (< 2.5 kb) mobile genetic elements, found in bacteria, that only carry information related to their transposition and its regulation (Mahillon and Chandler 1998). The number and locations of IS

elements vary among bacterial genomes (Deoiner 1987; Schneider et al. 2002), and these elements are a significant source of new mutations (Naas et al. 1994; Hall 1999; Papadopoulos et al. 1999; Schneider et al. 2000; Cooper et al. 2001b; de Visser et al. 2004; Schneider and Lenski 2004). IS insertions can have diverse effects on gene expression, including gene inactivation and polar effects (Jordan et al. 1968), activation of cryptic genes (Reynolds et al. 1981; Hall 1999), inactivation of adjacent genes (Blasband et al. 1986), and altered gene expression caused by IS-encoded promoters (Charlier et al. 1982; Ciampi et al. 1982; Jaurin and Normark 1983; Bongers et al. 2003).

IS and other mobile genetic elements have been viewed as genomic parasites, which have mostly deleterious effects on their hosts but are maintained in genomes by transposition and horizontal transfer (Charlesworth et al. 1994). However, these elements also sometimes have beneficial consequences by producing mutations that increase the genetic variation available for selection (Blot 1994; Kidwell and Lisch 2001; Schneider and Lenski 2004). Some authors have suggested that IS transposition may occur at higher rates in bacteria under stressful conditions, including low (Reif and Saedler 1975) or high temperature (Ohtsubo et al. 2005), starvation (Naas et al. 1995; Hall 1999; Twiss et al. 2005), oxygen stress (de Visser et al. 2004), and UV radiation (Eichenbaum and Livneh 1998), but direct tests of the effects are few (Hall 1999) and IS-mediated mutations certainly occur in non-stressful environments as well. For example, the average number of IS-mediated substitutions in *E. coli* genomes after 30 years of starvation (Naas et al. 1995) was roughly the same as

after only 4 years of growth (Papadopoulos et al. 1999). A study directly comparing the rates of IS-associated mutations substituted under growth and starvation conditions found no significant differences between these two treatments (de Visser et al. 2004). In this study, we do not test whether the stresses of freezing and thawing contributed to IS activity per se; instead, we seek to determine whether IS mutations that were substituted in the evolving lines contributed to their adaptation to the FTG regime.

#### MATERIALS AND METHODS

#### **Derivation of bacterial strains**

The bacteria used in this study derive from a common ancestor via two successive evolution experiments, as summarized in Figure 14. In the first experiment, 12 populations independently evolved for 20,000 generations (3,000 days) starting from two variants of the same ancestral strain of *E. coli* B (Lenski et al. 1991; Lenski 2004). One ancestral variant (REL606) cannot grow on arabinose, while the other (REL607) is a spontaneous Ara<sup>+</sup> mutant. The Ara marker is selectively neutral under the conditions of that long-term experiment (Lenski et al. 1991) as well as in the freeze-thaw-growth environment used in this study (Sleight and Lenski 2007). For the purposes of this paper, we will refer to both variants as the "ancestor" unless we need to discriminate between them for methodological reasons, or as the "original ancestor" to minimize confusion with clones derived from the first evolution experiment that served as progenitors for the second evolution experiment. The long-term experiment involves daily transfers in DM25 (Davis Minimal medium supplemented with glucose at 25

μg/mL) with incubation at 37°C. The 100-fold dilution and re-growth allow about 6.6 (= log<sub>2</sub> 100) generations per day. One clone was sampled from each of the 12 populations after 20,000 generations, and these twelve clones are designated as A-1 to A-6 and A+1 to A+6 for this study.

The second evolution experiment involves 15 populations that were propagated under the freeze-thaw-growth (FTG) regime. Three populations were founded by the Ara<sup>+</sup> variant of the original ancestor, and a single population was founded by each clone sampled from each of the 12 long-term populations. These 15 populations evolved for 150 two-day FTG cycles, which equals at least 1,000 generations based on the 100-fold dilution and growth in alternating days. Somewhat more generations occurred because growth also offset death during the freeze-thaw cycle in alternating days. To start the FTG evolution experiment, 1 mL of DM25 stationary-phase culture was transferred into a freezer tube and put in a -80°C freezer for 22.5 h. The tube then thawed at room temperature (~22°C) for 1.5 h, after which time the culture was diluted 100-fold into fresh DM25 and incubated at 37°C without shaking for 24 h. Thus, the evolving populations experienced cycles of a day of freezing and thawing that alternated with a day of growth in the same medium and at the same temperature as during the long-term evolution experiment. Populations and clones were sampled and stored every 100 generations (30 days) in freezer vials with glycerol for future studies. Note that glycerol was added as a cryoprotectant for long-term storage of samples, but no cryoprotectant was present during the actual FTG evolution experiment itself. The three populations derived from the original ancestor are

designated as AncA/FTG, AncB/FTG, and AncC/FTG, while the other twelve are designated as A-1/FTG to A-6/FTG and A+1/FTG to A+6/FTG (Fig. 14).

During the first evolution experiment, unique mutations were substituted in each of the 12 populations after 20,000 generations, including different alleles in *nadR* (Woods et al. 2006). To check for the possibility of inadvertent crosscontamination during the second evolution experiment, the *nadR* gene was resequenced in all 15 of the FTG lines. In all cases, the *nadR* alleles precisely matched that of their intended progenitors, thereby excluding any crosscontamination.

## DNA extractions, PCR, and sequencing

DNA was extracted from cultures grown overnight in LB medium using the Qiagen genomic-tip 100/G kit and quantified using a spectrophotometer.

Polymerase Chain Reaction (PCR) was performed using the Promega High Fidelity Taq Polymerase kit in a PTC-200 thermocycler (MJ). PCR products were purified using GFX PCR DNA and Gel Band Purification Kit (Amersham Biosciences). Purified PCR products were sequenced on both strands by the dideoxy chain termination method (Sanger et al. 1977). DNA sequences were aligned in the SeqMan program (DNA Star). All mutations were verified by repeating this entire process at least twice.

#### Candidate genes and sequencing strategy

As our first approach to identify the genetic bases of adaptation to the FTG regime, we sequenced six candidate genes. These candidates were chosen *a priori* because their described functions involve coping with the multi-

faceted stresses of freezing and thawing, which include low temperature, dehydration, osmotic shock, oxygen radicals, and intracellular ice formation (Cox and Heckly 1973; Grecz et al. 1980; Calcott and Gargett 1981; Mazur 1984; Gao and Critser 2000). Moreover, previous studies have shown that cold-shock proteins (Willimsky et al. 1992), membrane fluidity (Sinensky 1974; Calcott 1985), oxygen radical scavenging (Stead and Park 2000), and production of compatible solutes (Kandror et al. 2002) contribute to survival and recovery from freezing and thawing. Therefore, the six candidate genes were: cspA, the major cold-shock gene; fabF, involved in fatty acid unsaturation; otsA, involved in synthesizing the cryoprotectant trehalose; rpoS, encoding the alternative sigma factor involved in general stress responses (including transcription of otsA); rrsA, which encodes the 16S rRNA portion of the rmA operon; and sodA, encoding a superoxide dismutase. Moreover, some of these genes appear to have unusual sequence signatures in cold-adapted microorganisms (Hebraud and Potier 1999; Pruss et al. 1999). We sequenced all six candidate genes, including their adjacent regulatory regions, in the original ancestor and in two FTG-evolved clones (A-1/FTG and A+1/FTG) using the primer pairs shown in Appendix 2, Table A2.1.

# Southern hybridizations with IS probes

Extracted genomic DNA from each clone was digested with *Eco*RV (for IS1, IS2, IS3, IS4, IS30, and IS186) or *Hinc*II (for IS150), separated on a 0.8% agarose gels with a 1 kb ladder (New England Biolabs), and transferred to nylon membranes (Southern 1975). Hybridizations were performed at high stringency

(68°C) using internal fragments of each IS probe (Appendix 2, Table A2.2) that were PCR amplified, purified, and labeled using the DIG DNA Labeling and Detection Kit (Roche).

## Characterization of sequences adjacent to IS elements by inverse PCR

Genomic DNA from each clone was digested with *Eco*RV or *Hinc*II, and separated on agarose gels. Gel fragments containing IS elements were cut and purified using the GFX PCR DNA and the Gel Band Purification Kit (Amersham Biosciences). The fragments were self-ligated (end-to-end) with T4 DNA Ligase (New England Biolabs) at 10 μg/mL, and the ligated mixtures were used as templates in PCR reactions using primers directed outward from the appropriate IS element (Appendix 2, Table A2.3). PCR products were purified, sequenced, and the sequences adjacent to the IS element were compared to the whole genome sequence for *E. coli* K-12 (Riley et al. 2006; Genbank accession number NC\_000913). Once the location of these adjacent sequences was determined, primers were designed to PCR amplify the IS-insertion allele on the chromosome. The PCR products were sequenced with the same primers (Appendix 2, Table A2.3) to determine the exact position, orientation, and target-site duplication caused by the IS insertion.

#### Isogenic strain construction

Isogenic constructs and reconstructs were created using the "gene gorging" replacement technique (Herring et al. 2003). In the case of the A-2/FTG evolved clone, which has an 11-bp deletion in the *cls* gene, we performed two allelic replacements. First, the ancestral *cls* allele was moved into this evolved

clone. Next, the evolved clone with the introduced ancestral cls allele was reconstructed to the evolved cls deletion allele to verify that phenotypic differences were caused by the mutation and not a side-effect of the gene gorging process. Second, the evolved cls deletion allele was introduced into the A-2 progenitor and then reconstructed back to the ancestral cls allele. We used the A-2/FTG evolved line, rather than other evolved lines that had IS insertions in the cls gene, because this small mutation (11-bp deletion) is easier to manipulate. In the case of the AncB/FTG evolved clone, which acquired an IS 150 insertion in the uspA/B intergenic region, we independently made two isogenic constructs from which this IS150 insertion was removed, thereby restoring the ancestral allele of uspA/B. In this case, we did not attempt to move the uspA/B::IS150 allele back into this construct, nor into the ancestor, because of recombination events, during the strain construction process, with the various IS 150 copies present in the chromosome. The two independently constructed isogenic strains from which the IS150 insertion was removed did not differ significantly from one another in any respect, supporting their isogenicity, and the data obtained for them is combined in the competition, growth curve, and realtime PCR experiments reported in this paper. See Appendix 2, Figure A2.1, for a schematic representation of these isogenic constructs and reconstructs.

For all constructs, we used one primer with a *I-Sce-I* restriction site on its 5' end. Fragments that included about 500 bp on each side of the mutation site or its ancestral equivalent were PCR-amplified and purified. Primers used to make the *cls* constructs were RL594 (5' GGA CCT GCG CCA ACA TC 3') and

RL595 (5' TAG GGA TAA CAG GGT AAT CCG CCG GAT CGA ATA ACT C 3'). The primers for the *uspA/B* constructs were RL567 (5' TAG GGA TAA CAG GGT AAT ATG TAG GCC TGA TAA GCG TAG C 3') and RL568 (5' CCC GGT GTA TAG GTC AGA GTA GTT 3'). The resulting ~1 kb fragment was cloned into pCRII-Topo and transformed into *E. coli* cells using the Topo TA Cloning kit (Invitrogen). Transformants were selected and grown in LB supplemented with ampicillin, and the plasmids were purified using the Promega Wizard Plus SV Miniprep DNA Purification System. All cloned fragments were checked by DNA sequencing and no additional mutations were detected.

The donor plasmid (encoding kanamycin resistance and the ~1 kb cloned fragment) and the mutagenesis plasmid (encoding the *I-Sce-I* restriction enzyme, λ red recombination enzymes, and chloramphenicol resistance) were cotransformed into competent cells of the desired clone. Transformants were selected using LB agar with supplemental kanamycin and chloramphenicol, and then grown in a medium containing arabinose; this medium induces the enzymes produced by the mutagenesis plasmid that promote homologous recombination between the fragment on the donor plasmid and the chromosome (Herring et al. 2003). Putative constructs were then screened for the desired genotype using PCR with primers specific to the corresponding gene on the chromosome, and also checked for kanamycin and chloramphenicol sensitivity to ensure loss of both plasmids. All constructs and reconstructs were sequenced twice to verify the presence or absence, as intended, of the evolved mutation, and to ensure that no other mutations were introduced in the vicinity of the replacement allele.

## Quantifying FTG fitness and its components

We performed competition experiments to measure the relative fitness levels of various ancestral, evolved, and constructed genotypes. The neutrally marked variants of the ancestral strain allowed competitors to be distinguished on the basis of colony color on tetrazolium-arabinose (TA) indicator agar (Lenski et al. 1991; Sleight and Lenski 2007). For each replicate competition assay, each competitor's realized (net) growth rate, r, was measured over the two-day FTG cycle, as follows:

$$r = \ln((N_2 \times 100) / N_0)$$

where  $N_2$  is that competitor's final cell density,  $N_0$  is its initial cell density, and the factor of 100 takes into account the 100-fold dilution between each FTG cycle. Thus, the overall FTG fitness of one competitor relative to another is simply the ratio of their respective realized growth rates over the complete cycle.

We also calculated each competitor's FT survival, s, and subsequent growth rate, g, over the two separate days of the FTG cycle as follows:

$$s = N_1 / N_0$$

$$g = \ln((N_2 \times 100) / N_1)$$

where  $N_1$  is the viable cell density measured after the first day of the cycle prior to the 100-fold dilution. Note that survival is a proportion, whereas growth is a rate. In any case, the relative survival and growth of two competitors are expressed as the ratio of the relevant parameters, so that both become dimensionless quantities, as is the overall FTG fitness. Note also that all of these quantities are calculated separately for each replicate assay, thus preserving

their statistical independence. The quantities were averaged across replicates, and analyzed statistically as described below.

#### Statistical methods

We performed paired t-tests to compare the properties of two clones, with pairing based on temporal and spatial proximity in the structure of the experiment. In those cases where we had a priori expectations about the direction of change, significance was computed using one-tailed t-tests; otherwise two-tailed tests were used. We expected the FTG-evolved lines to have improved performance relative to their progenitors in the FTG regime, including both FT survival and subsequent growth. We also expected that evolved alleles would confer an advantage under the FTG conditions, and when present in the evolved genetic background. However, we had no expectations for other phenotypic aspects of isogenic clones differing only by a specific allele. Two-way ANOVAs were performed to compare phenotypic measures between clones with the four combinations of ancestral and evolved backgrounds and alleles.

#### **Growth curves**

Growth curves, based on optical density (OD) measurements, were obtained for sets of isogenic constructs in order to compare the durations of their lag phase prior to growth as well as their doubling times during the growth phase. The OD measurements were performed at 420 nm with 0.2-mL cultures in a 96-well microtiter plate that was incubated at 37°C. Data were collected for cultures following either a FT cycle or stationary phase at 37°C, such that a comparison

between the two curves allows one to estimate the effect of the FT cycle on the time required to achieve exponential growth following dilution into fresh DM25 medium (Sleight and Lenski 2007).

## Measuring membrane fluidity

Fluorescence polarization (anisotropy) measures fluidity in the cytoplasmic membrane using various probes, each one specific to a particular region of the membrane (Harris et al. 2002; Vanounou et al. 2002). The sample incubated with the probe is excited by polarized light, and the emitted light from the probe is polarized differentially depending on how much rotation of the probe occurs. When the emitted light is simultaneously measured both parallel and perpendicular to the axis of excitation, a probe that can rotate more freely (i.e. in a more fluid membrane) will generate a larger emission signal in the perpendicular relative to the parallel direction, when compared to a probe that rotates less freely (i.e. in a less fluid membrane).

Fluorescence anisotropy was measured with a Spectramax M5 fluorometer (Molecular Devices) using two probes, 6-dodecanoyl-2-dimethylaminoaphthalene (laurdan) and 1,3-diphenyl-1,3,5-hexatriene (DPH). Laurdan is an amphipathic molecule that localizes near the lipid polar head groups in the cytoplasmic membrane, and is therefore sensitive to changes at the water-lipid interface (Harris et al. 2002; Vanounou et al. 2002). DPH is useful for detecting changes in saturation of fatty acyl chains in the cytoplasmic membrane (Beney et al. 2004; Aricha et al. 2004). Either laurdan (5 x 10<sup>-5</sup> M added from a stock solution in methanol) or DPH (5 x 10<sup>-5</sup> M added from a stock solution in

tetrahydrofuran) was incubated for one hour at room temperature in the dark with 0.2 mL of cultures sampled either at stationary phase or after a FT cycle.

Cultures without any probe were used as a scattering control, and were incubated under the same conditions for each individually measured sample.

The optimal ratio of probe to culture concentration was determined by using the minimal concentration giving an appropriate signal-to-noise ratio (Vanounou et al. 2002). Laurdan anisotropy was measured at the 355 nm excitation wavelength and 440 nm emission wavelength. DPH anisotropy was measured at the 360 nm excitation wavelength and 430 nm emission wavelength. Anisotropy (r) is calculated in the traditional manner (Harris et al. 2002) as follows:

$$r = (I_V - GI_H) / (I_V + 2GI_H),$$

where I<sub>V</sub> and I<sub>H</sub> are the fluorescence intensities determined at vertical and horizontal orientations of the emission polarizer when the excitation polarizer is set in the vertical position. G is a correction factor for dissymmetry associated with the horizontal and vertical positions of the polarizers. Lower anisotropy values indicate higher probe rotation and thus imply a more fluid membrane compared to higher anisotropy values.

# RNA extractions and real-time (RT) PCR

RNA was extracted from cultures at stationary phase (24 h after dilution into fresh media), after a FT cycle (frozen at -80°C for 22.5 h and then thawed for 1.5 h at room temperature), and in transitional growth conditions (2 h after the thawed culture was diluted 1:10 into DM25 and incubated at 37°C) using the

RNeasy Mini Kit (Qiagen). For that third treatment, two hours was chosen because it corresponds to a time period when the ancestor is still deep within its long FT-associated lag phase, whereas the evolved clone is approaching the time when it starts growth (Sleight and Lenski 2007); hence, that timepoint may offer the best opportunity to detect physiologically important differences in gene expression between the evolved clone and ancestor. A 1:10 dilution was used, instead of the 1:100 dilution used in the evolution experiment, in order to extract enough RNA for the RT-PCR procedure; control experiments confirmed that the difference between the ancestor and evolved clone in the duration of their lags after a FT cycle is comparable for 1:10 and 1:100 dilutions. The same culture volume was used for each clone to preserve the relevant cell density, while an endogenous control served to measure the total RNA present (see below). After extraction, RNA was treated with Rnase-free DNase (Ambion), and PCR experiments were run using the extracted RNA as a template to ensure the absence of DNA in the RNA samples. RT-PCR was performed using the TaqMan One-Step RT-PCR kit (Applied Biosystems) with primers and MCB probes specific to the uspA, uspB, and 16S rRNA genes in the ABI Prism 7900HT Sequence Detection System. Negative controls without any RNA were also used in RT-PCR experiments, and they produced no significant background noise. An RNA standard was obtained by mixing RNA from different samples, and a log<sub>10</sub> dilution series through 10<sup>-5</sup> was measured with the primers and probe for each gene. Regression was then performed on C<sub>T</sub> (threshold cycle) values against the dilution factor to determine the amount of RNA in unknown samples.

The mRNA levels for *uspA* and *uspB* levels were individually divided by the 16S rRNA levels for each clone and sample timepoint to ensure that any differences were not an artifact of the total amount of RNA extracted.

# **Ethanol sensitivity experiments**

Samples of an evolved clone in stationary phase or after a FT cycle were mixed with the reciprocally marked ancestor from the same condition, as in a competition experiment. The mixed culture was then incubated in 10% ethanol at 37°C for one hour. Cell densities were measured before and after ethanol exposure, and used to quantify relative sensitivity using the same equation used to quantify relative FT survival.

# **Novobiocin sensitivity experiments**

Stationary-phase cultures of ancestral and evolved clones were separately plated on both TA agar and TA agar supplemented with novobiocin (100 µg/mL). The plates without novobiocin were incubated at 37°C for one day, while those with antibiotic were incubated for two days. Novobiocin sensitivity was then calculated from the ratio of the resulting cell densities.

# Supporting data and supplementary analyses

Appendix 2, which can be found at the back of this dissertation, provides some supporting data and supplementary analyses relevant to this Chapter. All information pertaining to the Materials and Methods is included in the figure legend if not already described.

#### RESULTS

## Absence of mutations in candidate genes

We began our search for the beneficial mutations responsible for adaptation to the FTG regime by sequencing six candidate genes in two of the FTG-evolved lines. These candidates were chosen because their encoded functions affect a wide range of physiological processes important for FT survival and subsequent recovery. These processes (and candidate genes) include: the cold-shock response (*cspA*); membrane fluidity (*fabF*); synthesis of cryoprotectants (*otsA*); global regulation of stress responses (*rpoS*); protein translation (*rrsA*); and scavenging oxygen radicals (*sodA*). A total of ~10 kb was sequenced in two focal FTG-evolved lines, A-1/FTG and A+1/FTG, but no mutations were found relative to their progenitors. Therefore, we next sought to pursue a more open-ended approach that would find mutations anywhere in the genome, albeit only those mutations causing observable changes in DNA fingerprints.

# Discovery of several IS-associated mutations in FTG-evolved lines

To characterize genetic changes and genomic rearrangements associated with IS elements in FTG-evolved lines relative to their progenitors, a Restriction Fragment Length Polymorphism (RFLP) analysis was performed using internal fragments from each of the seven IS elements in *E. coli* B as probes. One clone sampled from 10 of the 15 independently evolved FTG populations was compared against its progenitor for each of the seven IS elements (Table 3). An IS-associated change is defined as either a gain or loss of a band; however, one IS-mediated mutation can produce more than one band change, and therefore this method may sometimes overestimate the number of underlying mutational

events (Papadopoulos et al. 1999; Schneider et al. 2000). Of the seven IS elements, three showed no changes (IS2, IS4, and IS30) in any of the 10 evolved lineages. The absence of any changes associated with these three elements does not necessarily mean that they had absolutely no transposition activity under FTG conditions, but rather that either no mutations produced by such activity were highly beneficial and thus substituted in any of the ten FTG-evolved lines chosen for analysis, or that no transposition event hitchhiked with other beneficial mutations. By contrast, there were 30 total changes in the other four IS elements (IS1, IS3, IS150, and IS186), with IS150 alone contributing to more than half of these changes (see Figure 15 and Appendix 2, Figures A2.2-5, for the RFLP images). This high level of activity is not specific to FTG conditions, since IS150 also shows high activity under benign growth conditions (Papadopoulos et al. 1999; Schneider et al. 2000; Cooper et al. 2001). See also the exact band differences between FTG-evolved lines and their progenitors in Appendix 2, Table A2.4.

The number of IS changes in FTG-evolved lines ranges from zero (A+3/FTG, A-1/FTG) to seven (A+1/FTG) among the ten lines tested. Four of them (A+3/FTG, A+6/FTG, A-2/FTG, A-4/FTG) had evolved mutator phenotypes during their prior experimental evolution (Sniegowski et al. 1997; Cooper and Lenski 2000). On average, there were more IS-associated changes in the non-mutator than the mutator populations, although that difference was not statistically significant (two-tailed t-test, p = 0.1946).

Localization of IS-associated mutations in FTG-evolved lines

Given the numerous IS-associated mutations that we found, and the fact that parallel changes are a strong indication of adaptive evolution, we focused our attention on characterizing those changes that arose independently in multiple FTG-evolved lines. Figure 15 shows the Southern hybridizations using the IS150 sequence to probe the genomes of the FTG-evolved lines and their progenitors. Bands present in more than one FTG-evolved line, but not in their progenitors, are circled and the chromosomal location is indicated. Two of the 10 FTG-evolved clones that were tested have an insertion in the *cls* gene, and four evolved clones have an insertion in the *uspA/B* intergenic region. Another IS150-associated change, which is not circled in this figure, is an insertion within the *uspD* gene in A+4/FTG. However, this insertion was found in only one of ten clones tested from this evolved population and, moreover, it was absent from all of the other 14 FTG-evolved populations for which we screened 10 clones from each. Therefore, this *uspD* mutation was not investigated further.

## Systematic screening of cls in FTG-evolved lines

After the *cls* and *uspA/B* insertion mutations were discovered, we screened 10 clones from all 15 FTG-evolved populations for the presence of insertion mutations in these loci using PCR with primers designed to detect mutations in regulatory as well as coding regions. For the *cls* gene, five FTG-evolved lines were found to have IS insertions in at least one clone, including the two lines in which IS*150* insertions were originally found (A+4/FTG and A-3/FTG). In a third line (A-1/FTG), an IS*150* insertion was found in a single clone that was not tested in the previous Southern hybridizations. In two other lines (A-

5/FTG and A-6/FTG), all clones tested in these populations had insertions of a different IS element, IS186, either in or immediately upstream of cls. Surprisingly, the progenitors of these two lines (A-5 and A-6), which had evolved for 20,000 generations at constant 37°C, already harbored the cls::IS186 insertions. Thus, while these last two mutations might have contributed to adaptation to the previous environment, they cannot be responsible for the fitness gains specific to the FTG regime. In all of the other FTG-evolved lines without any insertion mutations in cls. that gene and its adjacent regulatory region were sequenced. One additional substitution was found, in which the A-2/FTG evolved line had an 11-bp deletion that generates a premature stop codon downstream. The physical locations of all these *cls* mutations are listed in Table 4, while Figure 16 provides a schematic representation. Table 5 shows the substitution dynamics of the *cls* mutations in the corresponding FTG populations, based on testing clones isolated from freezer stocks that we saved every 100 generations during the evolution experiment. We presume that all of the cls mutations that evolved during the FTG experiment, including the deletion in line A-2/FTG, disrupt the function of the encoded enzyme, cardiolipin (CL) synthase. This enzyme is widely distributed across bacterial species and converts two phosphatidylglycerol molecules into CL and glycerol in the membrane (Hirschberg and Kennedy 1972) during stationary phase (Shibuya and Hiraoka 1992). As noted previously, a deletion mutation can be more precisely manipulated than a new insertion of an IS element, as recombination between multi-copy IS elements may produce unintended changes. Therefore, our

subsequent analyses of the effects of *cls* evolution on FTG performance will focus on the *cls* deletion allele.

## Systematic screening of uspA/B in FTG-evolved lines

By screening the same 10 clones from all 15 FTG-evolved lines, we found mutations in uspA/B and its associated regulatory region in eight populations, with one or more clones presenting an insertion. Remarkably, all of them were IS150 insertions in the same exact position and orientation in the uspA/B intergenic region (Table 4). Cross-contamination can be ruled out because these clones have different IS banding patterns in RFLP experiments, different cls mutations (as described above), and unique nadR alleles derived from their progenitors (see Materials and Methods). No mutations were found in the openreading frames of uspA or uspB in any of the FTG-evolved lines. Figure 17 shows that these identical IS 150 insertions are located 34 bp upstream of the uspB start codon and 95 bp downstream of the putative uspB  $\sigma^{S}$  promoter. The uspA and uspB genes encode Universal Stress Proteins (Usp) A and B, respectively. UspA is an autophosphorylating serine and threonine phosphoprotein that is induced under a wide variety of stress conditions; it is thought to play a role in protecting cells from DNA damage, although its exact function is unknown (Kvint et al. 2003). Even less is known about UspB, although it is differentially transcribed from UspA and may not be a truly universal stress protein (Farewell et al. 1998; Kvint et al. 2003). The effects of the IS150 insertions on transcription of uspA and uspB will be discussed later. In the seven other FTG lines without uspA/uspB::IS150 mutations, we sequenced uspA, uspB,

and the *uspA/B* intergenic region for individual clones, but no other mutations were found. Table 6 summarizes the temporal dynamics of the *uspA/uspB*::IS150 mutations in the eight FTG-evolved populations where they were found, based on testing clones from the freezer stocks saved every 100 generations during the evolution experiment.

## Isogenic strain constructions

We constructed strains that were isogenic except for the *cls* deletion and *uspA/B*::IS150 insertion in order to test the fitness and other phenotypic effects of these evolved mutations. For *cls*, we first restored the ancestral allele in an evolved clone from the A-2/FTG line. In order to verify that any phenotypic differences were specifically caused by the *cls* alleles (and not by some hypothetical mutation inadvertently introduced during genetic manipulations), we then "reconstructed" the evolved state by re-introducing the *cls* deletion mutation back into the same evolved clone. Similarly, in order to test the effect of the evolved allele in the ancestral genetic background, the *cls* deletion mutation was moved into the A-2 progenitor genome, and then that progenitor was reconstructed by reintroducing the ancestral *cls* allele. Thus, we produced a set of four isogenic strains comprising each of the ancestral and evolved *cls* alleles in each of the progenitor and FTG-evolved backgrounds.

For *uspA/B*, we made two independent constructs from one evolved clone in the AncB/FTG line in which the ancestral allele replaced the *uspA/uspB*::IS150. The clones with the evolved insertion allele in the same background served as the controls for the experiments reported below; the

evolved allele was not introduced into the ancestral background for this locus. We detected no significant differences between the two independent constructs; therefore, we pooled the data from these constructs in the analyses below. Details of the strain-construction procedures are provided in the Materials and Methods section.

#### Phenotypic consequences of evolved cls mutation

We performed several experiments to investigate the physiological effects of the cls deletion mutation in the evolved and progenitor genetic backgrounds. First, we measured the relative fitness levels of all four isogenic strains, including the ancestral and evolved cls alleles in the progenitor and FTG-evolved genetic backgrounds, under four conditions (Figure 18): the entire two-day FTG regime. FT survival, growth performance after the FT treatment, and growth performance after stationary phase (without a FT cycle). Over the entire FTG cycle, the evolved clone with the *cls* mutation has a significantly higher fitness than its progenitor with the ancestral cls<sup>+</sup> allele (Figure 18A; paired one-tailed t-test, p < 0.0001). This higher overall FTG fitness reflects both improved FT survival and subsequent growth after FT treatment (Figures 18B and 18C; paired one-tailed ttests, p = 0.0001 and p = 0.0006, respectively). This overall improvement is specific to FTG conditions, because the evolved clone has a small, but significant, decrease in its performance without the FT treatment (Figure 18D; paired two-tailed t-test, p = 0.0038). Note the scale differences between panels in Figure 18; thus the error bars on the fitness values that are not significantly different from 1.0 in panel D are, in fact, very tight. These comparisons

demonstrate that the evolved A-2/FTG line improved its FTG fitness relative to its progenitor, and that the adaptation is specific to the FTG regime.

The following comparisons allow us to test whether the evolved *cls*<sup>-</sup> mutation is responsible, at least in part, for this adaptation. Restoring the ancestral *cls*<sup>+</sup> mutation to the evolved strain reduces overall FTG fitness by about 31% (Figure 18A; paired two-tailed t-test, p = 0.0002). The evolved allele significantly improves both FT survival and subsequent growth (Figures 18B and 18C; paired two-tailed t-tests, p = 0.0054 and 0.0024, respectively). The improvement associated with the evolved *cls* allele is specific to the FTG regime, as there is no significant difference between the ancestral *cls*<sup>+</sup> and evolved *cls*<sup>-</sup> alleles in the same evolved A-2/FTG background during competition after stationary phase without a FT cycle (Figure 18D; paired two-tailed t-test, p = 0.5077). These comparisons demonstrate that the *cls*<sup>-</sup> allele contributes significantly to the FTG-specific adaptation.

When moved into the A-2 progenitor, the same evolved *cls*<sup>-</sup> allele shows however only a small (roughly 5%) and marginally non-significant advantage in overall FTG fitness (Figure 18A; paired two-tailed t-test, p = 0.0957). Also, neither FT survival nor subsequent growth after FT treatment show any significant effect of the *cls* allele in the progenitor's background (Figures 18B and 18C; paired two-tailed t-tests, p = 0.4686 and 0.2736, respectively). The ancestral allele has a small, but again non-significant, advantage during growth after stationary phase without the FT cycle (Figure 18D; paired two-tailed t-test, p = 0.1250). Evidently, the fitness effects of the evolved *cls*<sup>-</sup> allele are contingent

on interactions with one or more other mutations in the evolved A-2/FTG line. This conclusion is further supported by a two-way ANOVA using the overall FTG fitness data, which indicates a highly significant interaction between the genetic background and the cls allele (p = 0.0001).

The beneficial effect of the evolved cls deletion allele for survival and recovery, and the specificity of that effect with respect to the FT treatment, was also evident from the growth dynamics of each isogenic strain (Figure 19). Following a FT cycle, the evolved A-2/FTG strain with the evolved cls allele recovers much more quickly than any of the other three constructs (Fig. 19A). When we compare the recovery of the same four isogenic strains following stationary phase at 37°C with no FT treatment, the growth curves are almost identical (Fig. 19B). Comparing the dynamics with and without the FT treatment, we also see that the recovery of the A-2 progenitor with its ancestral cls<sup>+</sup> allele is delayed (i.e., shifted to the right) by almost 3 h by imposing a FT treatment. In striking contrast, recovery of the evolved A-2/FTG strain with its cls allele is delayed by less than 1 h when the FT treatment is imposed. As an aside, these four strains following a 2 h cold shock at 4°C recover at about the same rate at 37°C (data not shown), indicating that the adaptation is specific to FT recovery and is not related to recovery from low temperatures in general.

Previous research has shown that *cls* mutants have altered membrane phase-transitions during or after a temperature downshift (Pluschke and Overath 1981). To test whether the evolved *cls*<sup>-</sup> allele altered membrane fluidity, we measured fluorescence anisotropy of the same four strains after either FT

treatment or stationary phase at 37°C (see Materials and Methods for details). Laurdan is a fluorescent probe that localizes to the cytoplasmic membrane, and which is sensitive to changes in the water-lipid interface where the phospholipid head groups reside (Harris et al. 2002; Vanounou et al. 2002). The results of the experiments are summarized in Figure 20 (note that lower values for laurdan anisotropy indicate more fluid membranes).

Figure 20A shows that the evolved *cls*<sup>-</sup> allele significantly increases membrane fluidity (reduces laurdan anisotropy) relative to the ancestral cls<sup>+</sup> allele following FT treatment, and does so in both the progenitor and FTGevolved backgrounds. One or more other evolved alleles must also contribute to greater membrane fluidity, because the evolved construct has greater fluidity than the progenitor even when both strains have the same ancestral cls<sup>+</sup> allele. A two-way ANOVA indicates the effects of both genetic background and cls allele are highly significant, while there is no significant interaction with respect to this phenotype (Table 7). The evolved cls allele therefore generally increases membrane fluidity after freezing and thawing regardless of genetic background. However, recall from the fitness experiments that the evolved cls allele was beneficial under the FTG regime only in the evolved genetic background. Taken together, these findings indicate that the beneficial effect of increased membrane fluidity after the FT cycle must be dependent on other mutations in the A-2/FTG evolved line and that the beneficial effect conferred by cls must be linked to another phenotypic effect.

We see no significant differences in membrane fluidity when laurdan anisotropy is measured for the same four strains after stationary phase, without the FT treatment (Figure 20B, Table 8). Therefore, the effect of the evolved *cls* allele on membrane fluidity is specific to freezing and thawing. Notice also that the anisotropy value of the A-2/FTG evolved strain, with its evolved *cls* allele, is almost the same when measured after either FT treatment or stationary phase at 37°C. This similarity indicates that this FTG-evolved line is able to maintain its membrane fluidity at the water-lipid interface after a FT cycle, whereas the progenitor's membrane evidently becomes much more rigid. This effect is independent of the *cls* allele.

We also used the same approach to measure changes in membrane fluidity in two of the FTG-evolved lines with IS150 insertions in the *cls* gene (A+4/FTG and A-3/FTG) relative to their respective progenitors. Both of these evolved lines also have significantly increased membrane fluidity relative to their progenitors after a FT cycle, but not during stationary phase (Appendix 2, Table A2.5), paralleling the case of the A-2/FTG evolved clone with the *cls* deletion relative to its progenitor (Figure 20). By contrast, the two FTG-evolved lines whose progenitors (A-5 and A-6) had IS186 insertions in or near the *cls* gene (Figure 16) evolved no further changes in their membrane fluidity following the FT treatment (Appendix 2, Table A2.5). Taken together, these results indicate that the *cls* mutations are a major, but not sole, determinant of the evolved changes in membrane fluidity measured after the FT treatment.

To this point, our results on membrane fluidity are based on laurdan as a probe, which is sensitive to changes at the water-lipid interface. We also performed fluorescence polarization measurements using the probe DPH, which is used to detect differences in fatty acyl chains in the membrane. However, we found no differences between multiple FTG-evolved lines and their progenitors, either during stationary phase or after the FT treatment.

We also examined the effect of the evolved *cls* deletion mutation on sensitivity to the hydrophobic antibiotic novobiocin. The *cls* gene is known to affect resistance to novobiocin (Ivanisevic et al. 1995), although other genes are also involved. As we expected, the A-2 progenitor with its *cls*<sup>+</sup> allele is much more resistant to novobiocin than its isogenic counterpart with the evolved *cls* deletion, with the former producing >500 times as many colonies on plates supplemented with that antibiotic at 100 µg/mL (data not shown). Unexpectedly, the evolved strain A-2/FTG with the *cls* deletion allele is slightly less sensitive to novobiocin than its counterpart with the ancestral *cls*<sup>+</sup> allele, with the difference being about 3-fold. These results show that the evolution of the *cls* gene has a measurable effect on novobiocin resistance, while also supporting our other results that indicate epistatic interactions between *cls* and one or more other loci that evolved under the FTG regime.

## Phenotypic consequences of evolved *uspA/B* mutation

Recall that some or all clones tested in 8 of the 15 FTG evolved populations have identical IS150 insertions in the *uspA/B* intergenic region (Figure 17, Table 4). We constructed isogenic strains, in an evolved genetic

background only, by replacing the *uspA/uspB*::IS150 allele in clones from the AncB/FTG evolved line with the *uspA/B* ancestral allele. Figure 21 shows the relative fitness values measured for the ancestor (without the IS element), the AncB/FTG evolved line with its evolved *uspA/B*::IS150 allele, and the same evolved strain except with that IS150 insertion replaced by the ancestral allele.

As expected, the evolved clone has a large fitness advantage relative to its ancestor under the full two-day FTG regime (Figure 21A; paired one-tailed ttest, p < 0.0001). Both FT survival and subsequent growth performance contribute significantly to the overall improvement (Figures 21B and 21C; paired one-tailed t-tests, both p < 0.0001). Without the FT cycle, fitness increased slightly, but significantly, in this evolved line (Figure 21D; paired one-tailed t-test, p = 0.0003), indicating that its adaptation was not entirely specific to the FTG regime. Most of the benefit was however linked to the FT regime. Hence, this evolved line's fitness gain after freezing and thawing was about 60% (Fig. 21C) as compared to its improvement of less than 5% when measured without the FT treatment (Fig. 21D). Again, note the difference in scales between panels C and D of Figure 21; the confidence intervals on the values in panel D are very tight. The fact that this AncB/FTG evolved line shows some non-specific adaptation to the growth conditions, whereas the A-2/FTG line examined previously did not, is probably because AncB/FTG derives from the original ancestor, whereas A-2/FTG derives from a progenitor that had already adapted to the same growth conditions for 20,000 generations.

Eliminating the IS150 insertion from the *uspA/B* intergenic region in the evolved clone (AncB/FTG -IS150) causes a significant reduction in FTG fitness (Figure 21A; paired two-tailed t-test, p = 0.0022). Both FT survival and growth performance after the FT cycle benefit from the presence of this insertion (Figures 21B and 21C; paired two-tailed t-tests, p = 0.0358 and 0.0023, respectively). The effect of this mutation is specific to FTG conditions, as there is no significant benefit to the evolved clone of having the IS150 insertion in growth after stationary phase without an intervening FT treatment; in fact, there is a marginally significant advantage when the evolved *uspA/uspB*::IS150 allele is replaced by the insertion-free ancestral allele without the FT treatment (Figure 21D; paired two-tailed t-test, p = 0.0685).

Figure 22 shows the growth dynamics of these same three strains after the FT treatment and following stationary phase at 37°C. After a FT cycle, the evolved line with its IS150 insertion in *uspA/B* has a much shorter lag than the ancestor, while reverting the insertion to its ancestral state reduces the difference (Fig. 22A). Following stationary phase without a FT cycle, the IS150 insertion has no discernible effect in the FTG-evolved background, and the difference in growth trajectories between the evolved line and its ancestor appears to reflect solely a difference in their exponential growth rates (Fig. 22B). Following a 2 h cold shock at 4°C, the evolved line with or without the IS150 insertion recovers at about the same rate at 37°C (data not shown), indicating again that the *uspA/uspB*::IS150 allele is specific to FTG adaptation and is not related to cold temperatures in general.

The physiological basis for the advantage of the evolved *uspA/B*::IS150 allele is unknown, although the precise same allele evolved independently in 8 of the 15 FTG populations. As a step towards understanding the effect of the IS150 insertion, we measured the transcription levels of both *uspA* and *uspB* by performing real-time PCR (RT-PCR) in stationary phase, after a FT cycle, and in growth-permissive conditions 2 h after thawed cultures were diluted into fresh media (Figure 23). Under all three conditions, transcription of *uspB* is reduced by more than 10-fold in the evolved *uspA/B*::IS150 allele relative to both the evolved strain with the ancestral *uspA/B* allele restored and the ancestor itself. By contrast, the same evolved allele has only a small effect on *uspA* transcription under the same test conditions (Appendix 2, Figure A2.6). This difference is consistent with the physical location of the IS150 insertion between the putative  $\sigma^{S}$  promoter and start codon for *uspB*, whereas the upstream regulatory region for *uspA* is not interrupted by the insertion (Figure 17).

Although UspB is called a universal stress protein, it is evidently beneficial to reduce or even eliminate its expression for freeze-thaw survival and recovery. In fact, UspB is a predicted membrane protein, and *uspB* mutants are hypersensitive to ethanol during stationary phase (Farewell et al. 1998). Ethanol fluidizes membranes, and the physiological response to ethanol is to increase membrane rigidity (Dombek and Ingram 1984). We hypothesized, therefore, that the disruption of *uspB* transcription increases membrane fluidity, which would be beneficial in the FTG regime, but which should reduce survival during ethanol exposure. To test this hypothesis, we examined both predicted effects by

comparing the isogenic strains with and without the IS150 insertion that disrupts uspB transcription. Possible differences in membrane fluidity were measured by performing fluorescence anisotropy after a FT cycle, as well as during stationary phase, using both laurdan and DPH as probes. However, we saw no significant differences in any of these cases (Appendix 2, Table A2.5 for laurdan measurements). The strains were tested for ethanol sensitivity through co-cultures with the marked ancestor, as in competition assays, in medium containing 10% ethanol for 1 h either during stationary phase or after FT treatment. Again, however, we saw no significant differences between these strains under either treatment (data not shown). In summary, the IS150 insertion reduces uspB transcription, which is beneficial under the FTG regime, but the physiological basis for that benefit remains unknown.

### DISCUSSION

Fifteen populations of *E. coli* evolved for 150 two-day cycles of a freeze-thaw-growth (FTG) regime. Every other day, each population was diluted 1:100 in glucose minimal medium, during which time the cells grew to stationary phase and exhausted the available glucose; in alternating days, the population was frozen at –80°C, without cryoprotectant, for 22.5 h and then thawed for 1.5 h at room temperature; and the cycle was then repeated by diluting the cells in fresh medium. Our previous research found that this regime was highly stressful, with substantial mortality during each freeze-thaw (FT) cycle and with much longer lags prior to re-commencing growth following the FT treatment than after stationary phase at 37°C (Sleight and Lenski 2007). Our earlier work also

established that these FTG-evolved lines adapted to this regime by improving both their FT survival and the speed with which surviving cells began to grow following dilution in fresh medium and incubation at 37°C (Sleight and Lenski 2007). In this study, we sought to identify the genetic differences between the FTG-evolved lines and their progenitors, and to characterize the resulting mutations for evidence concerning their improved survival and recovery.

We pursued two approaches to find relevant mutational differences between the FTG-evolved lines and their progenitors. First, we identified six candidate genes whose described functions impact a number of physiological processes that are important for FT survival and subsequent recovery. These processes include cold-shock response, membrane fluidity, cryoprotectant synthesis, regulation of stress responses, protein translation, and scavenging of oxygen radicals (Cox and Heckly 1973; Sinensky 1974; Grecz et al. 1980; Calcott and Gargett 1981; Mazur 1984; Calcott 1985; Kandror et al. 2002; Willimsky et al. 1992; Gao and Crister 2000; Stead and Park 2000). We sequenced six key genes involved in these processes (*cspA*, *fabF*, *otsA*, *rpoS*, *rrsA*, and *sodA*) in each of two FTG-evolved lines and the ancestor, but we found no mutations in any of them.

We then pursued a global approach in which we screened the entire genomes of clones from many of the FTG-evolved lines and their progenitors by an RFLP approach using native IS elements as probes (Naas et al. 1994; Papadopoulos et al. 1999; Schneider et al. 2000; Cooper et al. 2001b; de Visser et al. 2004; Schneider and Lenski 2004). This approach led to the discovery of

new IS insertions in multiple FTG-evolved lines at each of two loci, cls and uspA/B, and we therefore systematically screened those loci for mutations in ten clones sampled from each of 15 FTG-evolved lines. In all, we found four FTGevolved lines with new cls mutations, including three different IS150 insertions and one 11-bp deletion (Figure 16). We also found IS186 insertions in two other FTG-evolved lines but, in both cases, these insertions were already present in their progenitors, which had evolved at constant 37°C for 20,000 generations as part of an earlier experiment; hence, these IS186 insertions do not contribute to adaptation specific to the FTG regime, and they were not considered further. The screening also revealed that 8 of the 15 FTG-evolved lines had IS150 insertions in the uspA/B intergenic region; remarkably, all these insertions had the same location and orientation (Figure 17). The possibility that inadvertent cross-contamination of lines might account for the identical mutations in uspA/B was excluded by showing that the FTG-evolved lines had different alleles at another locus, one in which their progenitors had evolved distinguishing alleles as part of the previous experiment at 37°C (nadR, Woods et al. 2006). Parallel genetic changes, as observed in cls and uspA/B, are widely regarded as strong evidence that the resulting phenotypic changes are adaptive (Bull et al. 1997; Ferea et al. 1999; Wichman et al. 1999; Cooper et al. 2001b, 2003; Colosimo et al. 2005; Wood et al. 2005; Pelosi et al. 2006; Woods et al. 2006). Therefore, we sought to examine the effects of the evolved cls and uspA/B alleles on fitness under the FTG regimes, as well as the physiological bases thereof, by making isogenic strains that differed only at those loci.

# Physiological significance of the evolved mutations in cls

The *cls* gene encodes the cardiolipin (CL) synthase enzyme, which catalyzes condensation of two phosphatidylglycerol (PG) molecules to form CL and glycerol (Hirschberg and Kennedy 1972). CL is one of the three main phospholipids in *E. coli*, the other two being phosphatidylethanolamine (PE) and PG (Ames 1968; Cronan 1968; Cronan and Vagelos 1972). The relative amounts of these phospholipids depend on the physiological condition of cells; PG is most abundant in exponentially growing cells, while CL is dominant in stationary-phase cells and also under other conditions when cellular energy levels are lowered (Ames 1968; Cronan 1968; Cronan and Vagelos 1972; Shibuya and Hiraoka 1992; Heber and Tropp 1991). Thus, loss-of-function mutations in the *cls* gene lead to excess PG that cannot be converted to CL during stationary phase (Cronan and Vagelos 1972; Pluschke et al. 1978; Pluschke and Overath 1981).

We used the *cls* deletion mutation that was substituted in population A-2/FTG to test for effects on fitness and cell physiology because it was more readily manipulable than the IS*150* insertions that arose in three other FTG populations. By replacing this evolved *cls* allele with the ancestral allele, we found that the evolved allele contributed substantially to the fitness gain of this line under the FTG regime (Figure 18A). It did so primarily by improving survival during the FT treatment (Figure 18B), although recovery of subsequent growth also improved somewhat in with the evolved *cls*<sup>-</sup> allele relative to the ancestral *cls*<sup>+</sup> allele (Figure 18C). The evolved *cls*<sup>-</sup> allele conferred no advantage in

competition under the same conditions except without a FT cycle (Figure 18D), showing the specificity of its beneficial effect with respect to the FTG regime. When this same *cls*<sup>-</sup> allele was moved into the genetic background of the progenitor, it provided only a slight advantage under the FTG regime (Figure 18A). Thus, while the *cls*<sup>-</sup> allele is highly beneficial to the FTG line in which it arose, much of its advantage depends on epistatic interactions with one or more other mutations that were substituted in that lineage. The same overall conclusions about the beneficial effect of the evolved *cls*<sup>-</sup> allele, and the dependence on genetic background, are supported by comparing growth trajectories of these strains following either the FT treatment or stationary phase at 37°C (Figure 19).

A temperature downshift causes a phase transition in a cell membrane from a fluid to a more rigid, gel-like state (Hazel 1995). Prior research has shown that the increased PG content in *cls* mutants increases membrane fluidity, leading to a 6°C decrease in the midpoint of this phase transition (Pluschke and Overath 1981). This increased fluidity probably occurs because PG has a smaller head group than CL, which is the condensation of two PG molecules. In general, phospholipids with smaller head groups are more cone-shaped than cylindrical, which increases hydrogen-bound interstitial water and allows the molecules to change shape more easily (Slater et al. 1994).

The effect of this evolved *cls* deletion mutation on membrane fluidity was tested using fluorescence anisotropy with the amphipathic probe laurdan. No single technique for characterizing membrane fluidity is sensitive to the entire

range of lipid motions, and estimates of fluidity therefore depend on the motions that can be detected by particular methods (Hazel 1995). Laurdan localizes near the phospholipid head groups in the cytoplasmic membrane, and hence is useful for examining differences in membrane fluidity at the water-lipid interface. This cls mutation significantly increases fluidity (i.e., reduces anisotropy) after a FT cycle in both the evolved and progenitor backgrounds (Figure 20A), but it has no significant effect on fluidity during stationary phase at 37°C (Figure 20B). The anisotropy value for this evolved line after freezing and thawing was nearly the same as when measured in stationary phase at 37°C, indicating that it was better able to maintain the same membrane fluidity in the face of the FT stress than was its progenitor, whose membrane became much more rigid (higher anisotropy) after the FT treatment. Similar changes in membrane fluidity after freezing and thawing were also seen in FTG-evolved lines that had new IS150 insertions in the cls gene; again we saw no differences in fluidity between these evolved lines and their progenitors during stationary phase at 37°C. Freezing and thawing cause changes in hydration, and so the fact that anisotropy values differ among strains only after the FT treatment might indicate a hydrationdependent molecular rearrangement in the head-group region, as other head groups are known to respond to changes in hydration (Hsieh et al. 1997).

Our findings support previous research showing that membrane fluidity plays an important role in allowing organisms to tolerate various stresses over physiological and evolutionary timescales (Ramos et al. 1997; Beney and Gervais 2001), including especially stresses related to temperature (Marr and

Ingraham 1962; Sinensky 1974; Behan-Martin et al. 1993; Herman et al. 1994; Nedwell 1999). To compensate for the increased membrane rigidity caused by a temperature downshift, adaptive responses often increase membrane fluidity, a phenomenon known as "homeoviscous adaptation" (Sinensky 1974; Hazel 1995). This physiological response is typically associated with an increase in the unsaturation of fatty acids. At the outset of our study, we therefore chose fabF as a candidate gene for evolutionary adaptation to the FTG regime. That gene encodes a long-chain acyl-ACP elongation enzyme that contributes to fatty-acid unsaturation. However, no mutations were found when we sequenced fabF in two of the FTG-evolved lines. Furthermore, fluorescence polarization measurements using the probe DPH, which detects differences in fatty acyl chains in the membrane, found no differences between multiple FTG-evolved lines and their progenitors either after a FT treatment or during stationary phase. Evidently, our choice of membrane fluidity as a candidate evolutionary response was appropriate, but the particular gene target was different from the one that we first chose to investigate.

In any case, the increased membrane fluidity associated with the evolved *cls* alleles, and other mutations not yet found, may promote FT survival in several ways. Disruption of the plasmid membrane is the primary cause of FT injury, which leads to changes in osmotic behavior and, potentially, mechanical failure leading to cell death (Steponkus 1984). Membrane fluidity reduces FT injury and promotes survival during freezing and thawing in bacteria and other organisms (Kruuv et al. 1978; Beney and Gervais 2001). We speculate that increased

membrane fluidity in FTG conditions may be beneficial for a number of reasons, including: improved membrane protein function (Letellier et al. 1977; Cronan 1978; Hazel 1995), greater membrane integrity during contractions and expansions caused by dehydration and rehydration, respectively (Steponkus 1984), reduced ice nucleation on the membrane surface (Mindock et al. 2001), and faster recovery of growth since DNA replication requires a fluid membrane (Castuma, et al. 1993).

## Physiological significance of the evolved uspA/B mutations

Eight of the 15 FTG-evolved lines acquired IS150 insertions in the exact same position and orientation in the *uspA/B* intergenic region (Figure 17). As noted earlier, the possibility of accidental cross-contamination was excluded because the FTG-evolved lines had the appropriate alleles at other loci that distinguished them. Removal of this insertion element (i.e. restoration of the ancestral *uspA/B* gene) from a FTG-evolved line caused a significant reduction in fitness under the FTG regime, indicating that the insertion is beneficial (Figure 21A). This effect was precisely duplicated for two independent strain constructions, and the fitness advantage of the *uspA/B*::IS150 accrues during both FT survival and subsequent recovery of growth (Figures 21B and 21C). The evolved *uspA/B* allele confers no significant advantage when fitness assays are performed under the same conditions except without the FT treatment (Figure 21D). Therefore, as we also saw for the *cls*, the benefit of the evolved *uspA/B* state is specific to the FTG regime.

The location of these *uspA/B*::IS150 insertions in relation to the known regulatory regions suggests that they should disrupt expression of *uspB* more strongly than they would interfere with *uspA* (Figure 17). This expectation was confirmed by performing RT-PCR, which showed that *uspB* transcription was severely reduced when the insertion was present under all conditions examined including during stationary phase, after FT treatment, and during subsequent recovery of growth (Figure 23), whereas the insertion had little effect on *uspA* transcription under these same conditions.

The *uspB* gene has a putative  $\sigma^{S}$  promoter (Figure 17), and it should therefore be up-regulated under various stressful conditions (Farewell et al. 1998). Yet, although UspB is named a universal stress protein, it is demonstrably beneficial for freeze-thaw survival and recovery to dramatically reduce its expression. Based on its sequence, UspB is probably a membraneassociated protein, and uspB mutants have been shown to be hypersensitive to ethanol in stationary phase (Farewell et al. 1998). Ethanol fluidizes membranes, and therefore the physiological response to ethanol is to increase membrane rigidity (Dombek and Ingram 1984). Based on these reported effects, we hypothesized that the IS-mediated disruption of uspB transcription increases membrane fluidity, which would benefit cells during freezing and thawing, but which should reduce their survival during exposure to ethanol. To test our hypothesis, we compared isogenic strains with and without the IS 150 insertion that disrupts uspB transcription with respect to both membrane fluidity and ethanol sensitivity. We saw no differences in membrane fluidity, either during

stationary phase or after the FT treatment, using both laurdan and DPH as probes for fluorescence anisotropy. There were also no significant differences between these strains in their ethanol-induced mortality during stationary phase or after FT treatment. The physiological basis for the advantage of the <code>uspA/B::IS150</code> mutant under the FTG regime therefore remains unknown. We are tempted to speculate that this mutation is somehow involved with changes in membrane fluidity, despite our failure to find any such effect, given the facts that membrane fluidity is sensitive to the entire range of lipid motions and that no single method can detect all the potentially relevant motions (Hazel 1995).

Finally, the fact that the *uspA/B*::IS150 insertion is demonstrably beneficial under the FTG regime does not exclude the possibility that the genomic position where it inserted is a "hotspot" for this class of mutation. For example, Cooper et al. (2001b) found that IS-mediated deletions of the ribose-catabolic operon evolved quickly and repeatedly in replicate populations of the long-term experiment in glucose at 37°C for two reasons: the deletion mutants had a competitive advantage and, moreover, an IS element adjacent to the operon in the ancestral strain evidently easily recombined with new insertions to produce deletions at a very high rate at this ribose locus. In the present context, to search for possibly relevant sequence motifs near IS150 insertion target sites in the FTG-evolved lines (Table 4), we employed the MAST program (Bailey and Gribskov 1998) to look for a specific sequence motif using 100-bp regions on either side of each target site. No obvious motifs were found among these sequences, although we found a 6-bp DNA stretch ('GGGGCT') 4-bp

downstream from the *uspA/B* target site that exactly matches an IS150 insertion into an existing IS1 element (Hall et al. 1989). A few other IS150 insertions in our study have some similarity to this 6-bp motif, although with mismatches. However, given the short length of the motif and the small sample of unique IS150 insertions in our study, its biological relevance remains unclear.

In conclusion, we found two loci, *cls* and *uspA/B*, in which several lines that had evolved under a FTG regime independently acquired mutations. Construction of, and competition between, isogenic strains that differ only at those loci demonstrate that the evolved alleles in both genes contribute significantly to the fitness gains under the FTG regime, including improved FT survival and faster recovery of subsequent growth. In the case of *cls*, which encodes an enzyme involved in the conversion of phospholipids, this mutation helps maintain membrane fluidity following FT treatment. The mutations in the *uspA/B* intergenic region severely disrupt transcription of *uspB*, but the physiological basis for the resulting benefit remains unknown. In addition, other mutations in unknown genes also contribute to adaptation to the FTG regime, some of which interact epistatically with the *cls* and *uspA/B* mutations.

#### FIGURES

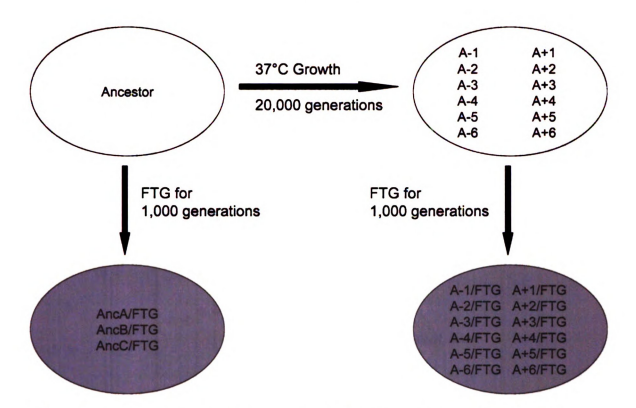


Figure 14. Evolutionary histories of individual freeze-thaw-growth (FTG) populations. The ancestor of a long-term evolution experiment (Lenski et al. 1991) was used to found three FTG-evolved populations. Twelve other FTG-evolved populations were founded by clones sampled from each of 12 populations that previously evolved for 20,000 generations at 37°C. All 15 of the FTG lines evolved for 1,000 generations under the FTG regime, with alternating days of a FT cycle and growth at 37°C. The culture medium used for growth was the same as the one used in the long-term evolution experiment.

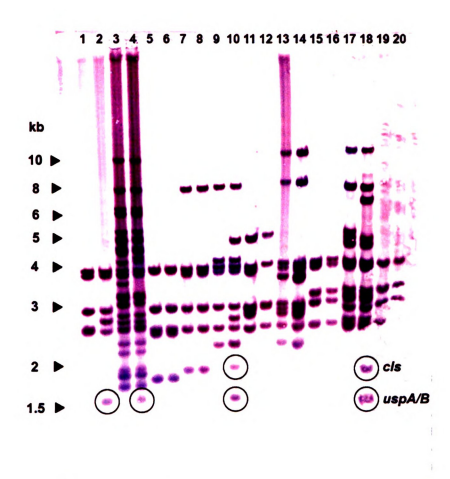


Figure 15. Southern hybridization of *Hinc*II-digested genomic DNA with the IS150 probe. Sizes of bands are given in kb (kilobases) on the left. Insertion bands that occur in multiple FTG-evolved clones are circled and labeled either *cls* or *uspA/B* for the affected genes. The clones are numbered for each lane at top, where each FTG-evolved clone follows its direct progenitor (odd numbers are progenitors and even numbers are FTG-evolved clones). Lanes 1-20 are as follows: 1) Ancestor, 2) AncB/FTG, 3) A+1, 4) A+1/FTG, 5) A+2, 6) A+2/FTG, 7) A+3, 8) A+3/FTG, 9) A+4, 10) A+4/FTG, 11) A+6/FTG, 13) A-1, 14) A-1/FTG, 15) A-2, 16) A-2/FTG, 17) A-3, 18) A-3/FTG, 19) A-4, 20) A-4/FTG.

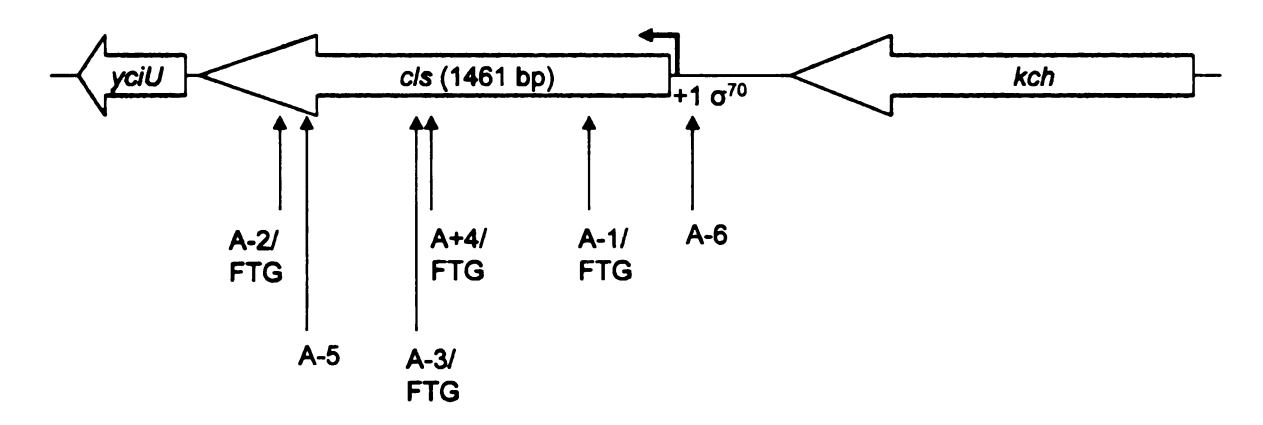


Figure 16. Schematic representation of mutations in cls. Block arrows indicate the direction of transcription for each gene and are drawn to scale. Upward pointing arrows indicate the location of IS150 (A+4/FTG, A-1/FTG, A-3/FTG) and IS186 (A-5, A-6) insertions, and an 11-bp deletion (A-2/FTG) in FTGevolved clones or progenitors already harboring insertions. The A+4/FTG and A-3/FTG insertions were originally discovered by the IS150 Southern hybridization (Figure 15), while all other mutations were found after screening clones in all other FTG-evolved lines for mutations within cls. The IS150 insertion in the A-1/FTG population occurred in a clone not tested in the original IS150 Southern hybridization. The A-2/FTG mutation causes a premature stop codon 43 bp downstream. All mutations occurred in the open reading frame (ORF) except in the case of A-6, which is upstream of the cls transcription start site. The bent arrow indicates the putative transcription start site of cls, and the sigma factor  $(\sigma^{70})$  responsible for its transcription is also shown (Ivanisevic et al. 1995). The yciU gene (330 bp) encodes a hypothetical protein and is predicted to be transcribed in the same direction as cls. In this case, the cls mutations may have polar effects on yciU transcription. The kch gene (1254 bp) is a potassium VIC (Voltage-gated Ion Channel).

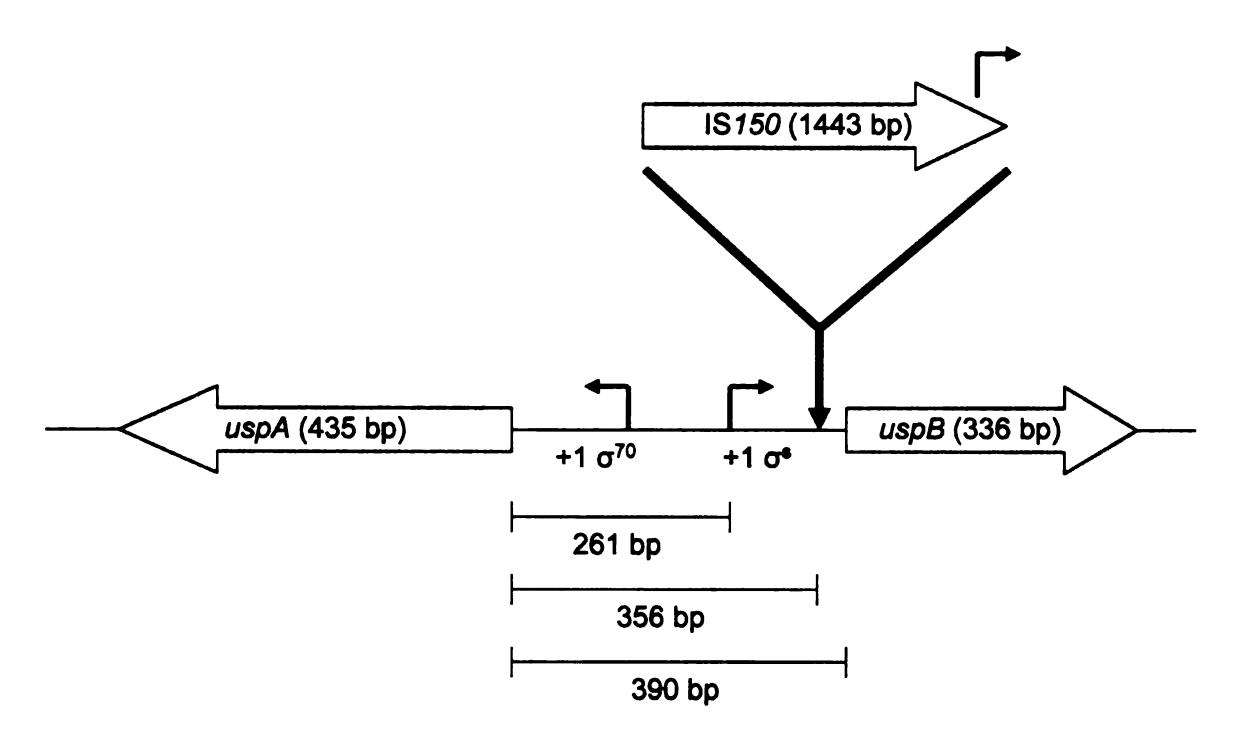
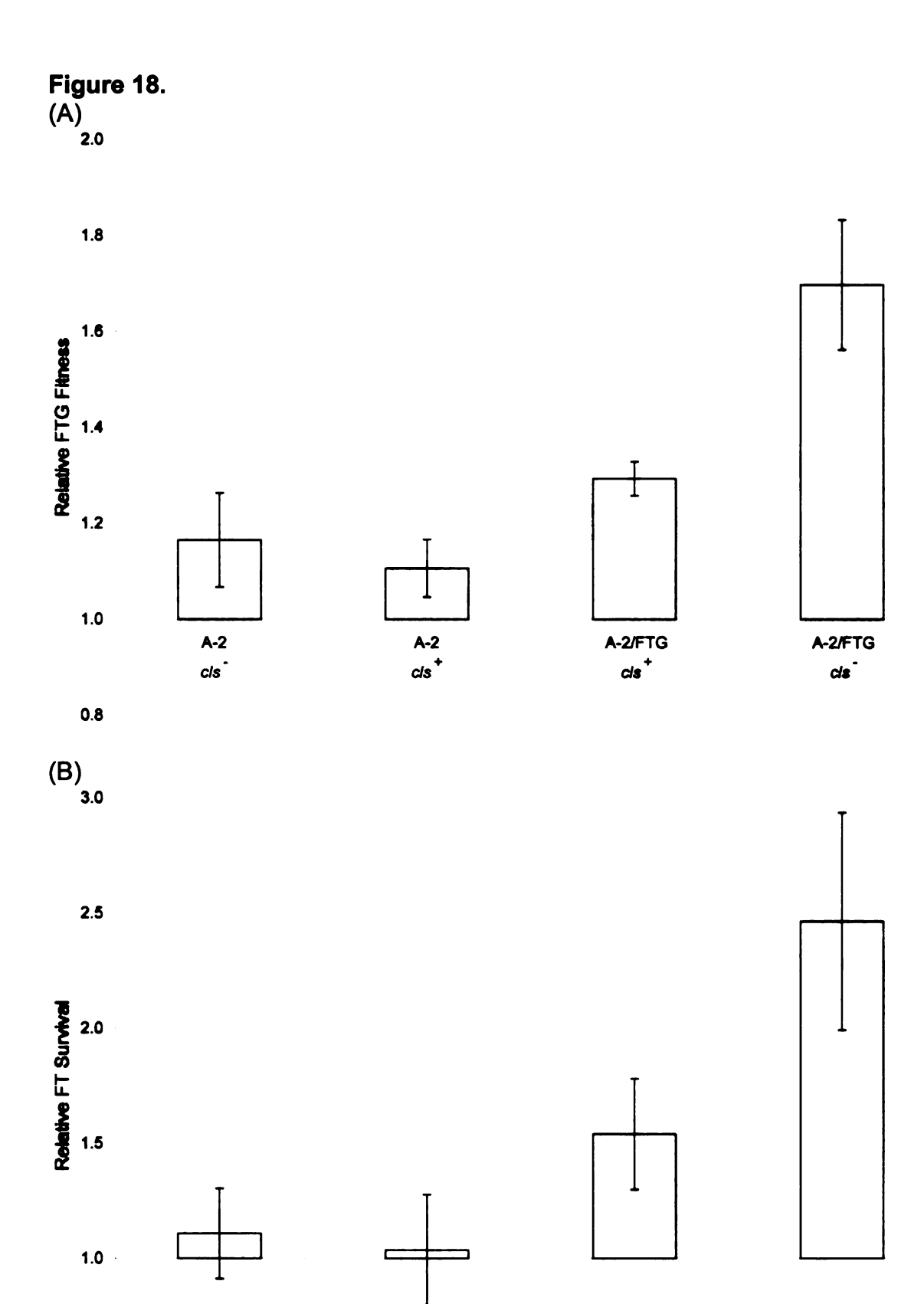


Figure 17. Schematic representation of IS150 insertions in uspA/B intergenic region. Block arrows indicate the direction of transcription for each gene and are not to scale. Eight of the 15 FTG populations had at least one tested clone with an IS150 insertion in the exact same position and orientation, 34 bp upstream of the uspB start codon. This insertion generated a 3-bp duplication at the target site and is 95 bp downstream of the putative uspB promoter ( $\sigma^S$ ). The IS150 element has at least one possible promoter-like sequence directed outward (Schwartz et al. 1988) towards uspB.



A-2/FTG

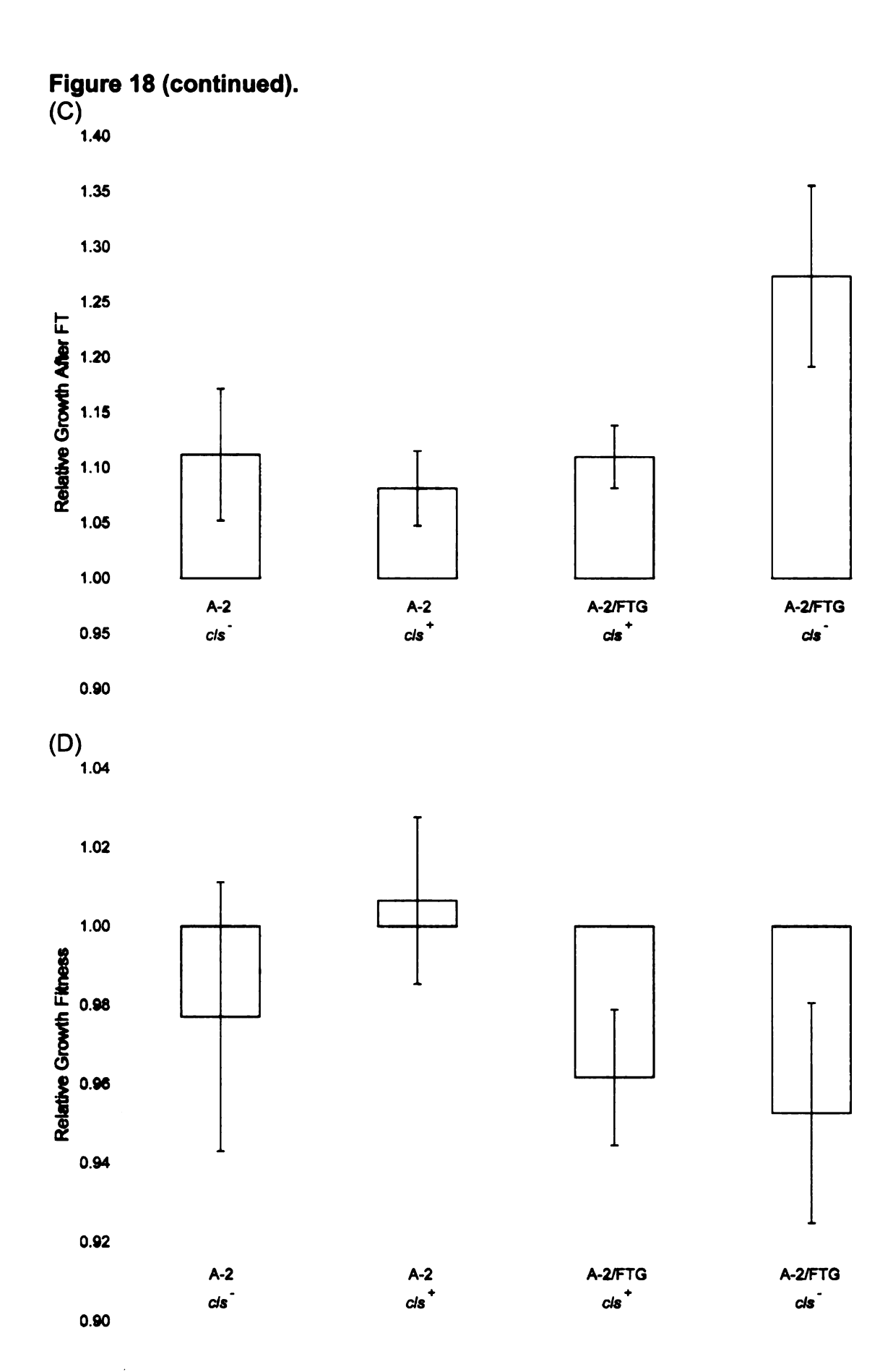
A-2/FTG

A-2 c/s

A-2

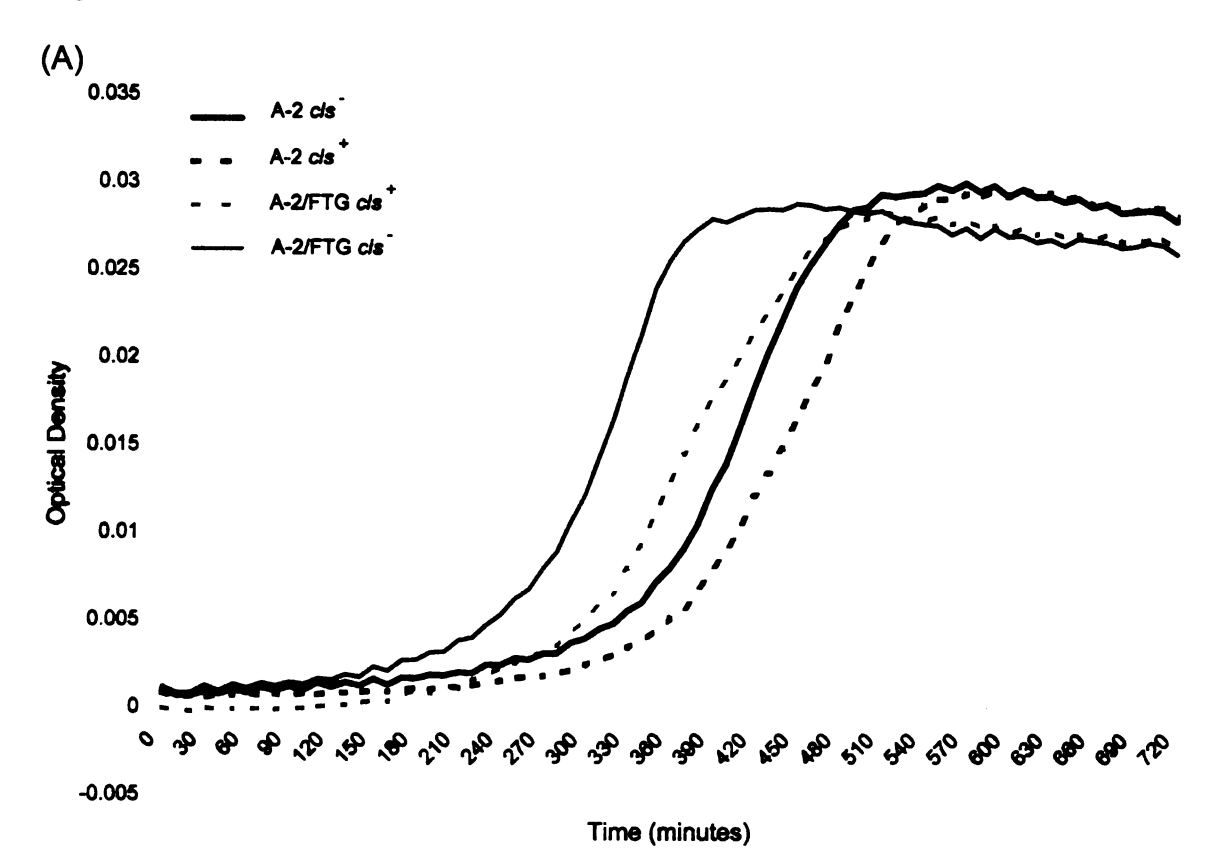
cls

0.5



**Figure 18. Relative fitness components of the following clones:** A-2 *cls*<sup>-</sup> construct, A-2 *cls*<sup>-</sup> progenitor, A-2/FTG *cls*<sup>-</sup> construct, and A-2/FTG *cls*<sup>-</sup> evolved clone. All four types competed against an Ara<sup>+</sup> mutant of the A-2 progenitor. Fitness components are as follows: (A) overall FTG fitness, (B) FT survival, (C) growth after FT, and (D) growth after stationary phase. Error bars are 95% confidence intervals based on eight replicate assays.

Figure 19.



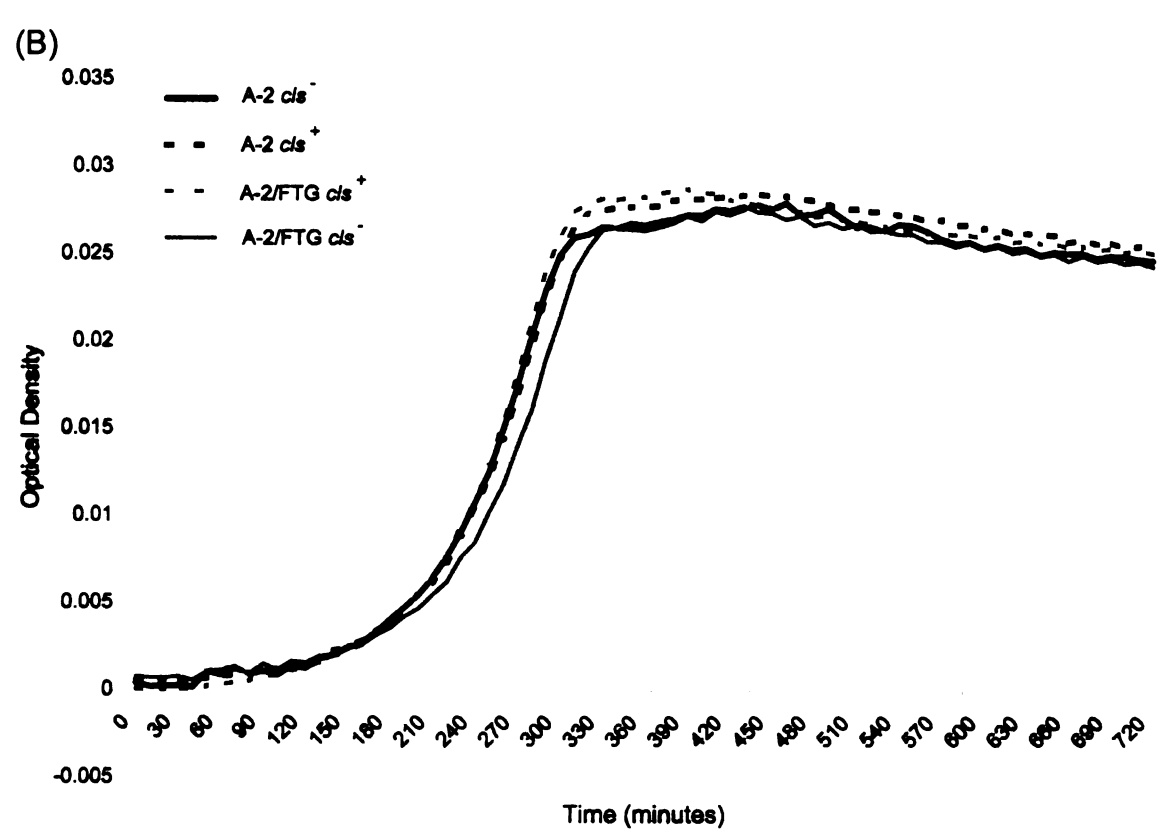


**Figure 19.** Growth dynamics following (A) FT treatment and (B) stationary phase at 37°C. Clones shown are as follows: A-2 *cls*<sup>-</sup> construct (solid black), A-2 *cls*<sup>-</sup> progenitor (dashed black), A-2/FTG *cls*<sup>-</sup> construct (dashed grey), and A-2/FTG *cls*<sup>-</sup> evolved clone (solid grey). Each curve is the average of 18 replicate trajectories.

Figure 20.

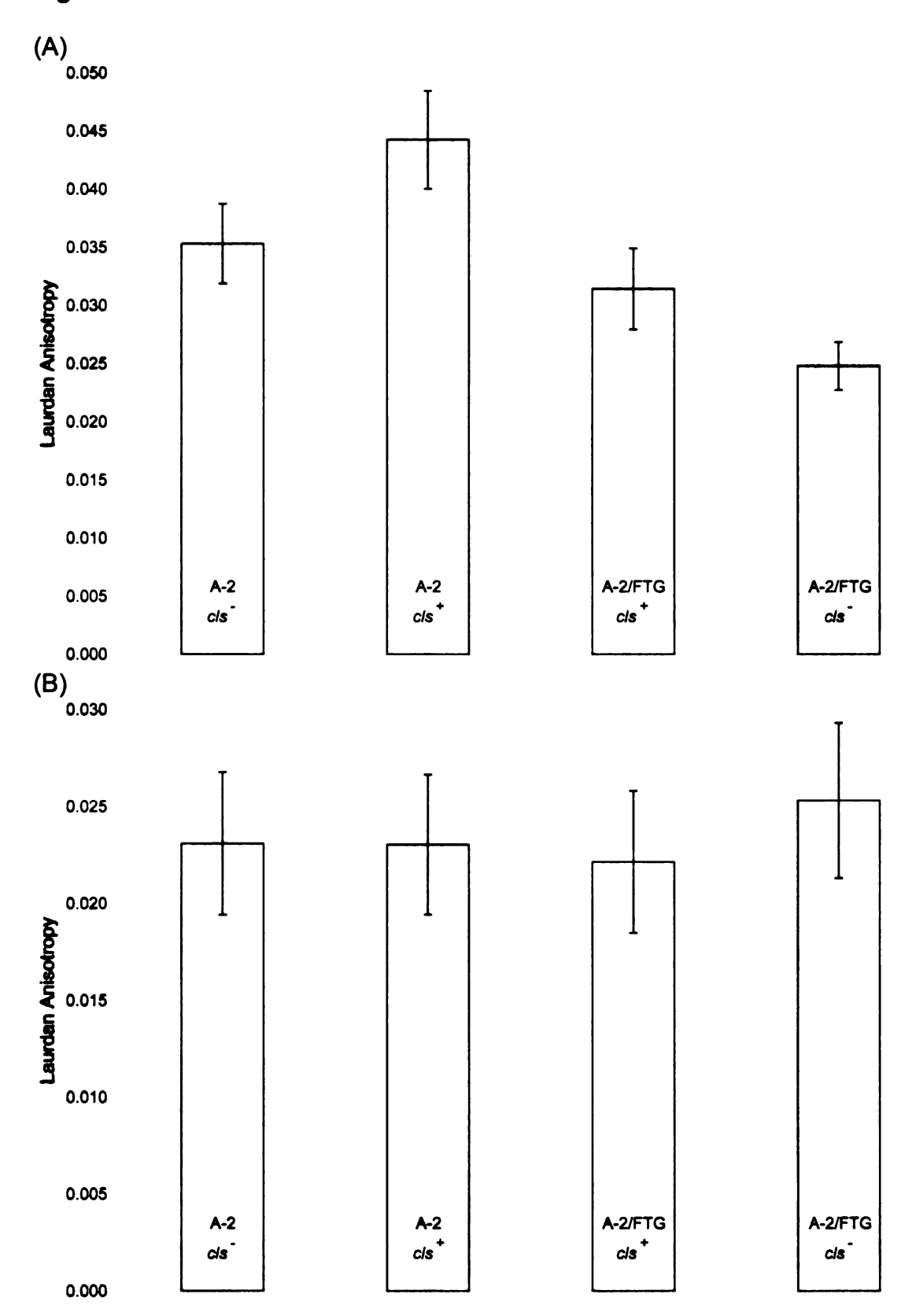
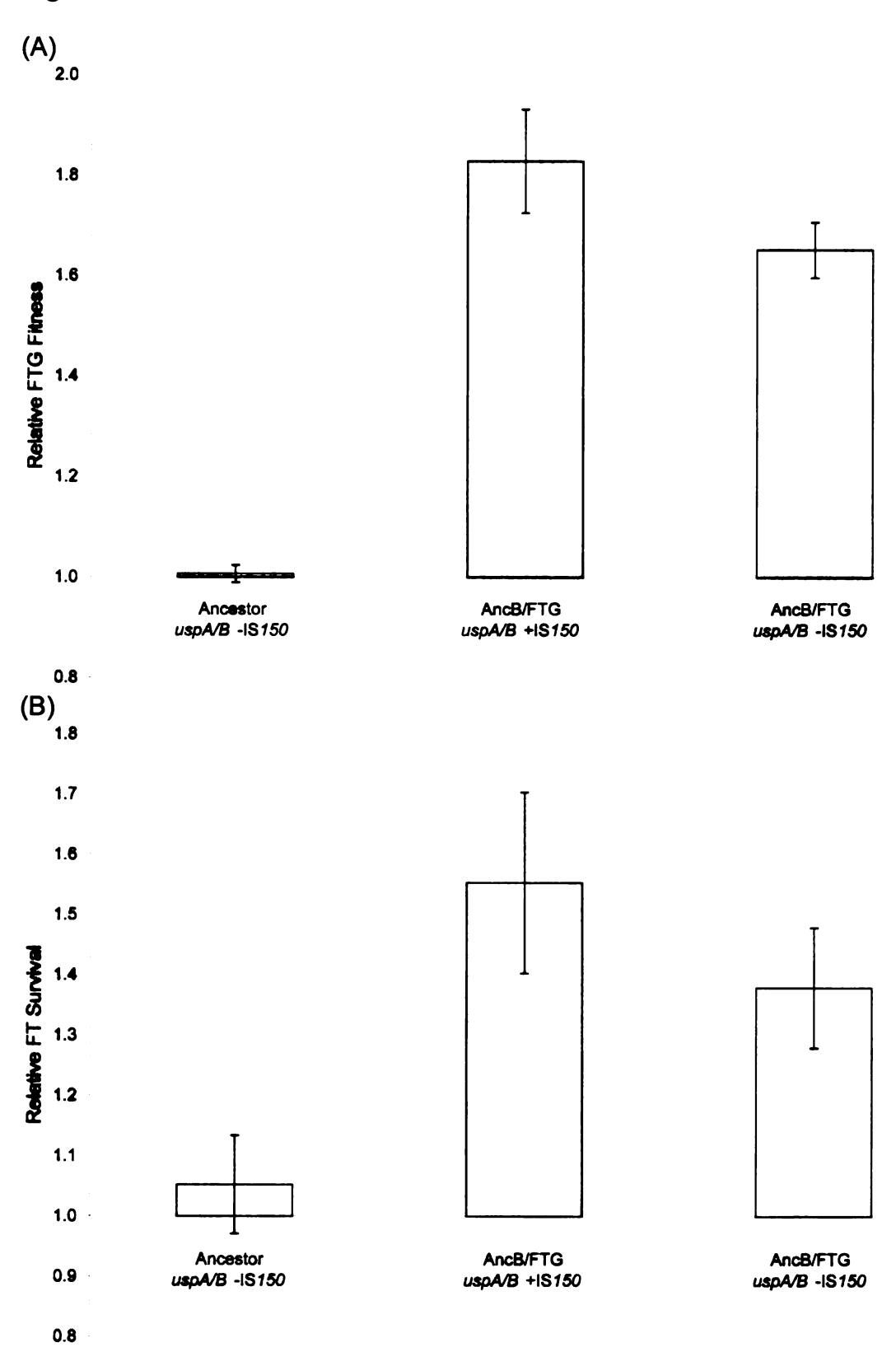


Figure 20. Laurdan anisotropy differences following (A) FT treatment and (B) stationary phase. Each clone was incubated with the fluorescent probe laurdan, and fluorescence anisotropy was measured individually in a fluorometer with 18-fold replication. Lower anisotropy values are indicative of a more fluid membrane in the context of the water-lipid interface. See Materials and Methods for details.





# Figure 21 (continued).

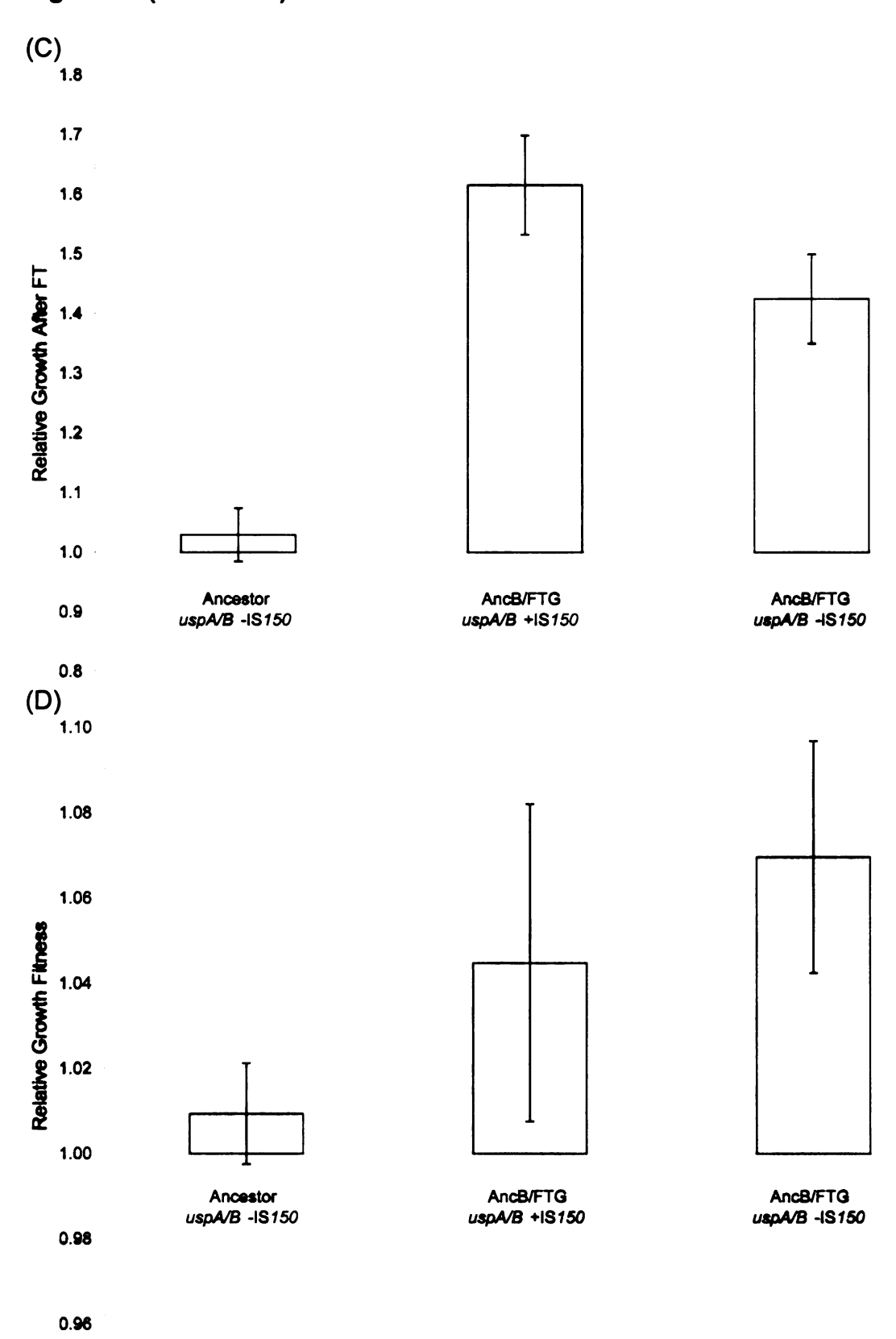
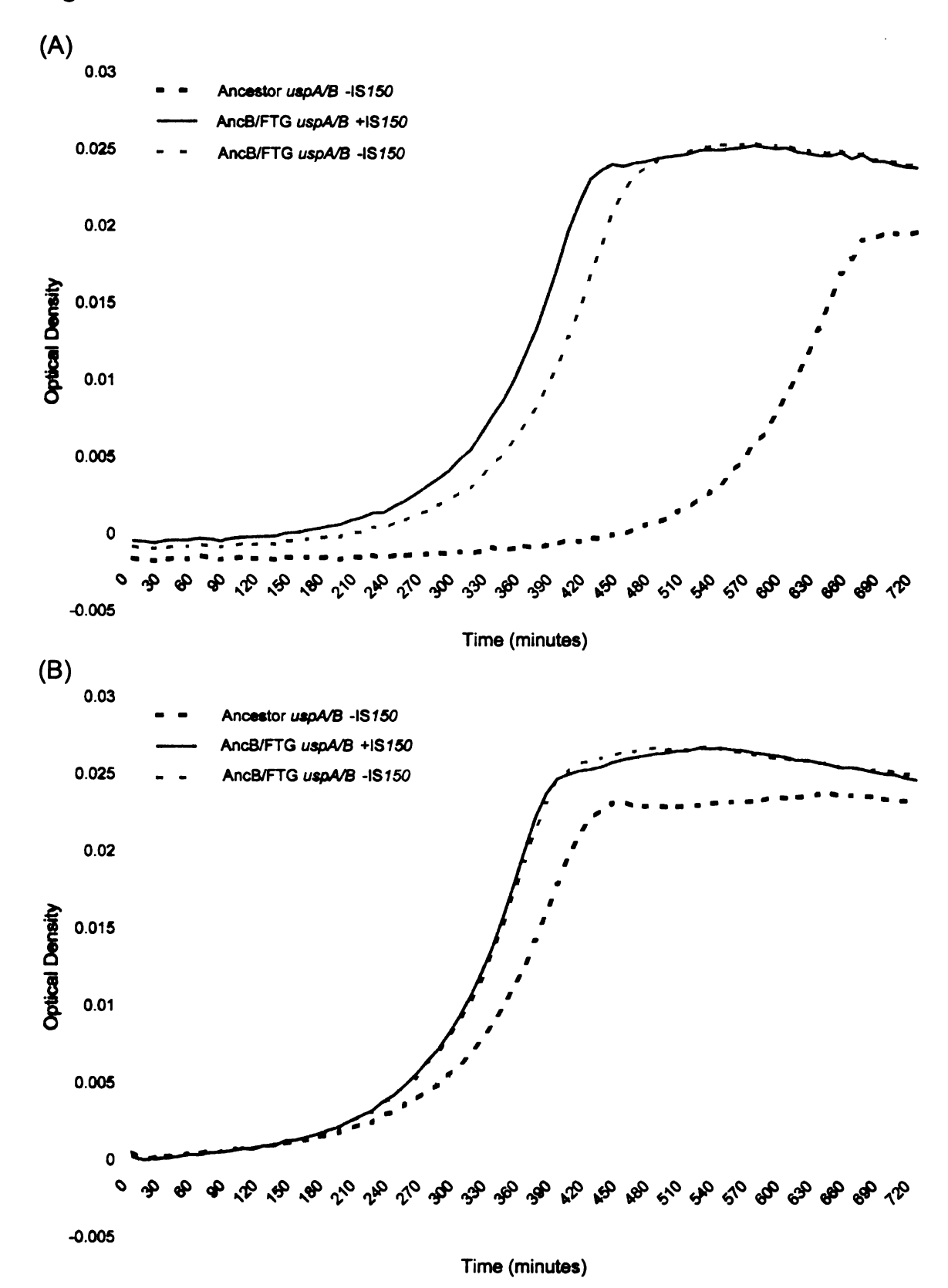


Figure 21. Relative fitness components of the following clones: ancestor (uspA/B-IS150), evolved clone AncB/FTG uspA/B+IS150, and the constructed clone AncB/FTG uspA/B-IS150. All three types competed against the ancestor with the opposite arabinose marker. Each relative fitness component is as follows: (A) overall FTG fitness, (B) FT survival, (C) growth after FT, and (D) growth after stationary phase. Error bars are 95% confidence intervals of 12 replicate assays.

Figure 22.



**Figure 22.** Growth dynamics following (A) FT treatment and (B) stationary phase at 37°C. Clones shown are as follows: Ancestor *uspA/B* –IS150 (dashed black), evolved clone AncB/FTG *uspA/B* +IS150 (solid grey), and constructed clone AncB/FTG *uspA/B* –IS150 (dashed grey). Each curve is the average of 18 replicate trajectories.

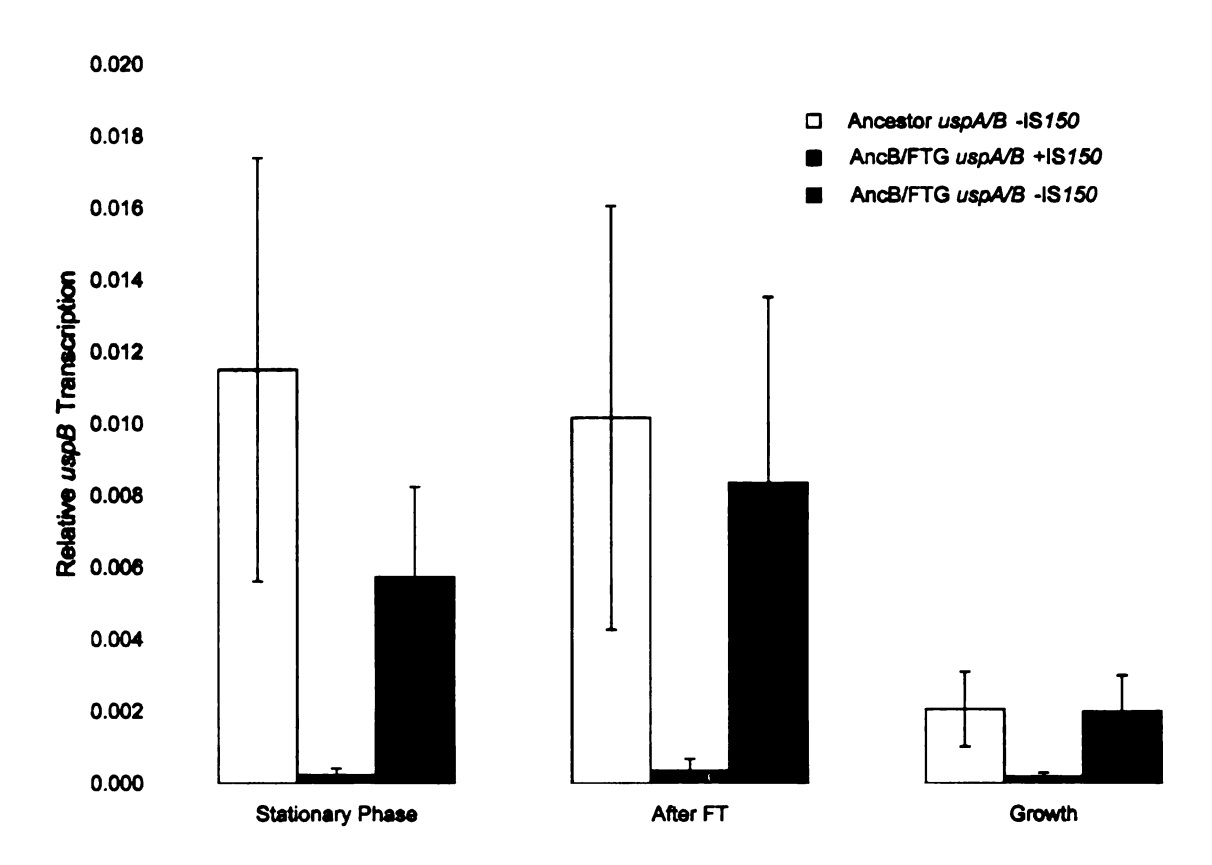


Figure 23. Relative *uspB* transcription differences using Real-Time PCR. *uspB* transcription was measured relative to 16S rRNA transcription as an endogenous control at stationary phase, after a FT cycle, and in growth conditions 2 h after thawed cultures were diluted into fresh media. Clones are as follows: Ancestor *uspA/B* –IS150 (white), evolved clone AncB/FTG *uspA/B* +IS150 (grey), and constructed clone AncB/FTG *uspA/B* -IS150 from which the insertion element was removed (black). The height of each bar represents the mean of two independent RNA extractions, each set with 3-fold replication. Error bars are 95% confidence intervals based on the six-fold replication.

**TABLES** 

Clone	IS1	IS2	IS3	IS4	IS30	IS150	IS186	Total
AncB/FTG	0	0	0	0	0	3	0	3
A+1/FTG	0	0	3	0	0	3	1	7
A+2/FTG	1	0	3	0	0	0	0	4
A+3/FTG	0	0	0	0	0	0	0	0
A+4/FTG	0	0	0	0	0	4	0	4
A+6/FTG	2	0	0	0	0	2	1	5
A-1/FTG	0	0	0	0	0	0	0	0
A-2/FTG	0	0	0	0	0	0	1	1
A-3/FTG	1	0	0	0	0	4	0	5
A-4/FTG	0	0	0	0	0	1	0	1
Total	4	0	6	0	0	17	3	30

**Table 3. IS changes in FTG-evolved lines relative to progenitors.** IS changes are defined as appearance or disappearance of a hybridizing band. A single IS-associated mutation may cause more than one IS change.

Population	Mutation	Target site duplication	Location in nc_000913 a
A+4/FTG	IS150 insertion in cls	3 bp (ATC)	1305917-19
A-1/FTG	IS150 insertion in cls	3 bp (GCG)	1306467-69
A-2/FTG	11-bp deletion in cls	N/A	1305473-83
A-3/FTG	IS150 insertion in cls	3 bp (CGA)	1305865-67
A-5 Progenitor	IS186 insertion in cls	6 bp (TGGATG)	1305580-85
A-6 Progenitor	IS186 insertion in cls	6 bp (GTATAA)	1306774-79
AncA/FTG	IS150 insertion in uspA/B	3 bp (CCC)	3637778-80
AncB/FTG	IS150 insertion in uspA/B	3 bp (CCC)	3637778-80
A+1/FTG	IS150 insertion in uspA/B	3 bp (CCC)	3637778-80
A+2/FTG	IS150 insertion in uspA/B	3 bp (CCC)	3637778-80
A+4/FTG	IS150 insertion in uspA/B	3 bp (CCC)	3637778-80
A-3/FTG	IS150 insertion in uspA/B	3 bp (CCC)	3637778-80
A-5/FTG	IS150 insertion in uspA/B	3 bp (CCC)	3637778-80
A-6/FTG	IS150 insertion in uspA/B	3 bp (CCC)	3637778-80

Table 4. Mutations in cls and uspA/B genes.

<sup>&</sup>lt;sup>a</sup> Pubmed Accession Number for the *E. coli* K-12 genome (Riley et al. 2006).

Timepoint	100	200	300	400	500	600	700	800	900	1000
A+4/FTG	1/8	1/9	2/8	6/9	6/8	4/5	0/3	5/6	5/5	3/10
A-1/FTG	0/5	0/5	0/5	0/5	0/1	0/4	n.d.	2/3	4/4	1/10
A-3/FTG	0/5	0/5	1/5	2/5	4/4	4/4	3/5	2/3	n.d.	10/10

**Table 5.** *cls* mutations in FTG-evolved lines through time. FTG-evolved populations having IS*150* mutations in *cls* at generation 1000 were tracked every 100 generations during FTG evolution. The numerator is the number of clones harboring an IS element as determined by PCR. The denominator is the number of clones tested (n.d., not determined).

Timepoint	100	200	300	400	500	600	700	800	900	1000
AncA/ FTG	0/9	0/8	0/9	0/9	0/17	0/10	1/6	0/10	6/12	1/10
AncB/ FTG	0/7	0/10	3/10	8/10	7/8	3/8	15/32	5/9	6/8	10/10
A+1/FTG	0/10	9/10	9/10	8/10	8/9	10/10	8/8	4/5	7/11	6/10
A+2/FTG	0/10	0/10	0/8	0/9	1/8	0/8	2/9	0/12	0/12	1/10
A+4/FTG	0/8	8/9	10/10	6/6	6/8	9/10	9/10	6/7	9/11	9/22
A-3/FTG	7/10	6/7	9/10	7/9	n.d.	9/9	8/8	12/12	10/10	10/10
A-5/FTG	0/10	9/12	0/9	9/9	10/10	12/12	10/10	8/8	9/9	10/10
A-6/FTG	0/10	1/7	0/8	0/8	0/10	0/5	2/8	0/12	5/6	10/10

**Table 6.** *uspA/B* mutations in FTG-evolved lines through time. FTG-evolved populations having IS*150* mutations in the *uspA/B* intergenic region at generation 1000 were tracked every 100 generations during FTG evolution. The numerator is the number of clones harboring an IS element as determined by PCR. The denominator is the number of clones tested (n.d., not determined).

Source of variation	DF	SS	MS	F	р
Allele	1	0.00109	0.00109	23.457	< 0.0001
Background	1	0.00245	0.00245	52.779	< 0.0001
Allele × Background	1	0.00002	0.00002	0.528	0.4700
Error	68	0.00316	0.00005		
Total	71	0.00672			

Table 7. 2-way ANOVA testing for differences in the *cls* allele, progenitor or evolved background, and interaction effects in laurdan anisotropy after freeze-thaw treatment.

Source of variation	DF	SS	MS	F	р
Allele	1	0.00005	0.00005	0.825	0.367
Background	1	0.00001	0.00001	0.141	0.708
Allele × Background	1	0.00004	0.00004	0.769	0.384
Error	68	0.00385	0.00006		
Total	71	0.00395			

Table 8. 2-way ANOVA testing for differences in the *cls* allele, progenitor or evolved background, and interaction effects in laurdan anisotropy after stationary phase.

## REFERENCES

- Ames, G.F. 1968. Lipids of *Salmonella typhimurium* and *Escherichia coli*: structure and metabolism. J Bacteriol 95:833-43.
- Aricha, B., I. Fishov, Z. Cohen, N. Sikron, S. Pesakhov, I. Khozin-Goldberg, R. Dagan, and N. Porat. 2004. Differences in membrane fluidity and fatty acid composition between phenotypic variants of *Streptococcus pneumoniae*. J Bacteriol 186:4638-44.
- Bailey, T.L., and M. Gribskov. 1998. Combining evidence using p-values: application to sequence homology searches. Bioinformatics 14:48-54.
- Bakermans C., A.I. Tsapin, V. Souza-Eqipsy, D.A. Gilichinsky, and K.H. Nealson. 2003. Reproduction and metabolism at –10°C of bacteria isolated from Siberian permafrost. Environ Microbiol 4:321-326.
- Behan-Martin, M.K., G.R. Jones, K. Bowler, and A.R. Cossins. 1993. A near perfect temperature adaptation of bilayer order in vertebrate brain membranes. Biochim Biophys Acta 1151:216-22.
- Bell G. 1997. Selection: The Mechanism of Evolution. New York: Chapman and Hall.
- Beney, L., and P. Gervais. 2001. Influence of the fluidity of the membrane on the response of microorganisms to environmental stresses. Appl Microbiol Biotechnol 57:34-42.
- Beney, L., Y. Mille, and P. Gervais. 2004. Death of *Escherichia coli* during rapid and severe dehydration is related to lipid phase transition. Appl Microbiol Biotechnol 65:457-64.
- Bennett A.F., R.E. Lenski, and J.E. Mittler. 1992. Evolutionary adaptation to temperature. I. Fitness responses of *Escherichia coli* to changes in its thermal environment. Evolution 46:16-30.
- Bennett A.F., and R.E. Lenski. 1993. Evolutionary adaptation to temperature. II. Thermal niches of experimental lines of *Escherichia coli*. Evolution 47:1-12.
- Bennett A.F., and R.E. Lenski. 1997. Phenotypic and evolutionary adaptation of a model bacterial system to stressful thermal environments. Pp. 135-154 in R. Bijlsma and V. Loeschcke, eds. Environmental Stress, Adaptation and Evolution. Birkhäuser, Basel, Switzerland.

- Bennett A.F., and R.E. Lenski. 1999. Experimental evolution and its role in evolutionary physiology. Am Zool 39:346-362.
- Blasband, A.J., W.R. Marcotte, Jr., and C.A. Schnaitman. 1986. Structure of the *Ic* and *nmpC* outer membrane porin protein genes of lambdoid bacteriophage. J Biol Chem 261:12723-32.
- Blot, M. 1994. Transposable elements and adaptation of host bacteria. Genetica 93:5-12.
- Böck A., R. Curtiss III, J.B. Kaper, F.C. Neidhardt, T. Nyström, K. E. Rudd, and C.L. Squires, eds. 2006. *Escherichia coli* and *Salmonella*: Cellular and Molecular Biology. ASM Press, Washington, DC. [Published online at www.ecosal.org]
- Bongers, R.S., M.H. Hoefnagel, M.J. Starrenburg, M.A. Siemerink, J.G. Arends, J. Hugenholtz, and M. Kleerebezem. 2003. IS981-mediated adaptive evolution recovers lactate production by *IdhB* transcription activation in a lactate dehydrogenase-deficient strain of *Lactococcus lactis*. J Bacteriol 185:4499-507.
- Bull, J.J., M.R. Badgett, H.A. Wichman, J.P. Huelsenbeck, D.M. Hillis, A. Gulati, C. Ho, and I.J. Molineux. 1997. Exceptional convergent evolution in a virus. Genetics 147:1497-507.
- Burch C.L, and L. Chao. 2000. Evolvability of an RNA virus is determined by its mutational neighbourhood. Nature 406:625-628.
- Calcott P.H., and R.A MacLeod. 1975. The survival of *Escherichia coli* from freeze-thaw damage: the relative importance of wall and membrane damage. Can J Microbiol, 12:1960-1968.
- Calcott P.H., and A.M. Gargett. 1981. Mutagenicity of freezing and thawing. FEMS Microbiol Lett 10:151-155.
- Calcott P.H., D. Wood, and L. Anderson. 1983. Freezing and thawing induced curing of drug-resistance plasmids from bacteria. Cryo-Lett 4:99.
- Calcott P.H. 1985. Cryopreservation of microorganisms. CRC Crit Rev Biotech 4:279-297.
- Castuma, C.E., E. Crooke, and A. Kornberg. 1993. Fluid membranes with acidic domains activate DnaA, the initiator protein of replication in *Escherichia coli*. J Biol Chem 268:24665-8.

- Charlesworth, B., P. Sniegowski, and W. Stephan. 1994. The evolutionary dynamics of repetitive DNA in eukaryotes. Nature 371:215-20.
- Charlier, D., J. Piette, and N. Glansdorff. 1982. IS3 can function as a mobile promoter in *E. coli*. Nucleic Acids Res 10:5935-48.
- Chippindale A. 2006. Experimental evolution. Pp. 482-501 in C.W. Fox and J.B. Wolf, eds. Evolutionary Genetics: Concepts and Case Studies. Oxford Univ Press, Oxford, UK.
- Ciampi, M.S., M.B. Schmid, and J.R. Roth. 1982. Transposon Tn10 provides a promoter for transcription of adjacent sequences. Proc Natl Acad Sci U S A 79:5016-20.
- Cloutier J., D. Prevost, P. Nadeau, and H. Antoun. 1992. Heat and cold shock protein synthesis in arctic and temperate strains of rhizobia. Appl Environ Microbiol 58:2846-53.
- Colosimo, P.F., K.E. Hosemann, S. Balabhadra, G. Villarreal, Jr., M. Dickson, J. Grimwood, J. Schmutz, R.M. Myers, D. Schluter, and D.M. Kingsley. 2005. Widespread parallel evolution in sticklebacks by repeated fixation of Ectodysplasin alleles. Science 307:1928-33.
- Cooper T.F., D.E. Rozen, and R.E. Lenski. 2003. Parallel changes in gene expression after 20,000 generations of evolution in *Escherichia coli*. Proc Natl Acad Sci USA 100:1072-1077.
- Cooper V.S., and R.E. Lenski. 2000. The population genetics of ecological specialization in evolving *E. coli* populations. Nature 407:736-739.
- Cooper V.S., A.F. Bennett, and R.E. Lenski. 2001a. Evolution of thermal dependence of growth rate of *Escherichia coli* populations during 20,000 generations in a constant environment. Evolution 55:889-896.
- Cooper V.S., D. Schneider, M. Blot, and R.E. Lenski. 2001b. Mechanisms causing rapid and parallel losses of ribose catabolism in evolving populations of *E. coli* B. J Bacteriol 183:2834-2841.
- Cox C.S., and R.J. Heckly. 1973. Effect of oxygen upon freeze-dried and freeze-thawed bacteria: viability and free radical production. Canadian J Microbiol 19:189-194.
- Cronan, J.E., Jr. 1968. Phospholipid alterations during growth of *Escherichia coli*. J Bacteriol 95:2054-61.

- Cronan, J.E., and P.R. Vagelos. 1972. Metabolism and function of the membrane phospholipids of *Escherichia coli*. Biochim Biophys Acta 265:25-60.
- Cronan, J.E., Jr. 1978. Molecular biology of bacterial membrane lipids. Annu Rev Biochem 47:163-89.
- Crozat E., N. Philippe, R.E. Lenski, J. Geiselmann, and D. Schneider. 2005. Long-term experimental evolution in *Escherichia coli*. XII. DNA topology as a key target of selection. Genetics 169:523-532.
- Cullum A.J., A.F. Bennett, and R.E. Lenski. 2001. Evolutionary adaptation to temperature. IX. Preadaptation to novel stressful environments by *E. coli* adapted to high temperature. Evolution 55:2194-2202.
- Deonier, R.C. 1996. Native insertion sequence elements: locations, distributions, and sequence relationships, pp. 2000–2011 in *Escherichia coli and Salmonella: Cellular and Molecular Biology*, edited by F.C. Neidhardt. ASM Press, Washington, DC.
- de Visser J.A., and R.E. Lenski. 2002. Long-term experimental evolution in Escherichia coli. XI. Rejection of non-transitive interactions as cause of declining rate of adaptation. BMC Evo Bio 2:19.
- de Visser, J.A., A.D. Akkermans, R.F. Hoekstra, and W.M. de Vos. 2004. Insertion-sequence-mediated mutations isolated during adaptation to growth and starvation in *Lactococcus lactis*. Genetics 168:1145-57.
- Dombek, K.M., and L.O. Ingram. 1984. Effects of ethanol on the *Escherichia coli* plasma membrane. J Bacteriol 157:233-9.
- Drouin P., D. Prevost, and H. Antoun. 2000. Physiological adaptation to low temperatures of strains of *Rhizobium leguminosarum* bv. viciae associated with *Lathyrus* spp. FEMS Microb Ecol 32:111-120.
- Eichenbaum, Z., and Z. Livneh. 1998. UV light induces IS10 transposition in *Escherichia coli*. Genetics 149:1173-81.
- Elena S.F., and R.E. Lenski. 2003. Evolution experiments with microorganisms: the dynamics and genetic bases of adaptation. Nature Rev Gen 4:457-469.
- Eriksson M., J.O. Ka, and W.W. Mohn. 2001. Effects of low temperature and freeze-thaw cycles on hydrocarbon biodegradation in Arctic tundra soil. Appl Environ Microbiol 67:5107-5112.

- Farewell, A., K. Kvint, and T. Nystrom. 1998. *uspB*, a new sigmaS-regulated gene in *Escherichia coli* which is required for stationary-phase resistance to ethanol. J Bacteriol 180:6140-7.
- Ferea, T.L., D. Botstein, P.O. Brown, and R.F. Rosenzweig. 1999. Systematic changes in gene expression patterns following adaptive evolution in yeast. Proc Natl Acad Sci U S A 96:9721-6.
- Funchain P., A. Yeung, J.L. Stewart, R. Lin, M.M. Slupska, and J.H. Miller. 2000. The consequences of growth of a mutator strain of *Escherichia coli* as measured by loss of function among multiple gene targets and loss of fitness. Genetics 154:959-970.
- Gao D., and J.K. Critser. 2000. Mechanisms of cryoinjury in living cells. ILAR 41:187-196.
- Gould S.J. 1989. Wonderful Life: The Burgess Shale and the Nature of History. New York: Norton.
- Grant P.R. 1999. *Ecology and Evolution of Darwin's Finches*. Princeton: Princeton University Press.
- Grecz N., T.L. Hammer, C.J. Robnett, and M.D. Long. 1980. Freeze-thaw injury: evidence for double strand breaks in *Escherichia coli* DNA. Biochem Biophys Res Comm 93:1110-1113.
- Hall, B.G., L.L. Parker, P.W. Betts, R.F. Dubose, S.A. Sawyer *et al.* 1989. IS103, a new insertion element in Escherichia coli: characterization and distribution in natural populations. Genetics 121:423-431.
- Hall, B.G. 1999. Spectra of spontaneous growth-dependent and adaptive mutations at *ebgR*. J Bacteriol 181:1149-55.
- Harris, F.M., K.B. Best, and J.D. Bell. 2002. Use of laurdan fluorescence intensity and polarization to distinguish between changes in membrane fluidity and phospholipid order. Biochim Biophys Acta 1565:123-8.
- Harvey P.H., and M.D. Pagel. 1991. *The Comparative Method in Evolutionary Biology.* Oxford: Oxford University Press.
- Hazel, J.R., 1995 Thermal adaptation in biological membranes: Is homeoviscous adaptation the explanation? Annu. Rev. Physiol. 57: 19-42.
- Heber, S., and B.E. Tropp. 1991. Genetic regulation of cardiolipin synthase in *Escherichia coli*. Biochim Biophys Acta 1129:1-12.

- Hebraud M., and P. Potier. 1999. Cold shock response and low temperature adaptation in psychrotrophic bacteria. J Mol Microbiol Biotechnol 1:211-9.
- Herman, P., I. Konopasek, J. Plasek, and J. Svobodova. 1994. Time-resolved polarized fluorescence studies of the temperature adaptation in *Bacillus subtilis* using DPH and TMA-DPH fluorescent probes. Biochim Biophys Acta 1190:1-8.
- Herring, C.D., J.D. Glasner, and F.R. Blattner. 2003. Gene replacement without selection: regulated suppression of amber mutations in *Escherichia coli*. Gene 311:153-63.
- Herring, C.D., A. Raghunathan, C. Honisch, T. Patel, M.K. Applebee, A.R. Joyce, T.J. Albert, F.R. Blattner, D. van den Boom, C.R. Cantor, and B.O. Palsson. 2006. Comparative genome sequencing of *Escherichia coli* allows observation of bacterial evolution on a laboratory timescale. Nat Genet 38:1406-12.
- Hirschberg, C.B., and E.P. Kennedy. 1972. Mechanism of the enzymatic synthesis of cardiolipin in *Escherichia coli*. Proc Natl Acad Sci U S A 69:648-51.
- Hoffmann A.A., and P.A. Parsons. 1993. Evolutionary Genetics and Environmental Stress. Oxford Univ Press, New York.
- Hsieh, C.H., S.C. Sue, P.C. Lyu, and W.G. Wu. 1997. Membrane packing geometry of diphytanoylphosphatidylcholine is highly sensitive to hydration: phospholipid polymorphism induced by molecular rearrangement in the headgroup region. Biophys J 73:870-7.
- Ingraham J. 1987. Effect of temperature, pH, water activity, and pressure on growth. *In: Escherichia coli and Salmonella: Cellular and Molecular Biology* (Edited by: Neidhardt FC). Washington, DC, ASM Press,1543-1553.
- Ivanisevic, R., M. Milic, D. Ajdic, J. Rakonjac, and D.J. Savic. 1995. Nucleotide sequence, mutational analysis, transcriptional start site, and product analysis of *nov*, the gene which affects *Escherichia coli* K-12 resistance to the gyrase inhibitor novobiocin. J Bacteriol 177:1766-71.
- Jaurin, B., and S. Normark. 1983. Insertion of IS2 creates a novel *ampC* promoter in *Escherichia coli*. Cell 32:809-16.
- Jeffreys A.G., K.M. Hak, R.J. Steffan, J.W. Foster, A.K. Bej. 1998. Growth, survival and characterization of *cspA* in *Salmonella enteritidis* following cold shock. Curr Microbiol 36:29-35.

- Jordan, E., H. Saedler, and P. Starlinger. 1968. O<sup>0</sup> and strong polar mutations in the *gal* operon are insertions. Mol. Gen. Genet. 102: 353-363.
- Kandror, O., A. DeLeon, and A.L. Goldberg. 2002. Trehalose synthesis is induced upon exposure of *Escherichia coli* to cold and is essential for viability at low temperatures. Proc Natl Acad Sci U S A 99:9727-32.
- Kidwell, M.G., and D.R. Lisch. 2001. Perspective: transposable elements, parasitic DNA, and genome evolution. Evolution Int J Org Evolution 55:1-24.
- Kruuv, J., J.R. Lepock, and A.D. Keith. 1978. The effect of fluidity of membrane lipids on freeze-thaw survival of yeast. Cryobiology 15:73-9.
- Kvint, K., L. Nachin, A. Diez, and T. Nystrom. 2003. The bacterial universal stress protein: function and regulation. Curr Opin Microbiol 6:140-5.
- Leebanon B., M.A. Drake. 2001. Acid stress, starvation, and cold stress affect post-stress behavior of *Escherichia coli* O157:H7 and non-pathogenic *Escherichia coli*. J Food Protect 64:970-974.
- Lenski R.E., M.R. Rose, S.C. Simpson, and S.C. Tadler. 1991. Long-term experimental evolution in *Escherichia coli*. I. Adaptation and divergence during 2,000 generations. Am Nat 138:1315-1341.
- Lenski R.E., and A.F. Bennett. 1993. Evolutionary response of *Escherichia coli* to thermal stress. Am Nat 142:S47-S64.
- Lenski R.E., V. Souza, L.P. Duong, Q.G. Phan, T.N.M. Nguyen, and K.P. Bertrand. 1994. Epistatic effects of promoter and repressor functions of the Tn10 tetracycline-resistance operon on the fitness of *Escherichia coli*. Molec Ecol 3:127-135.
- Lenski R.E., and M. Travisano. 1994. Dynamics of adaptation and diversification: a 10,000-generation experiment with bacterial populations. Proc Natl Acad Sci USA 91:6808-6814.
- Lenski R.E., J.A. Mongold, P.D. Sniegowski, M. Travisano, F. Vasi, P.J. Gerrish, T. Schmidt. 1998. Evolution of competitive fitness in experimental populations of *E. coli*: what makes one genotype a better competitor than another? Antonie van Leeuwenhoek 73:35-47.
- Lenski R.E., C.L. Winkworth, and M.A. Riley. 2003. Rates of DNA sequence evolution in experimental populations of *Escherichia coli* during 20,000 generations. J Mol Evol 56:498-508.

- Lenski R.E. 2004. Phenotypic and genomic evolution during a 20,000-generation experiment with the bacterium *Escherichia coli*. Plant Breed Rev 24:225-265.
- Leroi A.M., R.E. Lenski, and A.F. Bennett. 1994. Evolutionary adaptation to temperature. III. Adaptation of *Escherichia coli* to a temporally varying environment. Evolution 48:1222-1229.
- Letellier, L., H. Moudden, and E. Shechter. 1977. Lipid and protein segregation in Escherichia coli membrane: morphological and structural study of different cytoplasmic membrane fractions. Proc Natl Acad Sci U S A 74:452-456.
- Leu J.Y., and A.W. Murray. 2006. Experimental evolution of mating discrimination in budding yeast. Curr Biol 16:280-286.
- MacLean R.C., G. Bell, P.B. Rainey. 2004. The evolution of a pleiotropic fitness tradeoff in *Pseudomonas fluorescens*. Proc Natl Acad Sci USA 101:8072-8077.
- Maharjan R., S. Seeto, L. Notley-McRobb, and T. Ferenci. 2006. Clonal adaptive radiation in a constant environment. Science 313:514-517.
- Mahillon, J., and M. Chandler. 1998. Insertion sequences. Microbiol Mol Biol Rev 62:725-74.
- Marr, A.G., and J.L. Ingraham. 1962. Effect of Temperature on the Composition of Fatty Acids in *Escherichia coli*. J Bacteriol 84:1260-7.
- Mazur, P. 1984. Freezing of living cells: mechanisms and implications. Am J Physiol 247:C125-42.
- Mindock, C.A., M.A. Petrova, and R.I. Hollingswort. 2001. Re-evaluation of osmotic effects as a general adaptative strategy for bacteria in subfreezing conditions. Biophys Chem 89:13-24.
- Mongold J.A., A.F. Bennett, and R.E. Lenski. 1996. Evolutionary adaptation to temperature. IV. Adaptation of *Escherichia coli* at a niche boundary. Evolution 50:35-43.
- Mongold J.A., A.F. Bennett, and R.E. Lenski. 1999. Evolutionary adaptation to temperature. VII. Extension of the upper thermal limit of *Escherichia coli*. Evolution 53:386-394.

- Monnet C., C. Beal, G. Corrieu. 2003. Improvement of the resistance of Lactobacillus delbrueckii ssp bulgaricus to freezing by natural selection. J Dairy Sci 86:3048-3053.
- Mountfort D.O., H.F. Kaspar, R.A. Asher, and D. Sutherland. 2003. Influences of pond geochemistry, temperature, and freeze-thaw on terminal anaerobic processes occurring in sediments of six ponds of the McMurdo Ice Shelf, near Bratina Island, Antarctica. Appl Environ Microbiol 69:583-592.
- Muryoi N., M. Sato, S. Kaneko, H. Kawahara, H. Obata, M.W. Yaish, M. Griffith, and B.R. Glick. 2004. Cloning and expression of *afpA*, a gene encoding an antifreeze protein from the arctic plant growth-promoting rhizobacterium *Pseudomonas putida* GR12-2. J Bacteriol 17:5661-5671.
- Naas, T., M. Blot, W. M. Fitch, and W. Arber. 1994. Insertion sequence-related genetic variation in resting *Escherichia coli* K-12. Genetics 136:721-30.
- Naas, T., M. Blot, W. M. Fitch, and W. Arber. 1995. Dynamics of IS-related genetic rearrangements in resting *Escherichia coli* K-12. Mol Biol Evol 12:198-207.
- Nedwell, D. B. 1999. Effect of low temperature on microbial growth: lowered affinity for substrates limits growth at low temperature. FEMS Microbiol Ecol 30:101-111.
- Notley-McRobb L., and T. Ferenci. 2000. Experimental analysis of molecular events during mutational periodic selections in bacterial evolution. Genetics 156:1493-1501.
- Novak M., T. Pfeiffer, R.E. Lenski, U. Sauer, S. Bonhoeffer. 2006. Experimental tests for an evolutionary trade-off between growth rate and yield in *E. coli*. Am Nat 168:242-251.
- Ohtsubo, Y., H. Genka, H. Komatsu, Y. Nagata, and M. Tsuda. 2005. High-temperature-induced transposition of insertion elements in *burkholderia multivorans* ATCC 17616. Appl Environ Microbiol 71:1822-8.
- Packer E.L., J.L. Ingraham, and S. Scher. 1965. Factors affecting the rate of killing of *Escherichia coli* by repeated freezing and thawing. J Bacteriol 89:718-24.
- Panoff J.M., B. Thammavongs, and M. Gueguen. 2000. Cryoprotectants lead to phenotypic adaptation to freeze-thaw stress in *Lactobacillus delbrueckii* spp. *bulgaricus* CIP 101027T. Cryobiology 40:264-269.

- Papadopoulos, D., D. Schneider, J. Meier-Eiss, W. Arber, R.E. Lenski, and M. Blot. 1999. Genomic evolution during a 10,000-generation experiment with bacteria. Proc Natl Acad Sci USA 96:3807-3812.
- Parsons P.A. 1987. Evolutionary rates under environmental stress. Pp. 311-347 in M.K. Hecht, B. Wallace, and G.T. Prance, eds. Evolutionary Biology, Vol 21. Plenum, New York.
- Pelosi L., L. Kühn, D. Guetta, J. Garin, J. Geiselmann, R.E. Lenski, and D. Schneider. 2006. Parallel changes in global protein profiles during long-term experimental evolution in *Escherichia coli*. Genetics 173:1851-1869.
- Pluschke, G., Y. Hirota, and P. Overath. 1978. Function of phospholipids in *Escherichia coli*. Characterization of a mutant deficient in cardiolipin synthesis. J Biol Chem 253:5048-55.
- Pluschke, G., and P. Overath. 1981. Function of phospholipids in *Escherichia coli*. Influence of changes in polar head group composition on the lipid phase transition and characterization of a mutant containing only saturated phospholipid acyl chains. J Biol Chem 256:3207-12.
- Ponder M.A., S.J. Gilmour, P.W. Bergholz, C.A. Mindock, R. Hollingsworth, M.F. Thomashow, and J.M. Tiedje. 2005. Characterization of potential stress responses in ancient Siberian permafrost psychroactive bacteria. FEMS Microbiol Ecol 1:103-115.
- Poon, A., and L. Chao. 2005. The rate of compensatory mutation in the DNA bacteriophage phiX174. Genetics 170:989-99.
- Pruss, B.M., K.P. Francis, F. von Stetten, and S. Scherer. 1999. Correlation of 16S ribosomal DNA signature sequences with temperature-dependent growth rates of mesophilic and psychrotolerant strains of the *Bacillus cereus* group. J Bacteriol 181:2624-30.
- Queitsch C., T.A. Sangster, and S. Lindquist. 2002. Hsp90 as a capacitor of phenotypic variation. Nature 417:618-24.
- Ramos, J.L., E. Duque, J.J. Rodriguez-Herva, P. Godoy, A. Haidour, F. Reyes, and A. Fernandez-Barrero. 1997. Mechanisms for solvent tolerance in bacteria. J Biol Chem 272:3887-90.
- Reif, H.J., and H. Saedler. 1975. IS1 is involved in deletion formation in the *gal* region of *E. coli* K12. Mol Gen Genet 137:17-28.
- Reynolds, A.E., J. Felton, and A. Wright. 1981. Insertion of DNA activates the cryptic *bgl* operon in *E. coli* K12. Nature 293:625-9.

- Riehle M.M., A.F. Bennett, and A.D. Long. 2001. Genetic architecture of thermal adaptation in *Escherichia coli*. Proc Natl Acad Sci USA 98:525-530.
- Riehle M.M., A.F. Bennett, R.E. Lenski, and A.D. Long. 2003. Evolutionary changes in heat-inducible gene expression in lines of *Escherichia coli* adapted to high temperature. Physiol Genom 14:47-58.
- Riehle M.M., A.F. Bennett, and A.D. Long. 2005. Changes in gene expression following high-temperature adaptation in experimentally evolved populations of *E. coli*. Physiol Biochem Zool 78:299-315.
- Riley, M., T. Abe, M. B. Arnaud, M. K. Berlyn, F. R. Blattner, R. R. Chaudhuri, J. D. Glasner, T. Horiuchi, I. M. Keseler, T. Kosuge, H. Mori, N. T. Perna, G. Plunkett, 3rd, K. E. Rudd, M. H. Serres, G. H. Thomas, N. R. Thomson, D. Wishart, and B. L. Wanner. 2006. Escherichia coli K-12: a cooperatively developed annotation snapshot--2005. Nucleic Acids Res 34:1-9.
- Rivkina E.M., E.I. Friedmann, C.P. McKay, and D.A. Gilichinksy. 2000. Metabolic activity of permafrost bacteria below the freezing point. Appl Environ Microbiol 66:3230-3233.
- Rose M.R. 1984. Laboratory evolution of postponed senescence in *Drosophila melanogaster*. Evolution 38:1004-1010.
- Rozen D.E., and R.E. Lenski. 2000. Long-term experimental evolution in *Escherichia coli*. VIII. Dynamics of a balanced polymorphism. Am Nat 155:24-35.
- Rozen D.E., D. Schneider, R.E. Lenski. 2005. Long-term experimental evolution in *Escherichia coli*. XIII. Phylogenetic history of a balanced polymorphism. J Mol Evol 61:171-180.
- Russell N.J. 1990. Cold adaptation of microorganisms. Phil Trans R Soc Lond B Biol Sci 326:598-608.
- Rutherford S.L., and S. Lindquist. 1998. Hsp90 as a capacitor for morphological evolution. Nature 396:336-342.
- Sanger, F., S. Nicklen, and A.R. Coulson. 1977. DNA sequencing with chain-terminating inhibitors. Proc Natl Acad Sci U S A 74:5463-7.
- Scher S., E. Packer, and C. Sagan. 1964. Biological contamination of Mars. I. Survival of terrestrial microorganisms in simulated Martian environments. Life Sci Space Res 2:352-356.

- Schneider D., E. Duperchy, E. Coursange, R.E. Lenski, and M. Blot. 2000. Long-term experimental evolution in *Escherichia coli*. IX. Characterization of insertion sequence-mediated mutations and rearrangements. Genetics 156:477-488.
- Schneider D., E. Duperchy, J. Depeyrot, E. Coursange, R.E. Lenski, and M. Blot. 2002. Genomic comparisons among *Escherichia coli* strains B, K-12, and O157:H7 using IS elements as molecular markers. BMC Microbiol 2:18.
- Schneider, D., and R.E. Lenski. 2004. Dynamics of insertion sequence elements during experimental evolution of bacteria. Res Microbiol 155:319-27.
- Schoustra S.E., A.J. Debets, M. Slakhorst, and R.F. Hoekstra. 2006. Reducing the cost of resistance: experimental evolution in the filamentous fungus *Aspergillus nidulans*. J Evol Biol 19:1115-1127.
- Schwartz, E., M. Kroger, and B. Rak. 1988. IS150: distribution, nucleotide sequence and phylogenetic relationships of a new *E. coli* insertion element. Nucleic Acids Res 16:6789-802.
- Shendure J., G.J. Porreca, N.B. Reppas, X. Lin, J.P. McCutcheon, A.M. Rosenbaum, M.D. Wang, K. Zhang, R.D. Mitra, and G.M. Church. 2005. Accurate multiplex polony sequencing of an evolved bacterial genome. Science 309:1728-1732.
- Shibuya, I., and S. Hiraoka. 1992. Cardiolipin synthase from *Escherichia coli*. Methods Enzymol 209:321-30.
- Siddiqui K.S., and R. Cavicchioli. 2006. Cold-adapted enzymes. Annu Rev Biochem 75:403-433.
- Sinensky, M. 1974. Homeoviscous adaptation--a homeostatic process that regulates the viscosity of membrane lipids in *Escherichia coli*. Proc Natl Acad Sci U S A 71:522-5.
- Slater, S.J., M.B. Kelly, F.J. Taddeo, C. Ho, E. Rubin, and C.D. Stubbs. 1994. The modulation of protein kinase C activity by membrane lipid bilayer structure. J Biol Chem 269:4866-71.
- Sleight S.C., N.S. Wigginton, and R.E. Lenski. 2006. Increased susceptibility to repeated freeze-thaw cycles in *Escherichia coli* following long-term evolution in a benign environment. BMC Evol Biol 6:104.
- Sleight, S.C., and R.E. Lenski. 2007. Evolutionary adaptation to freeze-thaw-growth cycles in *Escherichia coli*. Phys. Biochem. Zool., in press.

- Sniegowski P.D., P.J. Gerrish, and R.E. Lenski. 1997. Evolution of high mutation rates in experimental populations of *E. coli*. Nature 387:703-705.
- Sokal R.R., and F.J. Rohlf. 1981. Biometry. W. H. Freeman, New York.
- Southern, E.M. 1975. Detection of specific sequences among DNA fragments separated by gel electrophoresis. J Mol Biol 98:503-17.
- Souzu H., M. Sato, and T. Kojima. 1989. Changes in chemical structure and function in *Escherichia coli* cell membranes caused by freezing and thawing. II. Membrane lipid state and response of cells to dehydration. Biochim Biophys Acta 978:112-118.
- Stead, D., and S.F. Park. 2000. Roles of Fe superoxide dismutase and catalase in resistance of *Campylobacter coli* to freeze-thaw stress. Appl Environ Microbiol 66:3110-2.
- Steponkus, P. L. 1984. Role of the plasma membrane in freezing injury and cold acclimation. Ann. Rev. Plant Physiol. 35:543-584.
- Thammavongs B., D. Corroler, J.M. Panoff, Y. Auffray, and P. Boutibonnes. 1996. Physiological response of *Enterococcus faecalis* JH2-2 to cold shock: growth at low temperatures and freezing/thawing challenge. Lett Appl Microbiol 23: 398-402.
- Travisano M., J.A. Mongold, A.F. Bennett, and R.E. Lenski. 1995. Experimental tests of the roles of adaptation, chance, and history in evolution. Science 267:87-90.
- Travisano, M. 1997. Long-term experimental evolution in *Escherichia coli*. VI. Environmental constraints on adaptation and divergence. Genetics 146: 471-479.
- Treves, D.S., S. Manning, and J. Adams. 1998. Repeated evolution of an acetate-crossfeeding polymorphism in long-term populations of *Escherichia coli*. Mol Biol Evol 15:789-97.
- Twiss, E., A.M. Coros, N.P. Tavakoli, and K.M. Derbyshire. 2005. Transposition is modulated by a diverse set of host factors in *Escherichia coli* and is stimulated by nutritional stress. Mol Microbiol 57:1593-607.
- Vanounou, S., D. Pines, E. Pines, A.H. Parola, and I. Fishov. 2002. Coexistence of domains with distinct order and polarity in fluid bacterial membranes. Photochem Photobiol 76:1-11.

- Vasi F., M. Travisano, and R.E. Lenski. 1994. Long-term experimental evolution in *Escherichia coli*. II. Changes in life-history traits during adaptation to a seasonal environment. Am Nat 144:432-456.
- Velicer G.J., G. Raddatz, H. Keller, S. Deiss, C. Lanz, I. Dinkelacker, and S.C. Schuster. 2006. Comprehensive mutation identification in an evolved bacterial cooperator and its cheating ancestor. Proc Natl Acad Sci USA 103:8107-8112.
- Walker V.K., G.R. Palmer, and G. Voordouw. 2006. Freeze-thaw tolerance and clues to the winter survival of a soil community. Appl Environ Microbiol 72:1784-1792.
- Wichman H.A., M.R. Badgett, L.A. Scott, C.M. Boulianne, and J.J. Bull. 1999.

  Different trajectories of parallel evolution during viral adaptation. Science 285:422-424.
- Wichman H.A., L.A. Scott, C.D. Yarber, and J.J. Bull. 2000. Experimental evolution recapitulates natural evolution. Phil Trans Roy Soc London B 355:1677-1684.
- Wichman H.A., J. Millstein, J.J. Bull. 2005. Adaptive molecular evolution for 13,000 phage generations: a possible arms race. Genetics 170:19-31.
- Willimsky, G., H. Bang, G. Fischer, and M. A. Marahiel. 1992. Characterization of *cspB*, a *Bacillus subtilis* inducible cold shock gene affecting cell viability at low temperatures. J Bacteriol 174:6326-35.
- Wood, T.E., J.M. Burke, and L.H. Rieseberg. 2005. Parallel genotypic adaptation: when evolution repeats itself. Genetica 123:157-70.
- Woods R., D. Schneider, C.L. Winkworth, M.A. Riley, and R.E. Lenski. 2006. Tests of parallel molecular evolution in a long-term experiment with *Escherichia coli*. Proc Natl Acad Sci USA 103:9107-9112.
- Wouters J.A., B. Jeynov, F.M. Rombouts, W.M. de Vos, O.P. Kuipers, T. Abee. 1999. Analysis of the role of 7 kDa cold-shock proteins of *Lactococcus lactis* MG1363 in cryoprotection. Microbiol 145:3185-3194.
- Wouters J.A., F.M. Rombouts, W.M. de Vos, O.P. Kuipers, and T. Abee. 1999. Cold shock proteins and low-temperature response of *Streptococcus thermophilus* CNRZ302. Appl Environ Microbiol 65:4436-4442.
- Young R.S., P.H. Deal, J. Bell, and J.L. Allen. 1964. Bacteria under simulated Martian conditions. Life Sci Space Res 2:105-111.

Zeyl C. 2006. Experimental evolution with yeast. FEMS Yeast Res 6:685-691.

Zinser, E.R., D. Schneider, M. Blot, and R. Kolter. 2003. Bacterial evolution through the selective loss of beneficial genes. Trade-offs in expression involving two loci. Genetics 164:1271-7.

## **APPENDIX 1**

This appendix provides some supporting data and supplementary analyses for Chapter 2 on "Adaptation to cycles of freezing, thawing, and growth: phenotypic evolution." It includes the following items:

- Figure A1.1. Relative freeze-thaw survival of the 15 FTG-evolved lines and their progenitors.
- Figure A1.2. Comparison of mortality rates between individual FTG-evolved lines and their progenitors under the repeated freeze-thaw regime.
- Figure A1.3. Comparison of mortality rates between the FTG-evolved groups and their progenitors under the repeated freeze-thaw regime.
- Figure A1.4. Relative growth fitness after freezing and thawing of the 15 FTG-evolved lines and their progenitors.
- Figure A1.5. FTG timecourse for two FTG-evolved lines and their progenitors.
- Figure A1.6. Growth timecourse after stationary phase for two FTG-evolved lines and their progenitors.
- Figure A1.7. Fluorescence microscopy of the Evolved Group A (AncB/FTG) clone and the ancestor at different timepoints in the FTG cycle.
- Figure A1.8. Fluorescence microscopy of the Evolved Group B (A+1/FTG) clone and its progenitor (A+1) at different timepoints in the FTG cycle.
- Table A1.1. Phenotypic measurements between individual FTG-evolved lines relative to their progenitors.
- Table A1.2. Statistical tests for FTG-evolved groups and their progenitors.

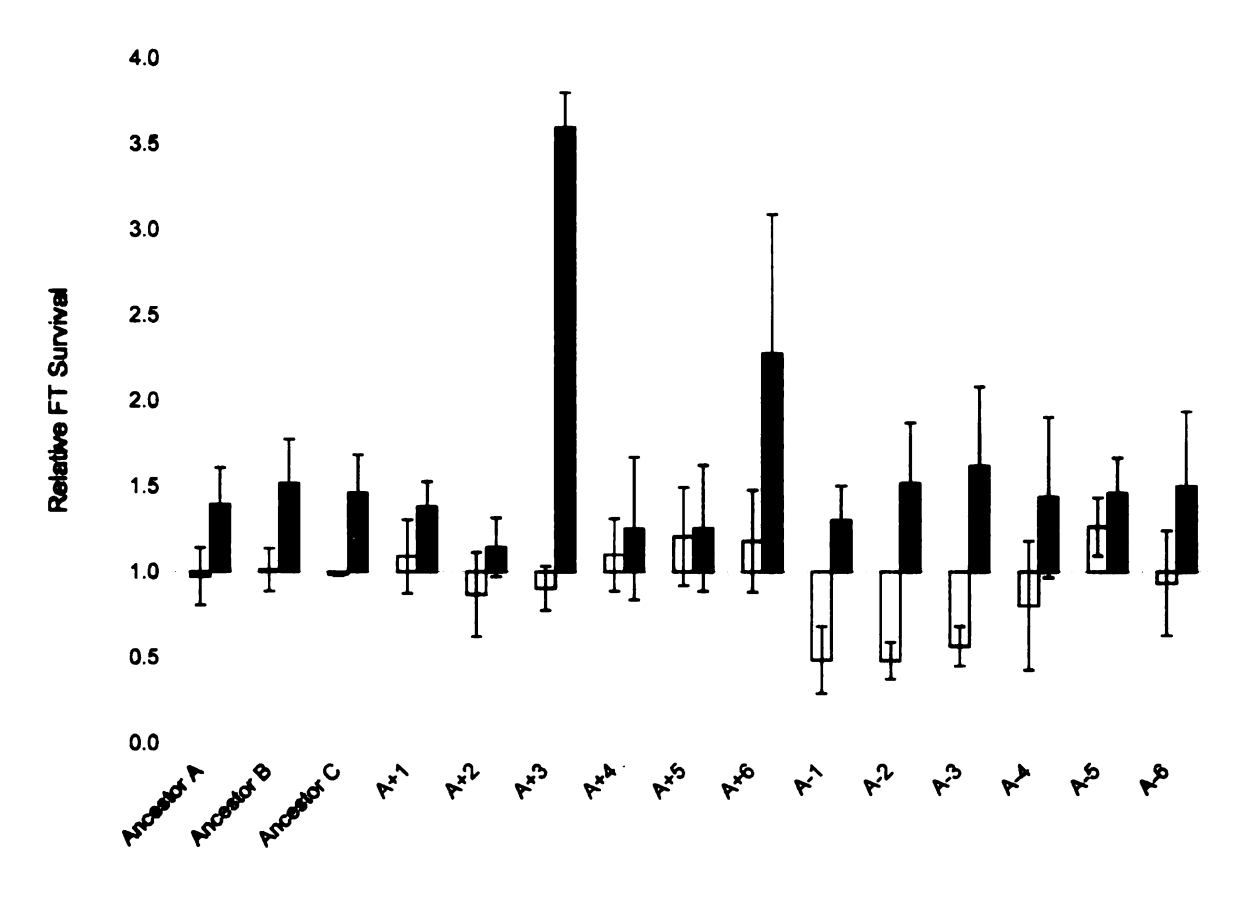


Figure A1.1. Relative freeze-thaw survival of the 15 FTG-evolved lines and their progenitors. FT survival values were measured in competition with the common ancestor during the first half of the two-day FTG cycle. Each evolved line (grey) is paired with its progenitor (white). The three group A lines are shown with different ancestral replicates (designated A, B, and C). The twelve group B lines were derived from long-term lines, designated A+1 to A-6, that previously evolved for 20,000 generations at 37°C. Error bars show 95% confidence intervals based on six replicate FT survival assays for each line or progenitor, except for the group A ancestor, where two of the replicate assays were paired with each of the three evolved lines in that group.

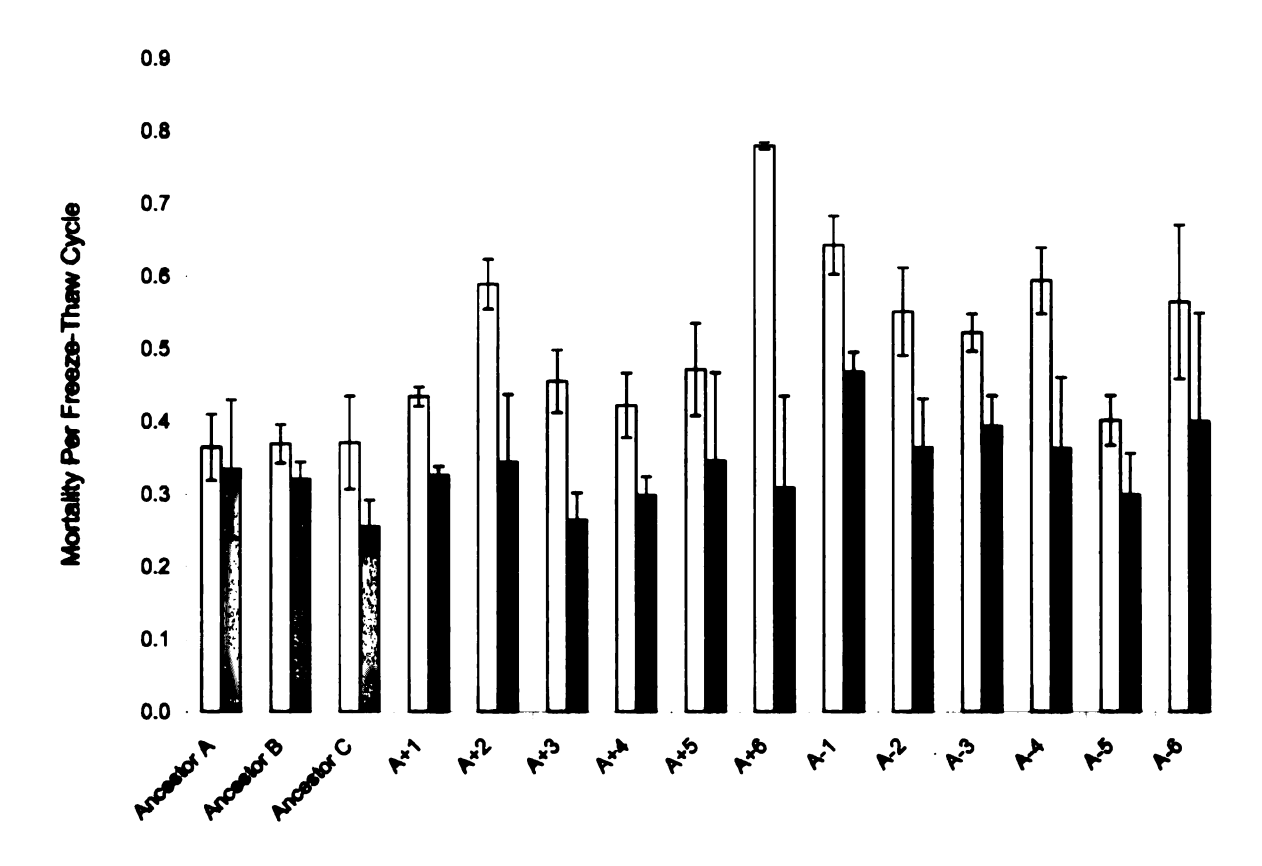


Figure A1.2. Comparison of mortality rates between individual FTG-evolved lines and their progenitors under the repeated freeze-thaw regime. The height of each bar shows the mean mortality rate per day for each of the evolved lines and their progenitors, measured individually over ten daily freeze-thaw cycles, calculated from three assays for each line. Each evolved line (grey) is shown paired with its progenitor (white). The three group A lines are shown with different ancestral replicates (designated A, B, and C). The twelve group B lines were derived from long-term lines, designated A+1 to A-6, that previously evolved for 20,000 generations at 37°C. See the Materials and Methods section in Chapter 1 for the mortality rate calculation. Error bars show 95% confidence intervals based on three replicate repeated FT survival assays for each evolved line or progenitor.

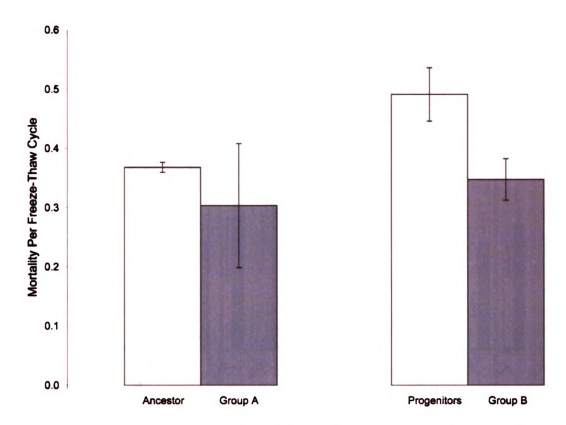


Figure A1.3. Comparison of mortality rates between the FTG-evolved groups and their progenitors under the repeated freeze-thaw regime. The height of each bar shows the mean mortality rate per day for each FTG-evolved group and their progenitor, measured over ten daily freeze-thaw cycles. The mean for each evolved group (grey) is adjacent to the corresponding mean for its progenitors (white). Means for each group were calculated from average values for each member in the group, except for the single ancestor of group A where the mean is based on nine independent measurements. See the Materials and Methods section in Chapter 1 for the mortality rate calculation. Error bars are 95% confidence intervals based on the number of independently evolved lines, except for the ancestor, for which the interval is based on the nine replicate assavs.

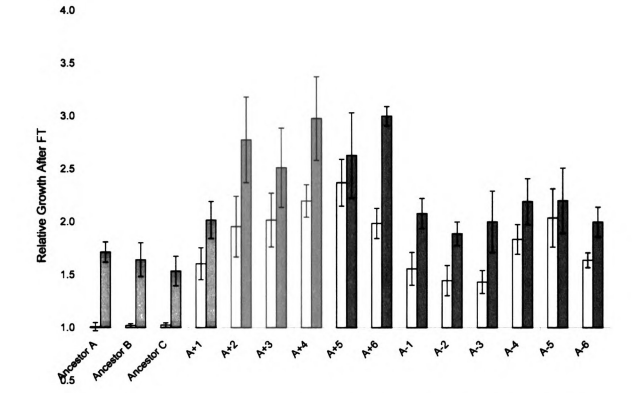
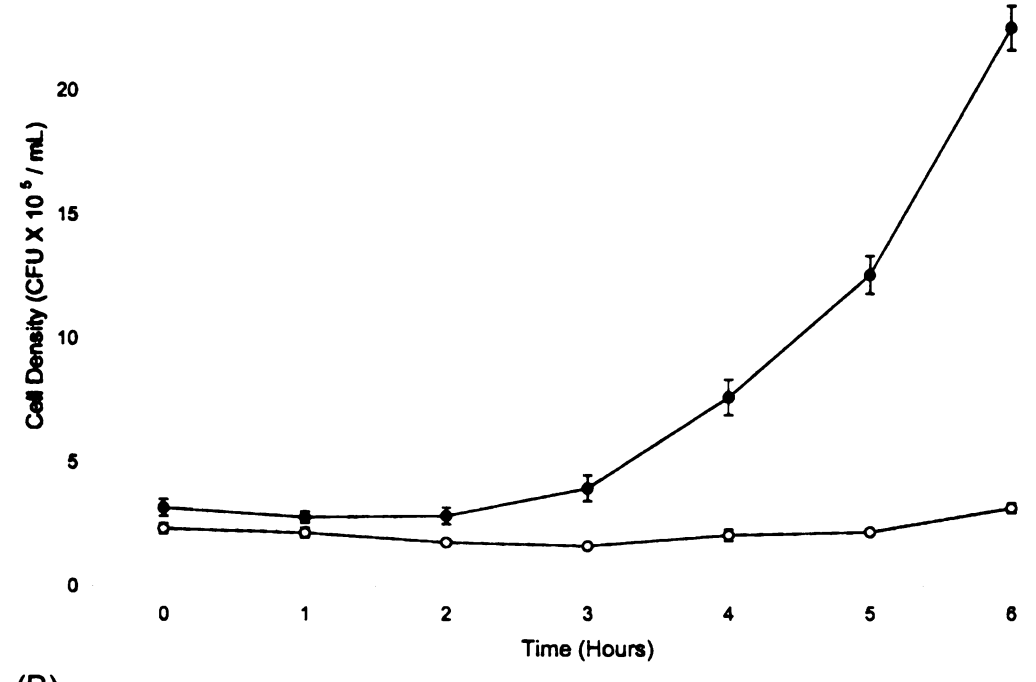


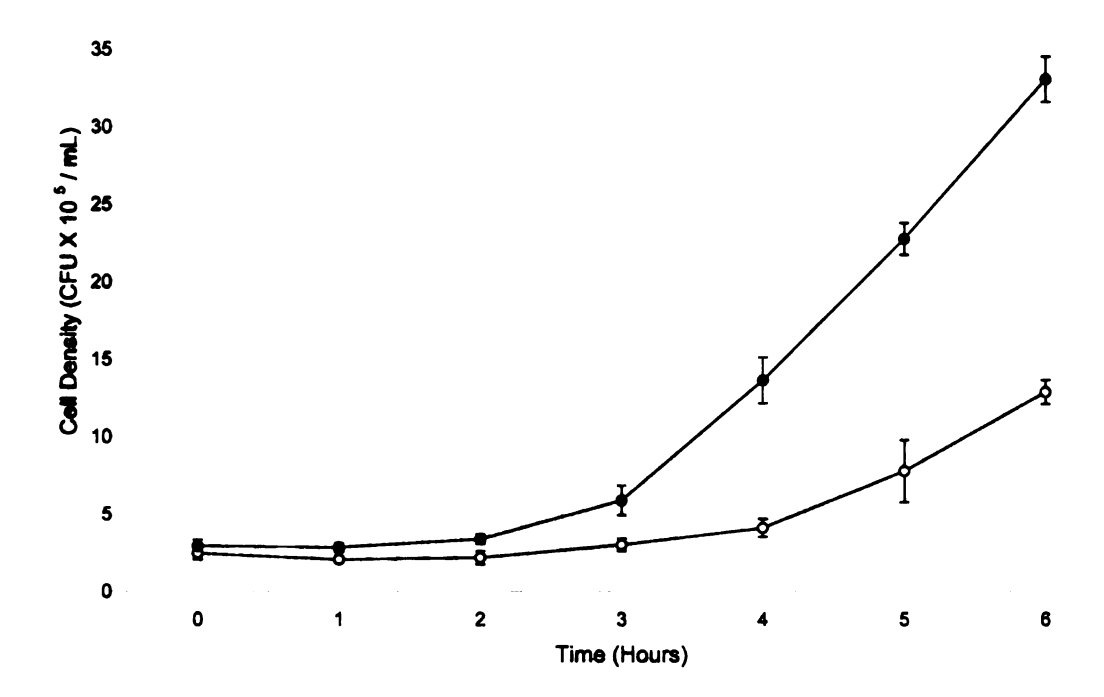
Figure A1.4. Relative growth fitness after freezing and thawing of the 15 FTG-evolved lines and their progenitors. Growth after FT values were measured in competition with the common ancestor during the second half of the two-day FTG cycle. Each evolved line (grey) is paired with its progenitor (white). The three group A lines are shown with different ancestral replicates (designated A, B, and C). The twelve group B lines were derived from long-term lines, designated A+1 to A-8, that previously evolved for 20,000 generations at 37°C. Error bars show 95% confidence intervals based on six replicate growth after FT assays for each line or progenitor, except for the group A ancestor, where two of the replicate assays were paired with each of the three evolved lines in that group.

Figure A1.5.



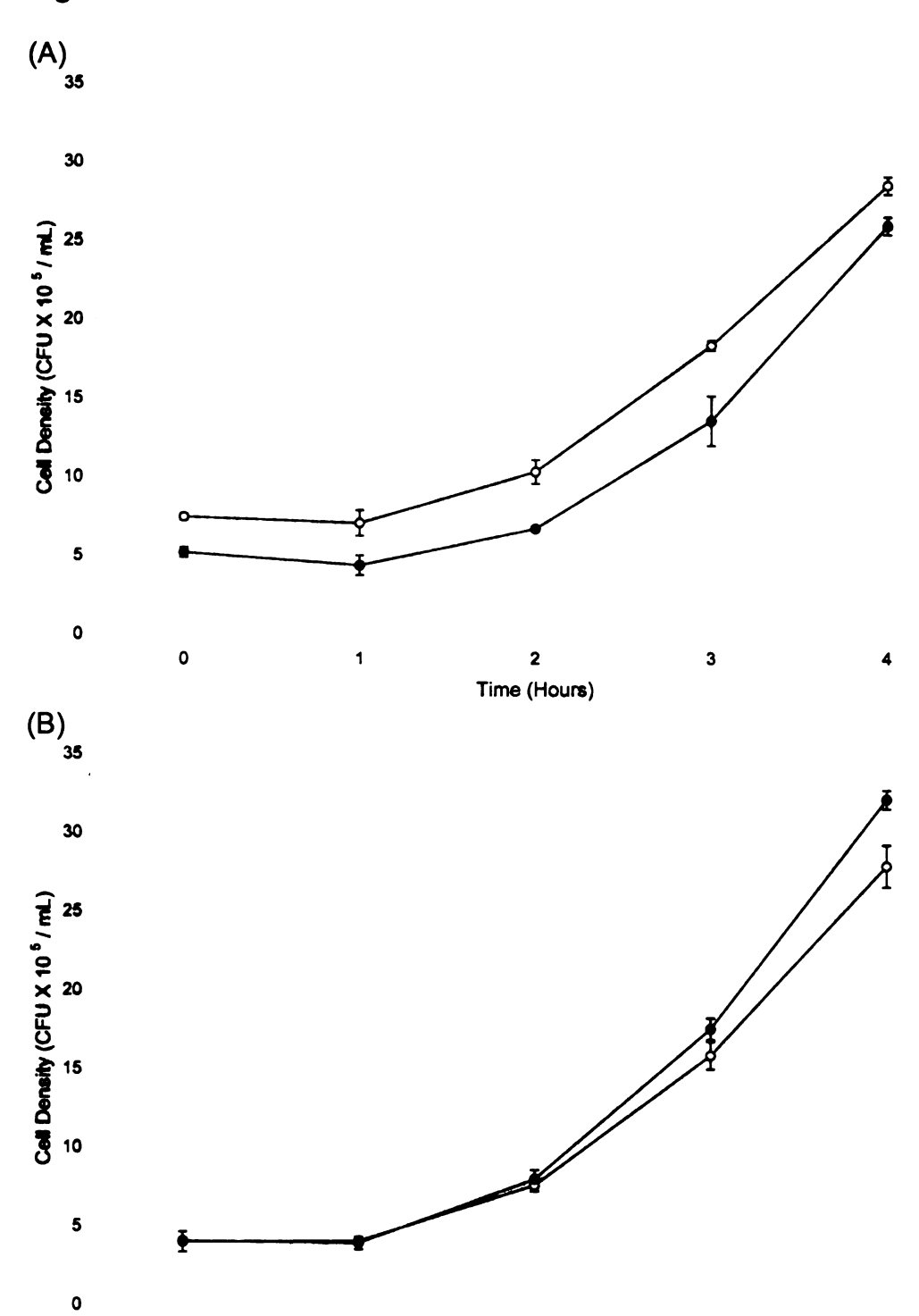






**Figure A1.5. FTG timecourse for two FTG-evolved lines and their progenitors.** (A) Group A evolved line (AncB/FTG) and the ancestor; (B) group B evolved line (A+1/FTG) and its immediate progenitor (A+1). Colony forming units (CFU) measured initially and every hour for six hours after the FT cycle in minimal glucose media. The evolved lines are shown as grey symbols, and their progenitors as black symbols. Each point is the average of each clone replicated sixfold. Error bars are 95% confidence intervals.

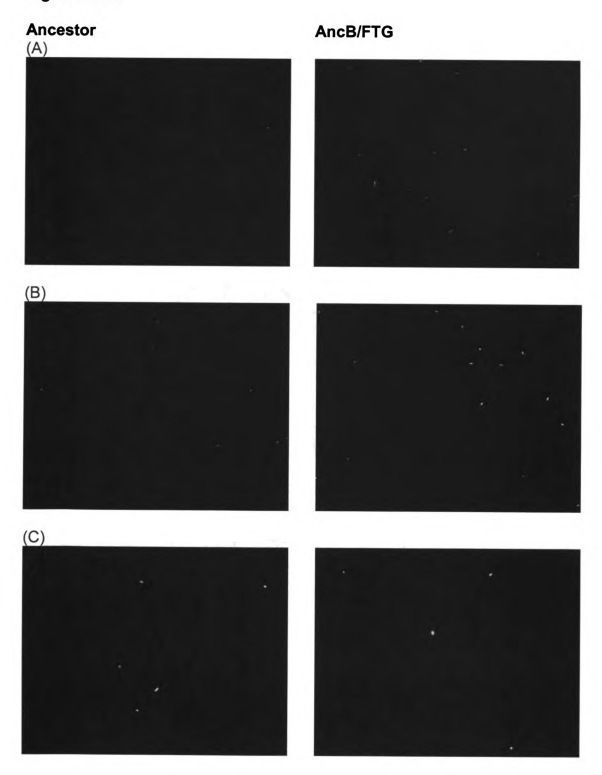




Time (Hours)

Figure A1.6. Growth timecourse after stationary phase for two FTG-evolved lines and their progenitors. (A) Group A evolved line (AncB/FTG) and the ancestor; (B) group B evolved line (A+1/FTG) and its immediate progenitor (A+1). Colony forming units (CFU) measured initially and every hour for four hours after stationary phase in minimal glucose media. The evolved lines are shown as grey symbols, and their progenitors as black symbols. Each point is the average of each clone replicated sixfold. Error bars are 95% confidence intervals.

Figure A1.7.



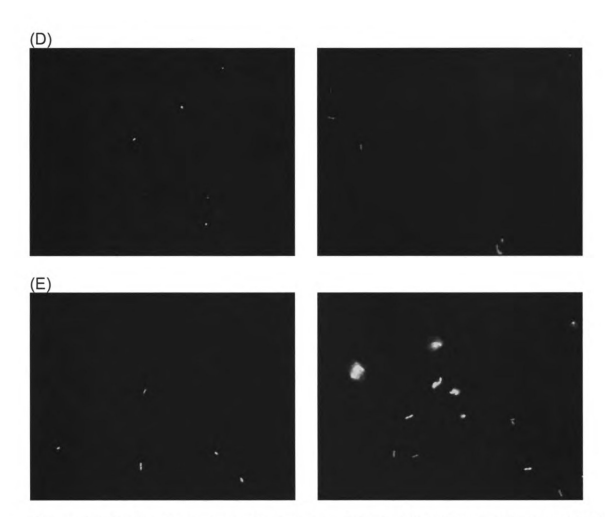
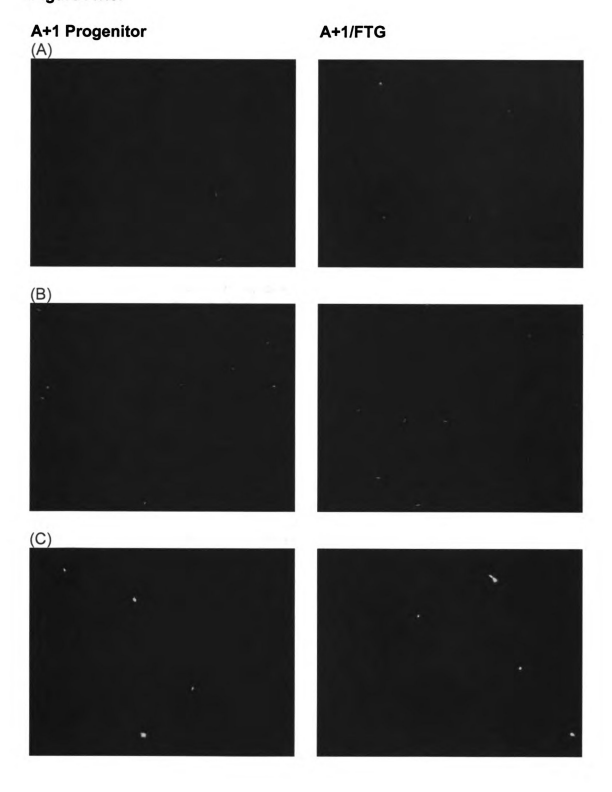


Figure A1.7. Fluorescence microscopy of the Evolved Group A (AncB/FTG) clone and the ancestor at different timepoints in the FTG cycle. (A) Stationary phase, (B) After a FT cycle, (C) 1.5 hours after growth, (D) 3 hours after growth, (E) 4.5 hours after growth. Cells at each timepoint were stained using the Live/Dead count kit (Invitrogen) according to protocol and a sample was put on a microscope slide for visualization with a fluorescent microscope. Live cells are stained green and dead cells are stained red. Images in this dissertation are presented in color.

Figure A1.8.



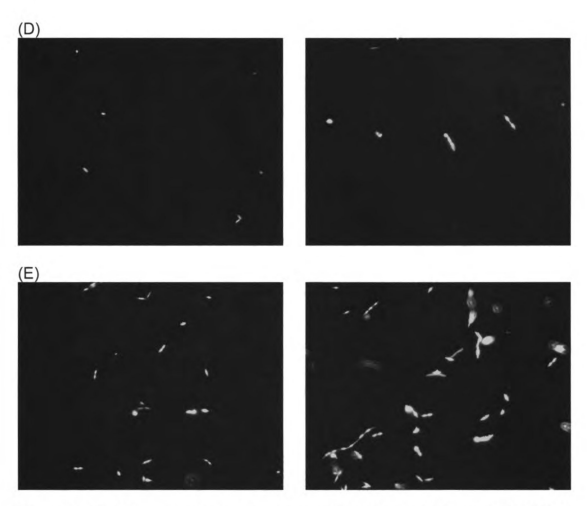


Figure A1.8. Fluorescence microscopy of the Evolved Group B (A+1/FTG) clone and its progenitor (A+1) at different timepoints in the FTG cycle. (A) Stationary phase, (B) After a FT cycle, (C) 1.5 hours after growth, (D) 3 hours after growth, (E) 4.5 hours after growth. Cells at each timepoint were stained using the Live/Dead count kit (Invitrogen) according to protocol and a sample was put on a microscope slide for visualization with a fluorescent microscope. Live cells are stained green and dead cells are stained red. Images in this dissertation are presented in color.

					Doubling	Lag Phase (After	Doubling Time (After	Repeated FT Survival
Clone	FTG Fitness	FT Survival	Growth After FT	Lag Phase (After FT)	Time (After FT)	Stationary Phase)	Stationary Phase)	(Mortality Rate)
Ancestor A/FTG	2.017	1.432	1.700	185.050	12.355	-9.005	9.479	0.918
Ancestor B/FTG	1.907	1.500	1.610	125.036	15.145	-26.655	10.491	0.869
Ancestor C/FTG	1.743	1.482	1.499	148.967	10.984	-48.234	7.580	0.689
Mean	1.889	1.471	1.603	153.018	12.828	-27.965	9.183	0.825
A+1/FTG	1.348	1.265	1.257	121.256	-1.371	31.077	-2.706	0.751
A+2/FTG	1.709	1.317	1.419	170.713	-8.038	38.008	-6.835	0.583
A+3/FTG	1.681	3.981	1.246	90.212	-3.925	-66.546	8.743	0.580
A+4/FTG	1.606	1.140	1.354	-1.379	8.013	-44.504	6.065	0.707
A+5/FTG	1.175	1.040	1.109	101.644	-13.109	-11.926	1.946	0.733
A+6/FTG	2.166	1.928	1.511	106.439	2.795	-6.353	7.595	0.396
A-1/FTG	1.726	2.677	1.335	76.624	8.837	38.555	-7.563	0.728
A-2/FTG	1.802	3.147	1.306	125.748	0.393	-64.301	15.764	0.661
A-3/FTG	1.876	2.854	1.398	224.527	-5.445	18.518	-3.923	0.753
A-4/FTG	1.472	1.786	1.194	135.187	-4.098	16.779	-4.520	0.611
A-5/FTG	1.185	1.156	1.080	4.114	4.510	-56.946	9.336	0.744
A-6/FTG	1.501	1.602	1.220	100.878	-2.901	65.219	-8.859	0.708
Mean	1.604	1.991	1.286	104.664	-1.195	-3.535	1.254	0.663

**Table A1.1. Phenotypic measurements between individual FTG-evolved lines relative to their progenitors.** The mean of eight different phenotypic measurements are shown for each individual FTG-evolved line relative to its progenitor.

Statistical test	One or two	p-value	Greater of
	tailed t-test		groups
FTG Fitness: A > Ancestor	One	0.0034	
FTG Fitness: B > Progenitors	One	< 0.0001	
FT Survival: A > Ancestor	One	0.0014	
FT Survival: B > Progenitors	One	0.0023	
Growth After FT: A > Ancestor	One	0.0042	
Growth After FT: B > Progenitors	One	< 0.0001	
Proportional FTG Fitness: A ?=? B	Two	0.0417	Α
Proportional FT Survival: A < B	One	0.0432	
Proportional Growth After FT: A > B	One	0.0056	
Final FTG Fitness: A ?=? B	Two	0.0003	В
Final FT Survival: A ?=? B	Two	0.3691	
Final Growth After FT: A ?=? B	Two	0.0001	В
Lag After FT: A > Ancestor	One	0.0066	
Lag After FT: B > Progenitors	One	0.0001	
Growth Rate After FT: A > Ancestor	One	0.0075	
Growth Rate After FT: B ?=?			
Progenitors	Two	> 0.5	
Lag After Stationary Phase: A ?=?	_		
Ancestor	Two	> 0.5	
Lag After SP: B ?=? Progenitors	Two	> 0.5	
Growth Rate After SP: A > Ancestor	One	0.0058	
Growth Rate After SP: B ?=?	Two	0.3007	
Progenitors	I I WO	0.3007	

**Table A1.2. Statistical tests for FTG-evolved groups and their progenitors.** Each statistical test between evolved groups and/or their progenitors is shown as a one or two-tailed t-test with the p-value. In the case of a one-tailed t-test, there was an *a priori* hypothesis about the direction of change (< or >) between two groups. In the case of a two-tailed t-test there is no *a priori* hypothesis about the direction of change. If the p-value is less than 0.05, then the far right column shows which of the groups being tested has a significantly greater value.

## **APPENDIX 2**

This appendix provides some supporting data and supplementary analyses for Chapter 3 on "Adaptation to cycles of freezing, thawing, and growth: genetic evolution." It includes the following items:

- Figure A2.1. cls and uspA/B isogenic constructs and reconstructs.
- Figure A2.2. Southern hybridization of *Eco*RV-digested genomic DNA to the IS1 probe.
- Figure A2.3. Southern hybridization of *Eco*RV-digested genomic DNA to the IS3 probe.
- Figure A2.4. Southern hybridization of *Eco*RV-digested genomic DNA to the IS186 probe.
- Figure A2.5. Southern hybridization of *Eco*RV-digested genomic DNA to the IS186 probe (second blot).
- Figure A2.6. Relative *uspA* transcription differences using Real-Time PCR.
- Table A2.1. Primer pairs used to PCR amplify candidate genes.
- Table A2.2. Primer pairs used to PCR amplify IS element probes for RFLP analysis.
- Table A2.3. Primer pairs used to PCR amplify sequences adjacent to IS elements.
- Table A2.4. IS band differences between individual FTG-evolved lines relative to their progenitors.
- Table A2.5. Laurdan anistropy differences between individual FTG-evolved clones, their progenitors, and isogenic constructs.

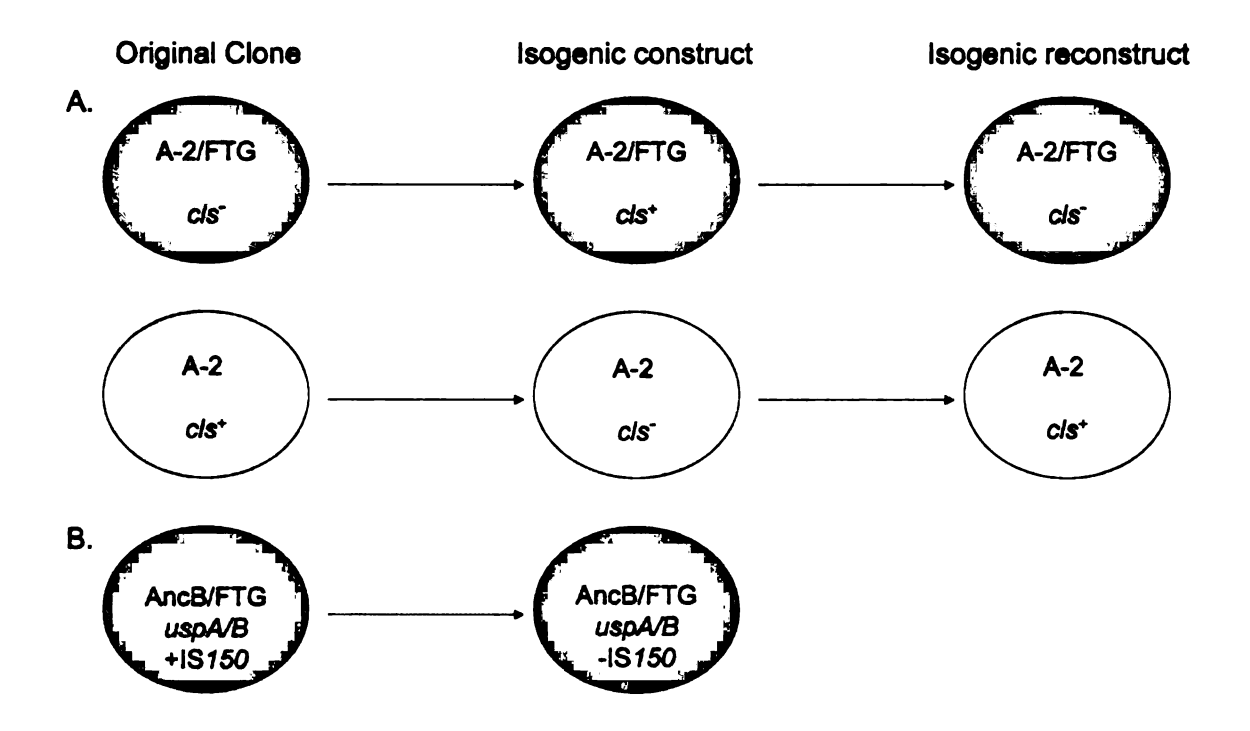


Figure A2.1. cls and uspA/B isogenic constructs and reconstructs. (A) The A-2/FTG population has an 11-bp deletion in the cls ORF in all clones tested within this population. An isogenic construct of the original A-2/FTG clone was made to reverse this mutation to the ancestral state. This isogenic construct was then reconstructed to possess the evolved mutation in order to verify that any FTG fitness differences are caused by the mutation itself (not some hypothetical mutation inadvertently introduced during genetic manipulations). Likewise, to test the effect of this mutation in the reciprocal case, the A-2 progenitor was constructed to have this evolved mutation and reconstructed back to the ancestral state. All constructs and reconstructs were sequenced twice to verify the presence or absence of the evolved mutation and that no other mutations were present within approximately 500 bp on either side. (B) All clones tested in the AncB/FTG population have an IS150 insertion in the uspA/B intergenic region. Two independent isogenic constructs were made to remove this IS150 element and control clones that retained the IS 150 insertion were isolated for FTG fitness competition and growth curve experiments to ensure that any differences are due to the IS150 insertion. In this case, no attempt was made to reconstruct the isogenic constructs back to have the IS150 insertion because in the process this IS150 may recombine with other IS150 elements and cause unwanted genomic rearrangements. All constructs and control clones were sequenced twice to verify the presence or absence of the IS150 insertion and that no other mutations were present 100 bp on either side of the insertion.

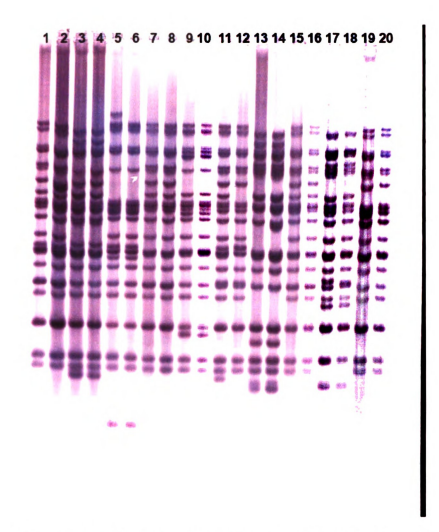


Figure A2.2. Southern hybridization of EcoRV-digested genomic DNA to the Is1 probe. The clones are numbered for each lane at top where each FTG-evolved clone follows its direct progenitor (odd numbers are progenitors and even numbers are FTG-evolved clones). Lanes 1-20 are as follows: 1) Ancestor, 2) AncB/FTG, 3) A+1, 4) A+1/FTG, 5) A+2, 6) A+2/FTG, 7) A+3, 8) A+3/FTG, 9) A+4, 10) A+4/FTG, 11) A+6, 12) A+6/FTG, 13) A-1, 14) A-1/FTG, 15) A-2, 16) A-2/FTG, 17) A-3, 18) A-3/FTG, 19) A-4, 20) A-4/FTG.

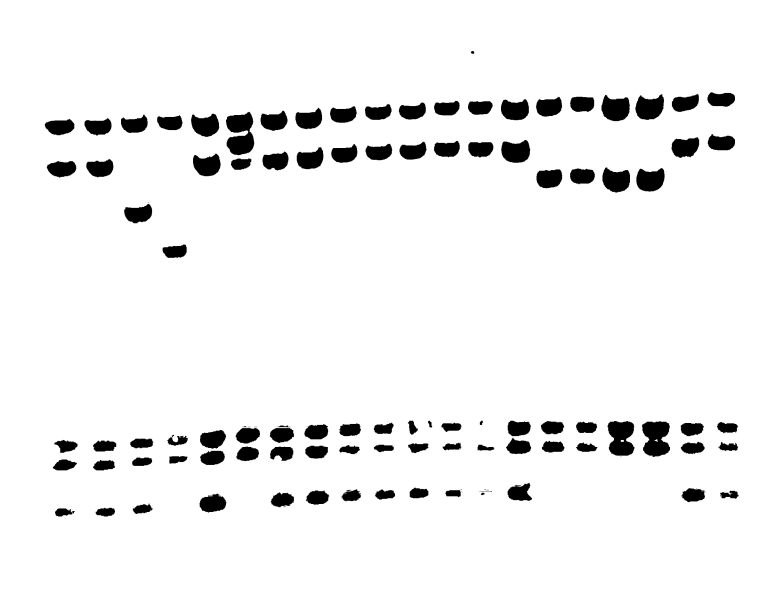


Figure A2.3. Southern hybridization of *Eco*RV-digested genomic DNA to the IS3 probe. The clones are numbered for each lane at top where each FTG-evolved clone follows its direct progenitor (odd numbers are progenitors and even numbers are FTG-evolved clones). Lanes 1-20 are as follows: 1) Ancestor, 2) AncB/FTG, 3) A+1, 4) A+1/FTG, 5) A+2, 6) A+2/FTG, 7) A+3, 8) A+3/FTG, 9) A+4, 10) A+4/FTG, 11) A+6, 12) A+6/FTG, 13) A-1, 14) A-1/FTG, 15) A-2, 16) A-2/FTG, 17) A-3, 18) A-3/FTG, 19) A-4, 20) A-4/FTG.

## 1 2 3 4 5 6 7 8 9 10 11 12 13 14 15 16 17 18 19 20

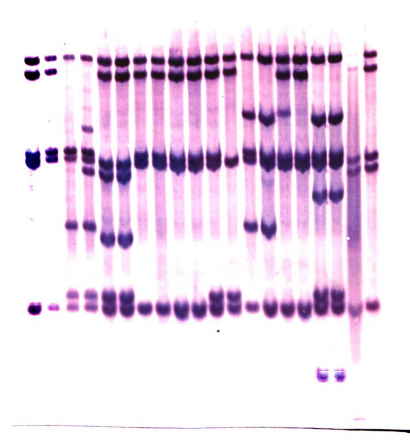


Figure A2.4. Southern hybridization of *EcoRV*-digested genomic DNA to the IS186 probe. The clones are numbered for each lane at top where each FTG-evolved clone follows its direct progenitor (odd numbers are progenitors and even numbers are FTG-evolved clones). Lanes 1-20 are as follows: 1) Ancestor, 2) AncB/FTG, 3) A+1, 4) A+1/FTG, 5) A+2, 6) A+2/FTG, 7) A+3, 8) A+3/FTG, 9) A+4, 10) A+4/FTG, 11) A+6, 12) A+6/FTG, 13) A-1, 14) A-1/FTG, 15) A-2, 16) A-2/FTG, 17) A-3, 18) A-3/FTG, 19) A-4, 20) A-4/FTG.

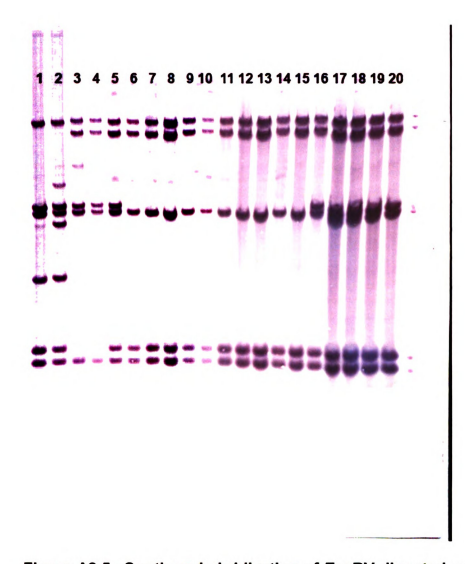
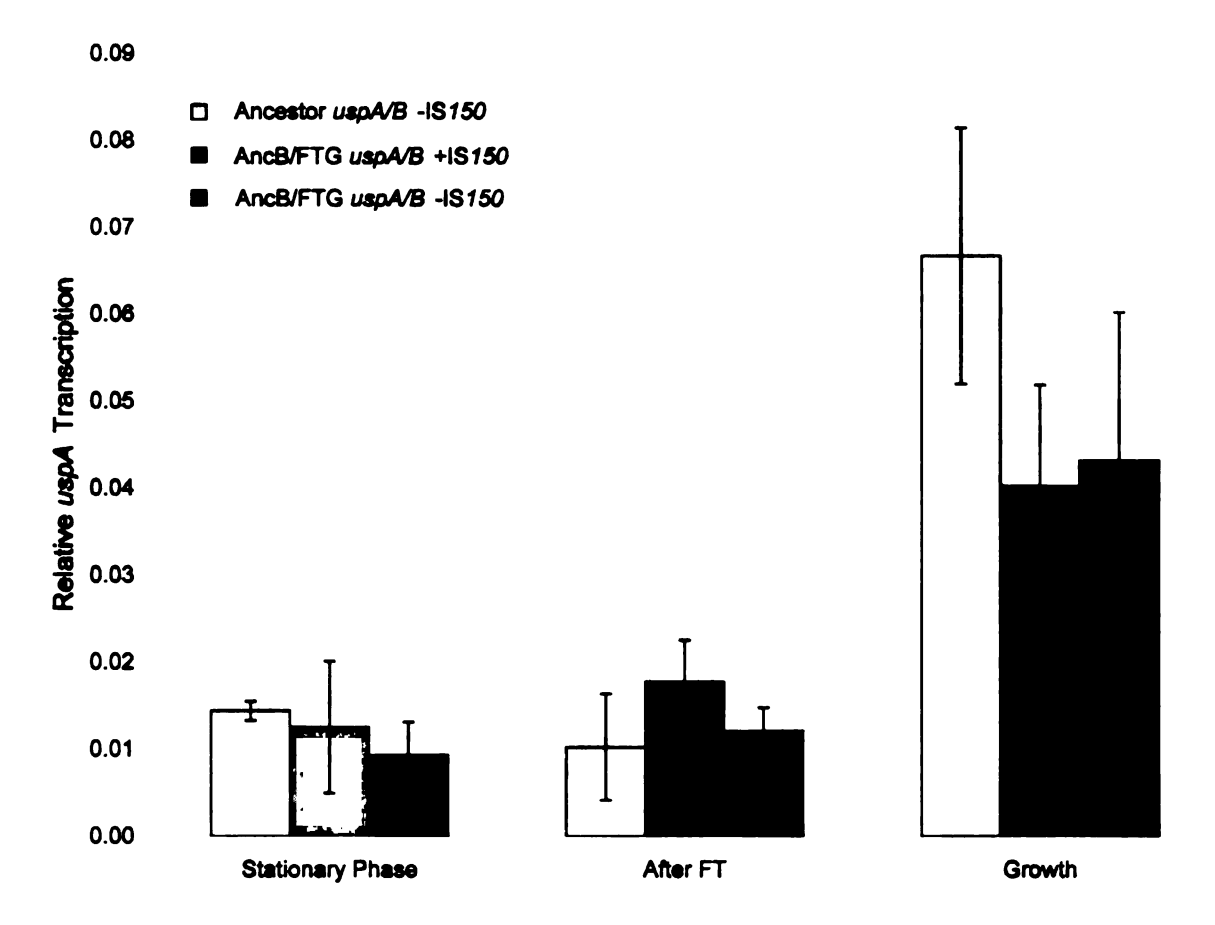


Figure A2.5. Southern hybridization of EcoRV-digested genomic DNA to the IS186 probe (second blot). This blot was performed to repeat four clones from the previous IS186 blot and determine whether other clones in the A+6/FTG population at the 500 generation and 1000 generation timepoints have deletion of a particular band as seen in the A+6/FTG clone. The clones are numbered for each lane at top. Lanes 1-20 are as follows: 1) A+1, 2) A+1/FTG, 3) A-2, 4) A-2/FTG, 5) A+6, 6-15) 10 different A+6/FTG clones from the 1000 generation population, 16-20) Five different A+6/FTG clones from the 500 generation population. The A+1/FTG and A-2/FTG clones have similar band changes as the previous IS186 blot and the reason for there being faint bands is unknown. All ten clones from the 1000 generation timepoint in the A+6/FTG population have a deleted band relative to the progenitor, but all five clones from the 500 generation timepoint have the same banding patterns as the progenitor. This deleted band in the 1000 generation clones was located near the hokE locus and is either a large deletion or complex genomic rearrangement. The exact mutation was not determined



**Figure A2.6.** Relative *uspA* transcription differences using Real-Time PCR. *uspA* transcription was measured relative to 16S rRNA transcription as an endogenous control at stationary phase, after a FT cycle, and in growth conditions 2 h after thawed cultures were diluted into fresh media. Clones are as follows: Ancestor *uspA/B* –IS150 (white), evolved clone AncB/FTG *uspA/B* +IS150 (grey), and constructed clone AncB/FTG *uspA/B* -IS150 from which the insertion element was removed (black). The height of each bar represents the mean of two independent RNA extractions, each set with 3-fold replication. Error bars are 95% confidence intervals based on the six-fold replication.

Gene	Gene Product	Primers	
cspA	Cold Shock Protein A	5' ATGGTAAAGGAATGGGAATC 3'	
		5' CTGGCGGCGTTTTTAGC 3'	
fabF	Beta-ketoacyl-ACP synthase II	5' TCCTGGCATCCGACGAA 3'	
		5' CTTATCAGAGAATTGTTAGTGTGG 3'	
		5' CAGGCTGCCATTGATTACAT 3'	
		5' TCATACCAAAGCCGACGAGTT 3'	
	Nicotinamide-Nucleotide		
nadR	adenylyltransferase	5' GTCTGGCAATCCTGCTGGCT 3'	
		5' GGTCACCCGTGCAGGTTT 3'	
		5' CGCATTCATGCTTTCAACGAAG 3'	
		5' GCGCACCGCTGATACTCATA 3'	
otsA	Trehalose synthase	5' TGCGGTAATCACAATCACAG 3'	
		5' CACAAATGGCGTTACAGC 3'	
_		5' AGCCCACGTCAGAGTAGCGGAATA 3'	
		5' GCGAACAGGACCTTGACGAATACT 3'	
rpoS	σS subunit	5' TGGGGTTGTCGGTAGCAGA 3'	
		5' TGATATCGCAGGCAGCAAAGGAC 3'	
		5' TATCGTCATCTTGCGTGGTATC 3'	
		5' CGAAAAGGCCTTAGTAGAACA 3'	
rrsA	16S rRNA	5' CGCCCATTTAACCGACAA 3'	
		5' TTTTTATTTAATCACTACAGAGA 3'	
		5' GTGGGGAGCAAACAGGATTAGATA 3'	
		5' CTCCGGAAGCCACGCCTCAAG 3'	
sodA	Manganese superoxide dismutase	5' CTGCCCGGCGCGAGTTACAATC 3'	
		5' GCCAAGGAATAGCGGGACGAGCAT 3'	
		5' TTCCTGCAAAACCATACC 3'	
		5' ACCCATCAGCGGAGAAT 3'	

Table A2.1. Primer pairs used to PCR amplify candidate genes.

IS	Primer name and sequence	Size of PCR product	
IS1	IS1F: 5' CTCCAGTGGCTTCTGTTTCT 3'	668 bp	
	IS1R: 5' TGACTTTGTCATGCAGCTCC 3'	000 бр	
IS2	IS2F: 5' GATGTCTTAGGGCCGGAGAA 3'	1,181 bp	
102	IS2R: 5' AGCCCGCTGCCGCAGATATT 3'	1,101 bp	
IS3F: 5' TCAGAGGTGACTCACATGAC 3'		1,158 bp	
100	IS3R: 5' CAAATTGTTCCGGACTGAGG 3'	1,130 Бр	
IS4	IS4F: 5' ATCCGGAAACGCTCACTTGT 3'	1,325 bp	
.07	IS4R: 5' ATTTCCAGGGCCTCTCCTTT 3'	1,323 bp	
	IS30F:	1,111 bp	
IS30	5'GAATGAGACGAACTATTACAGCAG 3'		
	IS30R:		
	5' GTTTTGAACTTCAGTGTCTTTCTC 3'		
IS150	IS150F: 5' GCGCCTTGAAGTCGTGAATC 3'		
	IS <i>150</i> R: 5' GGCTAATTCTTCTGCTGTTGTAG	1,279 bp	
	3'		
IS186	IS186F: 5' GCCGATGAATTACTCTCACG 3'	1,235 bp	
15786	IS186R: 5' GCCTCGTTAAGACGATGCCT 3'	1,200 bp	

Table A2.2. Primer pairs used to PCR amplify IS element probes for RFLP analysis.

IS element	Primer sequence	
IS1	5' GTCATCGGGCATTATCTGAAC 3'	
	5' AGAAGCCACTGGAGCACC 3'	
IS2	5' CATAGTGCGCTGGGTTATCG 3'	
	5' GTCTGCGTTTCTCCGGCCTA 3'	
IS3	5' AGTAACACCGATGCGTTCAG 3'	
	5' CTGCTACGATAATGCCTGCG 3'	
IS4	5' ACCAGATCAAGAGCCTGTCC 3'	
	5' CCTTCCCGAGAGTGGTAAAG 3'	
IS30	5' CCTCTGCTGTAAATGTTCGTCTCA 3'	
	5' GGTTGCTCAGCTAAACAACAG 3'	
IS150	5' GATCCTGTAACCATCATCAG 3'	
	5' CTGAAGGATGCTGTTACGG 3'	
IS186	5' CGGCATTACGTGCCGAAG 3'	
	5' GGTGGCCATTCGTGGGAC 3'	

Table A2.3. Primer pairs used to PCR amplify sequences adjacent to IS elements.

Clone	IS1	IS3	IS150	IS186
			2.75 kb	
AncB/FTG			insertion	
			2.5 kb deletion	
			1.5 kb insertion	
				7 kb
A+1/FTG		4.75 kb deletion	4 kb insertion	insertion
		4 kb insertion	3.5 kb deletion	
		1.8 kb deletion	1.5 kb insertion	
A+2/FTG	11 kb deletion	6 kb insertion		
		5.5 kb band	2	
		fainter		
		1.8 kb band		
A : 0/FTO		fainter		
A+3/FTG			511 1	
A+4/FTG			5 kb insertion	
			2.75 insertion	
			2 kb insertion	
	<u> </u>		1.5 kb insertion	
A+6/FTG	6 kb deletion,		3.75 kb deletion	6 kb deletion
	1.75 kb deletion		2.75 kb deletion	
A-1/FTG				
A-2/FTG				8 kb deletion
A-3/FTG	3.25 kb deletion		7 kb insertion	
			5 kb deletion	
			2 kb insertion	
			1.5 kb insertion	
A-4/FTG			2.5 kb insertion	

Table A2.4. IS band differences between individual FTG-evolved lines relative to their progenitors. For each FTG-evolved clone, the IS band differences are shown for the four IS elements with changes.

Clone	Genotype	Laurdan Anisotropy	Laurdan Anisotropy
		At Stationary Phase	After FT
A-2	cls <sup>-</sup> uspA/B -IS150	0.0231 ± 0.0037	0.0353 ± 0.0034
A-2	cls⁺ uspA/B -IS150	0.0231 ± 0.0036	0.0443 ± 0.0042
A-2/FTG	cls⁺ uspA/B -IS150	0.0222 ± 0.0037	0.0314 ± 0.0035
A-2/FTG	cls <sup>-</sup> uspA/B -IS150	0.0253 ± 0.0040	0.0248 ± 0.0021
A+4	cls⁺ uspA/B -IS150	0.0193 ± 0.0059	0.0408 ± 0.0078
A+4/FTG	cls uspA/B +IS150	0.0200 ± 0.0051	0.0248 ± 0.0033
A-3	cls⁺ uspA/B -IS150	0.0202 ± 0.0103	$0.0330 \pm 0.0053$
A-3/FTG	cls uspA/B +IS150	0.0197 ± 0.0023	0.0240 ± 0.0044
Ancestor	cls⁺ uspA/B -IS150	0.0263 ± 0.0033	0.0424 ± 0.0032
Anc B/FTG	cls⁺ uspA/B +IS150	0.0244 ± 0.0021	0.0375 ± 0.0027
Anc B/FTG	cls⁺ uspA/B -IS150	0.0274 ± 0.0012	0.0362 ± 0.0032
A-5	cls <sup>-</sup> uspA/B -IS150	0.0328 ± 0.0038	0.0343 ± 0.0040
A-5/FTG	cls uspA/B +IS150	0.0339 ± 0.0032	0.0376 ± 0.0044
A-6	cls uspA/B -IS150	0.0249 ± 0.0018	0.0363 ± 0.0050
A-6/FTG	cls uspA/B -IS150	0.0275 ± 0.0021	0.0395 ± 0.0052

Table A2.5. Laurdan anistropy differences between individual FTG-evolved clones, their progenitors, and isogenic strains. For each clone, the genotype is shown with relation to the *cls* and *uspA/B* loci, and laurdan anisotropy values are shown at stationary phase or after FT. The ± value indicates the 95% confidence interval from at least eight independent assays.